

# Metropolis Adjusted Langevin Trajectories: a robust alternative to Hamiltonian Monte Carlo

Lionel Riou-Durand and Jure Vogrinc

*University of Warwick, Coventry, CV4 7AL, United Kingdom.  
e-mail: [lionel.riou-durand@warwick.ac.uk](mailto:lionel.riou-durand@warwick.ac.uk); [jure.vogrinc@warwick.ac.uk](mailto:jure.vogrinc@warwick.ac.uk).*

**Abstract:** Hamiltonian Monte Carlo (HMC) is a widely used sampler, known for its efficiency on high dimensional distributions. Yet HMC remains quite sensitive to the choice of integration time. Randomizing the length of Hamiltonian trajectories (RHMC) has been suggested to smooth the Auto-Correlation Functions (ACF), ensuring robustness of tuning. We present the Langevin diffusion as an alternative to control these ACFs by inducing randomness in Hamiltonian trajectories through a continuous refreshment of the velocities. We connect and compare the two processes in terms of quantitative mixing rates for the 2-Wasserstein and  $\mathbb{L}_2$  distances. The Langevin diffusion is presented as a limit of RHMC achieving the fastest mixing rate for strongly log-concave targets. We introduce a robust alternative to HMC built upon these dynamics, named Metropolis Adjusted Langevin Trajectories (MALT). Studying the scaling limit of MALT, we obtain optimal tuning guidelines similar to HMC, and recover the same scaling with respect to the dimension without additional assumptions. We illustrate numerically the efficiency of MALT compared to HMC and RHMC.

**AMS 2000 subject classifications:** Primary: 60J25; secondary: 60H10, 60H30, 65C05.

**Keywords and phrases:** Markov Chain Monte Carlo, Hamiltonian Monte Carlo, Langevin diffusion, Mixing rate, Optimal scaling.

## Contents

1	Introduction	1
2	Control of the worst autocorrelation	6
3	Quantitative exponential mixing rates	8
4	Metropolis Adjusted Langevin Trajectories	11
5	Optimal scaling	14
6	Numerical illustrations	17
7	Conclusion	23
8	Acknowledgements	23
A	Proofs of the quantitative mixing rates	23
B	Proofs of the properties of MALT	29
C	Proofs of optimal scaling	32

## 1. Introduction

We consider the problem of sampling approximately from a probability distribution on  $\mathbb{R}^d$  with smooth density  $\Pi$  with respect to Lebesgue's measure. A widely used method for tackling this problem consists on building a discrete time Markov chain targeting the stationary distribution corresponding to  $\Pi$ , for which updates can be sampled exactly through a tractable algorithm. These recursive sampling methods are commonly referred as Markov Chain Monte Carlo (MCMC) algorithms. Beyond providing an approximate sampling solution by drawing a long run of the Markov chain, these algorithms also enable the approximation of intractable expectations with respect to

$\Pi$ . Indeed, empirical averages built upon random samples drawn from a Markov chain are convergent estimators of such expectations by the ergodic theorem. MCMC algorithms are powerful tools for providing numerical approximations to statistical models involving intractable integrals. The use of MCMC algorithms is now particularly spread in Bayesian statistics for instance, where the goal is to approximate estimators defined as moments of a high-dimensional posterior distribution.

When the dimension  $d$  gets large, efficient sampling algorithms often relies on discretizations of Markov processes built upon the gradient of the logarithm of  $\Pi$ . This family of MCMC algorithms is commonly referred as gradient-based samplers. In general, the resulting discrete time Markov chain possesses a flawed stationary distribution induced by the discretization. A common way to adjust the flaw of the stationary distribution is to apply the Metropolis-Hastings correction; see [37, 52]. This correction was applied to various discretized Markov processes and lead to several algorithms, among the most prominent algorithms are the Metropolis Adjusted Langevin Algorithm (MALA) and Hamiltonian Monte Carlo (HMC); see [4, 27, 67]. Unadjusted sampling approximations can be controlled by solving a trade-off between running the chain long enough to get close enough to the stationary measure, while choosing a time-step small enough in order to control the discretization error. Solving this tradeoff with respect to log-concave target densities  $\Pi$  has received a lot of attention lately; see [22, 23, 28, 29, 30, 41] for the overdamped Langevin diffusion, [20, 24, 25, 47, 56, 69] for the Langevin diffusion, and [8, 12, 14, 19, 48, 49, 50] for Hamiltonian dynamics. One limitation of unadjusted samplers is that whenever the discretization error scales polynomially with the time-step, the number of gradient evaluations required to reach a given precision will increase polynomially with the precision level at best. For Metropolis-adjusted samplers however, a logarithmic scaling with respect to the precision level is achievable as soon as the Markov chain is geometrically ergodic. In this work, we focus on Metropolis adjusted samplers. An extensive comparison between adjusted and unadjusted samplers is beyond the scope of our study.

Assessing and comparing the sampling efficiency of Metropolis adjusted samplers with respect to the dimension was initiated by the study of scaling limits established in [5, 63, 65, 68] and many others. These results suggest that the number of iterations required to reach a given accuracy scales as  $d^{1/3}$  for MALA and  $d^{1/4}$  for HMC, improving the scaling of order  $d$  obtained for the standard Random Walk Metropolis algorithm (RWM). Non-asymptotic bounds for the mixing times of Metropolis adjusted samplers were investigated more recently; see [18, 21, 32, 43]. It is now well established that in a typical application gradient-based samplers can outperform the others in terms of computational cost for high dimensional target distributions. However their lack of robustness to tuning is often a major issue for their practical implementations. The challenge of developing gradient-based samplers that combine high dimensional efficiency and robustness to tuning has received a particular interest lately; see [11, 38, 45, 75]. The focus of our work is motivated by this main challenge, and falls under the continuity of these recent studies.

Throughout this work, the target density  $\Pi$  is assumed to be positive everywhere. It can therefore be expressed in terms of a function  $\Phi : \mathbb{R}^d \rightarrow \mathbb{R}$  satisfying  $\int_{\mathbb{R}^d} \exp\{-\Phi(\mathbf{y})\} d\mathbf{y} < \infty$ , as follows

$$\Pi(\mathbf{x}) \propto \exp\{-\Phi(\mathbf{x})\}, \quad \mathbf{x} \in \mathbb{R}^d.$$

The function  $\Phi$  is called potential. For any vector  $\mathbf{x} \in \mathbb{R}^d$  we denote  $|\mathbf{x}| \triangleq (\mathbf{x}^\top \mathbf{x})^{1/2}$  its Euclidean norm. We assume in the sequel that  $\Phi$  satisfies the following smoothness assumption.

**Assumption 1.** *The potential  $\Phi \in C^1(\mathbb{R}^d)$  has a Lipschitz gradient*

$$\exists M > 0, \quad |\nabla \Phi(\mathbf{x}) - \nabla \Phi(\mathbf{y})| \leq M |\mathbf{x} - \mathbf{y}|, \quad \mathbf{x}, \mathbf{y} \in \mathbb{R}^d.$$

Among the family of gradient-based MCMC algorithms, HMC is often presented as a state-of-the-art sampler for high dimensional targets, justified by its gold standard  $d^{1/4}$  scaling with respect to dimension; see [5]. The HMC algorithm and many of its variations are built upon a

system of Ordinary Differential Equations (ODE), known as Hamiltonian dynamics. The solution of these deterministic dynamics at time  $t \geq 0$  is composed by a position  $\mathbf{X}_t \in \mathbb{R}^d$  and a velocity  $\mathbf{V}_t \in \mathbb{R}^d$  (a.k.a momentum). These correspond to the solution of the ODE

$$d \begin{bmatrix} \mathbf{X}_t \\ \mathbf{V}_t \end{bmatrix} = \begin{bmatrix} \mathbf{V}_t \\ -\nabla \Phi(\mathbf{X}_t) \end{bmatrix} dt. \quad (1)$$

These dynamics preserve the measure on  $\mathbb{R}^{2d}$  characterized by the density

$$\Pi_*(\mathbf{x}, \mathbf{v}) \propto \exp\{-\Phi(\mathbf{x}) - |\mathbf{v}|^2/2\}, \quad (\mathbf{x}, \mathbf{v}) \in \mathbb{R}^{2d}.$$

We use the notations  $\Pi$  and  $\Pi_*$  to refer both to the densities and to their corresponding probability distributions, when the context is clear. The density  $\Pi_*$  on  $\mathbb{R}^{2d}$  writes as the product of two marginal densities, corresponding to independent position and velocity drawn respectively from  $\Pi$  and from a standard Gaussian distribution. Therefore, approximate sampling from  $\Pi_*$  directly yields approximate sampling from  $\Pi$  by simply restricting our attention to the positions of the random draws. The distribution  $\Pi_*$  is invariant in the sense that if  $(\mathbf{X}_0, \mathbf{V}_0) \sim \Pi_*$  then  $(\mathbf{X}_t, \mathbf{V}_t) \sim \Pi_*$  for any  $t \geq 0$ . Yet the trajectories driven by Hamiltonian dynamics are both deterministic and periodic, as they follow the contours of the density  $\Pi_*$ . Consequently the trajectories cannot be ergodic without introducing random updates, this point is discussed further in the sequel.

In general no closed form solutions are available and the Hamiltonian trajectories need to be approximated by a tractable discretization. Many such discretizations have been proposed and studied, the most well known is probably the Störmer-Verlet integrator (a.k.a leapfrog method), defined as follows. For a time-step  $h > 0$ , let  $\theta_h : (\mathbf{x}_0, \mathbf{v}_0) \mapsto (\mathbf{x}_1, \mathbf{v}_1)$  such that

$$\begin{aligned} \mathbf{v}_{1/2} &= \mathbf{v}_0 - (h/2)\nabla\Phi(\mathbf{x}_0) \\ \mathbf{x}_1 &= \mathbf{x}_0 + h\mathbf{v}_{1/2} \\ \mathbf{v}_1 &= \mathbf{v}_{1/2} - (h/2)\nabla\Phi(\mathbf{x}_1). \end{aligned}$$

A Hamiltonian trajectory of length  $T > 0$  is then approximated by following  $L = \lfloor T/h \rfloor$  successive leapfrog steps. This approximation corresponds to the  $L^{th}$ -composition of the Störmer-Verlet update, denoted  $\theta_h^L \triangleq \theta_h \circ \dots \circ \theta_h$ . The Störmer-Verlet integrator preserves several properties of Hamiltonian dynamics; see [57]. In particular, it is known to be time reversible. Let  $\varphi(\mathbf{x}, \mathbf{v}) \triangleq (\mathbf{x}, -\mathbf{v})$  stands for the flip of velocity. Time reversibility means that flipping the velocity along the trajectory boils down to going backwards in time, or equivalently, that the map  $\varphi \circ \theta_h^L$  is an involution.

The hybrid, or Hamiltonian Monte Carlo algorithm was first introduced in [27]. It consists on proposing a Hamiltonian trajectory of length  $T > 0$ , approximated with the leapfrog method for a step-size  $h > 0$ , faced with a Metropolis accept-reject test. The velocity is updated by a fresh standard Gaussian draw at the start of each trajectory, inducing the randomness necessary to produce an ergodic sampler. This principle was later extended in [40] to allow for partial momentum refreshments through the choice of a persistence parameter  $\alpha \in [0, 1)$  (a.k.a cosines of the angle of refreshment). The resulting algorithm, called Generalized Hamiltonian Monte Carlo (GHMC), is presented explicitly hereafter; see [Algorithm 1](#). It boils down to the standard HMC algorithm for  $\alpha = 0$ .

The Metropolis-Hastings kernel is known to be a reversible Markov kernel with respect to its invariant measure. The notion of time reversibility for an (approximate) Hamiltonian trajectory is different from the notion of reversibility for a Markov chain (a.k.a detailed balance). Yet the two notions can be related when the Markov kernel is composed with a momentum flip (a.k.a skew detailed balance); see [2, Proposition 3.5] for explicit definitions. Essentially: in [Algorithm 1](#) the proposal trajectory is decomposed as  $\theta_h^L = \varphi \circ \varphi \circ \theta_h^L$  so that the involution  $\varphi \circ \theta_h^L$  is faced with a Metropolis accept-reject. When composing with  $\varphi$  the output of the test, overall a momentum

**Algorithm 1:** Generalized Hamiltonian Monte Carlo

---

**Input** : Starting point  $(\mathbf{X}^0, \mathbf{V}^0) \in \mathbb{R}^{2d}$ , number of MCMC samples  $N \geq 1$ , step-size  $h > 0$ , integration time  $T \geq h$ , and persistence  $\alpha \in [0, 1)$ .

---

```

1 Set  $L \leftarrow \lfloor T/h \rfloor$ 
2 for  $n \leftarrow 1$  to  $N$  do
3   draw  $\xi \sim \mathcal{N}_d(\mathbf{0}_d, \mathbf{I}_d)$  and refresh the momentum  $\mathbf{V}' \leftarrow \alpha \mathbf{V}^{n-1} + \sqrt{1-\alpha^2} \xi$ 
4   propose a Hamiltonian trajectory  $(\mathbf{X}^n, \mathbf{V}^n) \leftarrow \theta_h^L(\mathbf{X}^{n-1}, \mathbf{V}')$ 
5   compute the energy difference  $\Delta \leftarrow \Phi(\mathbf{X}^n) - \Phi(\mathbf{X}^{n-1}) + (|\mathbf{V}^n|^2 - |\mathbf{V}'|^2)/2$ 
6   draw a uniform random variable  $U$  on  $(0, 1)$ 
7   if  $U > \exp\{-\Delta\}$  then
8     | reject and flip the momentum  $(\mathbf{X}^n, \mathbf{V}^n) \leftarrow (\mathbf{X}^{n-1}, -\mathbf{V}')$ 
9   end
10 end
11 return  $(\mathbf{X}^1, \mathbf{V}^1), \dots, (\mathbf{X}^N, \mathbf{V}^N)$ .

```

---

flip occurs whenever a move is rejected. In practice, this is of little importance when choosing  $\alpha = 0$  (HMC), in which case momentum flips are erased by full refreshments of the velocity, ensuring reversibility of the Markov kernel; see [3, Remark 13]. However, as soon as  $\alpha \in (0, 1)$  the momentum is only partially refreshed, and reversibility is no longer ensured. Beyond these technicalities, perhaps one of the most natural question concerning [Algorithm 1](#) is the following.

**Q1.** How should we choose  $T > 0$ ,  $h > 0$  and  $\alpha \in [0, 1)$  in practice?

In the sequel, we give an overview of the main solutions proposed in the literature. We also highlight several problems often encountered when tuning (G)HMC. In particular, we explain why providing a simple answer to **Q1** is unfeasible. We first discuss the choice of the persistence parameter  $\alpha \in [0, 1)$ , then we discuss optimal scaling results established for the time-step  $h > 0$ , finally we focus on the choice of integration time  $T > 0$ .

By construction, larger values of  $\alpha$  induce more persistence in successive trajectories when accepted, but momentum flips are also erased more partially, causing backtracking upon rejection. The resulting trade-off was discussed and investigated in [40, 42]. The authors highlight the fact that no significant advantage over HMC was established, mainly due to the perturbations in the dynamics induced by momentum flips. For this reason, GHMC had limited success and the choice  $\alpha = 0$  was often considered as a default solution. This was even more upsetting as one original objective in [40] was to choose  $\alpha \rightarrow 1$  as  $T = h \rightarrow 0$  in order to converge to a Langevin diffusion. Several variations of [Algorithm 1](#) were proposed with a similar purpose [13, 60, 64, 70]. To overcome the perturbations induced by the momentum flips, these analyses required considering small enough time-steps to ensure a negligible amount of rejections. Connections between these frameworks and our methodology are discussed further below; see (2). This upset incited several authors to suggest variations of GHMC in the purpose of reducing the number of flips/rejections to facilitate the exploration of the space; see [16, 72, 76]. These suggestions are broadly related to delayed rejection methods, introduced in [36, 55, 73]; see [61] for recent developments. Reducing flips/rejections in these samplers always comes at the price of a higher number of proposals, inducing another trade-off to solve in terms of computational cost. An explicit comparison with these approaches is beyond our scope.

A simple solution for tuning  $h > 0$  was proposed in [5], relying on a scaling limit of the HMC algorithm. The study of scaling limits for Metropolis adjusted samplers is often referred in the literature as *optimal scaling*; see [5, 63, 65, 68]. These works are devoted to an asymptotic study of the acceptance rate when  $d \rightarrow \infty$  for product form targets. The independence assumption, although quite unrealistic, happens to be useful for illustrating the connections between the choice

of the time-step  $h > 0$  and the behaviour of the Metropolis accept-reject test. In particular for HMC, choosing  $h = \ell_T d^{-1/4}$  for a constant  $\ell_T > 0$  corresponds to a phase-transition regime in which the acceptance probability converges to a non trivial value  $a(\ell_T) \in (0, 1)$ . The neatness of the mathematical framework allows for an explicit optimization of several measures of efficiency (e.g. the expected square jump distance) with respect to the constant  $\ell_T$ . The optimal constant  $\ell_T^*$  corresponds to an asymptotic acceptance probability  $a(\ell_T^*)$  close to 65%. This result yields a simple way of choosing  $h$  in practice by calibrating the average acceptance probability. Given its simplicity, this strategy was widely adopted for tuning the time-step of HMC, even for distributions far beyond the original mathematical framework. As useful as it may be, this solution answers **Q1** only partially, since the optimal scaling problem in [5] is studied conditionally on  $T > 0$  and for a single value of  $\alpha = 0$ .

The choice of integration time  $T > 0$  is particularly challenging. The sampling efficiency of HMC is known to be quite sensitive to this choice, which incited many authors to propose and study several tuning solutions; see [6, 7, 10, 38, 39, 57, 71, 77]. We first illustrate how challenging the tuning problem for  $T > 0$  can be, even in a simple Gaussian framework. We consider Gaussian potentials of the form  $\Phi(\mathbf{x}) = \sum_{i=1}^d x_i^2 / (2\sigma_i^2)$  with heterogeneous scales  $\sigma_1, \dots, \sigma_d$ . In this framework, the ODE (1) possesses an explicit solution, known as the harmonic oscillator. We note  $\rho_i(T) = \mathbb{E}[\mathbf{X}_0(i)\mathbf{X}_T(i)]$  the Auto-Correlation Function (ACF) of the  $i^{\text{th}}$  component of  $\mathbf{X}_T$ . Direct computations of the ACFs yield  $\rho_i(T) = \cos(T/\sigma_i)$  for  $i = 1, \dots, d$ . These functions are periodic with arbitrary bandwidths, therefore the map  $T \mapsto \max_i |\rho_i(T)|$  can be arbitrarily erratic and close to 1. In other words, choosing  $T > 0$  to control the worst ACF can be rather difficult, if not impossible. This phenomenon was discussed in [57, Section 3.2] and in [10, 38] more recently, it is further illustrated in [Section 2](#). This main issue relates to the periodicity of Hamiltonian dynamics, and therefore extends beyond the Gaussian framework. Since one cannot hope to get a satisfactory solution for fixed  $T > 0$ , a recurrent strategy suggested in the literature consists on drawing randomly a new integration time at each iteration, therefore inducing an averaging effect on the correlations. In the Gaussian framework, drawing  $T$  from an exponential distribution with rate  $\lambda > 0$  yields expected ACFs of the form  $\mathbb{E}[\rho_i(T)] = \sigma_i^2 / (\sigma_i^2 + \lambda^{-2})$ ; see [10]. Each of these average ACFs are controlled by the average ACF of the largest scale  $\max_i \sigma_i$ , furthermore they vanish monotonously as the average integration time  $\lambda^{-1}$  goes to infinity. Other choices of distribution have been suggested; e.g. uniform in [6, 38, 77]. In [Section 3](#), we consider Hamiltonian trajectories with exponentially distributed integration times updated by Gaussian refreshments. This piecewise deterministic Markov process is referred as (exact) Randomized HMC; [10, 26]. Its discretization yields an analogue of [Algorithm 1](#), for which  $T$  is drawn at each iteration from the exponential distribution with rate  $\lambda$ , while  $L = \lfloor T/h \rfloor$  is updated accordingly.

Finally, several authors have proposed adaptive tuning strategies for variations of HMC; see [38, 39, 71, 77]. Among these, the No-U-Turn Sampler (NUTS) introduced in [39] can be implemented with quite limited tuning by the user, and it is now widely used in statistical softwares; see [17]. In particular, NUTS enables automatic selection of  $T > 0$  in the goal of maximizing the Euclidean jump distance while maintaining skew detailed balance. Since the objective criterion being a global metric, the sampler cannot provide mixing guarantees for individual components. We highlight that, intrinsically, adaptive tuning does not guarantee control of the worst ACF. This control can however be obtained when adaptive tuning is combined with a randomized strategy; see [38]. An extensive comparison with adaptive algorithms is also beyond our scope.

In this work we focus on an alternative strategy to introduce randomness in the Hamiltonian trajectories. This strategy consists on updating the Hamiltonian trajectories with a continuous refreshment of the velocities induced by a Brownian motion  $(\mathbf{W}_t)_{t \geq 0}$  on  $\mathbb{R}^d$ . The resulting process is referred in the molecular dynamics literature as Langevin diffusion (a.k.a kinetic, geometric, underdamped, or second order Langevin). Under [Assumption 1](#), the Langevin diffusion can be defined as the strong solution of the following Stochastic Differential Equation (SDE), with respect

to a damping parameter  $\gamma \geq 0$  (a.k.a friction).

$$d \begin{bmatrix} \mathbf{X}_t \\ \mathbf{V}_t \end{bmatrix} = \begin{bmatrix} \mathbf{V}_t \\ -\nabla \Phi(\mathbf{X}_t) \end{bmatrix} dt + \begin{bmatrix} \mathbf{0}_d \\ -\gamma \mathbf{V}_t dt + \sqrt{2\gamma} d\mathbf{W}_t \end{bmatrix}. \quad (2)$$

The Langevin diffusion preserves  $\Pi_*$  as well. Contrary to Hamiltonian dynamics, the randomness induced by the Brownian motion yields ergodicity of the Langevin diffusion as soon as  $\gamma > 0$ . This process is sometimes confused with its highly overdamped limit obtained by letting  $\gamma \rightarrow \infty$  while rescaling the time as  $\bar{\mathbf{X}}_t = \mathbf{X}_{\gamma t}$ ; see [58]. However, quantitative rates of convergence were established for various other damping regimes; see [24, 33]. The organization of the article is presented hereafter.

- In [Section 2](#), we show that a positive damping enables control of the worst ACF of a Langevin trajectory, without need of randomizing the integration time.
- In [Section 3](#), we present the Langevin diffusion as a limit of Randomized HMC that achieves faster exponential mixing rate for strongly log-concave targets. We prove the convergence of the generators, and derive quantitative bounds on the 2-Wasserstein mixing time and on the autocorrelations of  $\mathbb{L}_2(\Pi)$ . In particular, the rate obtained for Randomized HMC is optimized when  $\alpha \rightarrow 1$  and matches the rate obtained for the Langevin diffusion. Our results extend and interpolate the rates established in [24] and [26].
- In [Section 4](#), we introduce a sampler built upon Metropolis Adjusted Langevin Trajectories (MALT). Our approach is different from [13, 40, 60, 64, 70] in the sense that the Metropolis correction is applied to the whole trajectory of the Langevin diffusion. In particular, MALT yields a neat extension of HMC, in which momentum flips are erased by full Gaussian refreshments for any choice of friction  $\gamma \geq 0$ .
- In [Section 5](#), we establish optimal scaling limits for MALT. Our study extends the results of [5] to any choice of friction  $\gamma \geq 0$ . Similarly to HMC, we show that the  $d^{1/4}$  scaling and the 65.1% acceptance rate are optimal without further assumptions.
- In [Section 6](#), we compare MALT to several variations of Hamiltonian Monte Carlo, and illustrate its robustness through numerical experiments.

## 2. Control of the worst autocorrelation

The efficiency of HMC is known to be quite sensitive to the choice of integration time  $T > 0$ , especially under heterogeneity of scales. In this section we show how randomness induced in a Langevin trajectory yields robustness to the choice of integration time  $T > 0$ . We illustrate this phenomenon in the framework of independent centered Gaussians with arbitrary standard deviations  $\sigma_1, \dots, \sigma_d$ , i.e.  $\Phi(\mathbf{x}) = \sum_{i=1}^d \mathbf{x}(i)^2 / (2\sigma_i^2)$ . This setting was discussed several times for Hamiltonian dynamics; see [11, 38, 57]. In this section, we highlight that choosing a positive damping  $\gamma$  enables control of the worst ACF.

In the Gaussian context, the Langevin diffusion boils down to an Ornstein-Uhlenbeck process defined through an independent system of SDEs for  $t \geq 0$  and  $1 \leq i \leq d$  by

$$d \begin{bmatrix} \mathbf{X}_t(i) \\ \mathbf{V}_t(i) \end{bmatrix} = -\mathbf{A}_{i,\gamma} \begin{bmatrix} \mathbf{X}_t(i) \\ \mathbf{V}_t(i) \end{bmatrix} dt + \begin{bmatrix} 0 \\ \sqrt{2\gamma} d\mathbf{W}_t(i) \end{bmatrix}, \quad \mathbf{A}_{i,\gamma} \triangleq \begin{bmatrix} 0 & -1 \\ \sigma_i^{-2} & \gamma \end{bmatrix}.$$

It is well known that Ornstein-Uhlenbeck SDEs admit explicit solutions; see [35]. For any square matrix  $\mathbf{A}$  we note its matrix exponential  $e^{\mathbf{A}} \triangleq \sum_{k=0}^{\infty} \mathbf{A}^k / k!$ . We derive the solution corresponding to the  $i^{th}$  component of a trajectory of length  $T > 0$ :

$$\begin{bmatrix} \mathbf{X}_T(i) \\ \mathbf{V}_T(i) \end{bmatrix} = e^{-T\mathbf{A}_{i,\gamma}} \begin{bmatrix} \mathbf{X}_0(i) \\ \mathbf{V}_0(i) \end{bmatrix} + \int_0^T e^{-(T-t)\mathbf{A}_{i,\gamma}} \begin{bmatrix} 0 \\ \sqrt{2\gamma} d\mathbf{W}_t(i) \end{bmatrix} dt. \quad (3)$$

We define  $T \mapsto \rho_{i,\gamma}(T)$  the ACF corresponding to the  $i^{th}$  component of the position at stationarity. We also note  $\mathbf{A}(i,j)$  the  $(i,j)^{th}$  element of  $\mathbf{A}$ . By construction, we have

$$\rho_{i,\gamma}(T) \triangleq \text{Corr}(\mathbf{X}_T(i), \mathbf{X}_0(i)) = \mathbb{E}[\mathbf{X}_T(i)\mathbf{X}_0(i)]/\sigma_i^2 = e^{-T\mathbf{A}_{i,\gamma}}(1,1).$$

The computation of this ACF follows from an eigen value decomposition of  $\mathbf{A}_{i,\gamma}$ . Denoting  $\omega_{i,\gamma} \triangleq |(\gamma/2)^2 - (1/\sigma_i)^2|^{1/2}$ , this computation yields

$$\rho_{i,\gamma}(T) = \begin{cases} e^{-\gamma T/2}(\cos(T\omega_{i,\gamma}) + (\gamma/(2\omega_{i,\gamma}))\sin(T\omega_{i,\gamma})) & \text{if } 0 \leq \gamma < 2/\sigma_i \\ e^{-T/\sigma_i}(1 + T/\sigma_i) & \text{if } \gamma = 2/\sigma_i \\ e^{-\gamma T/2}(\cosh(T\omega_{i,\gamma}) + (\gamma/(2\omega_{i,\gamma}))\sinh(T\omega_{i,\gamma})) & \text{if } \gamma > 2/\sigma_i. \end{cases} \quad (4)$$

Choosing  $\gamma = 0$  yields the periodic ACFs of Hamiltonian dynamics, i.e.  $\rho_{i,0}(T) = \cos(T/\sigma_i)$ . When  $\gamma > 0$ , the Langevin diffusion becomes ergodic and the correlations  $\rho_{i,\gamma}(T)$  vanish as  $T \rightarrow +\infty$ . The exponential rate of convergence is maximized for  $\gamma = 2/\sigma_i$ . This choice of friction corresponds to a phase transition. In the underdamped regime, i.e. when  $0 < \gamma < 2/\sigma_i$ , the complex eigenvalues of  $\mathbf{A}_{i,\gamma}$  induce an oscillatory behaviour in the convergence of  $\rho_{i,\gamma}(T)$ . In the overdamped regime, i.e. when  $\gamma \geq 2/\sigma_i$ , the eigen values of  $\mathbf{A}_{i,\gamma}$  are real numbers and the convergence of the ACFs is monotonous. In [Figure 1](#) and [Figure 2](#), we plot  $\rho_{i,\gamma}(T)$  as a function of the duration  $T > 0$ , respectively with fixed scale  $\sigma_i = 1$  for different values of damping  $\gamma \geq 0$ , and with fixed  $\gamma \in \{0, 2\}$  for different component's scales  $\sigma_i > 0$ .

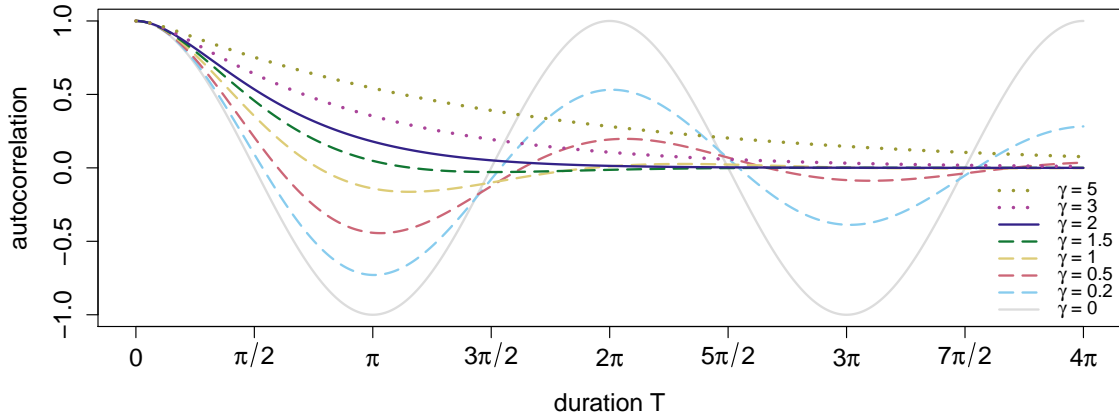


FIG 1. ACFs of Langevin dynamics for a fixed scale  $\sigma_i = 1$ , and various damping parameters  $\gamma \geq 0$ . The solid grey line corresponds to Hamiltonian dynamics ( $\gamma = 0$ ). The solid blue line corresponds to the fastest exponential rate of convergence ( $\gamma = 2$ ). Dashed lines corresponds to the underdamped regime ( $0 < \gamma < 2$ ). Dotted lines corresponds to the overdamped regime ( $\gamma > 2$ ).

As illustrated on [Figure 1](#) for a fixed scale  $\sigma_i$ , although the long term convergence to zero is optimized for  $\gamma = 2/\sigma_i$ , on the short run the ACF of a Hamiltonian trajectory ( $\gamma = 0$ ) decays faster than any other choice of  $\gamma > 0$ . In particular, it reaches zero the soonest, i.e. for  $T = \sigma_i\pi/2$ . Hamiltonian dynamics can therefore produce low correlated samples faster than Langevin dynamics for one particular component. Under heterogeneity of scales however, choosing the length  $T$  of a Hamiltonian trajectory to control the ACF of a particular scale  $\sigma_i$  can result in very high correlations for other scales. The left part of [Figure 2](#) illustrates that the worst ACF can become arbitrarily erratic and close to one in absolute terms. In other words, choosing  $T$  to simultaneously control all the correlations of Hamiltonian dynamics can be next to impossible. The right part of [Figure 2](#) illustrates that, if the damping parameter is chosen as  $\gamma = 2/\sigma_i$  for a given  $i \in \{1, \dots, d\}$ , then the ACF of any smaller component's scale  $\sigma_j < \sigma_i$  is always dominated by the  $i^{th}$  ACF. This observation suggests a simple tuning rule to control uniformly the correlations over  $\sigma_1, \dots, \sigma_d$ : first choose  $\gamma = 2/\sigma_{\max}$  according to the maximum scale  $\sigma_{\max} \triangleq \max_i \sigma_i$ , then select  $T$  in order to control the ACF corresponding to  $\sigma_{\max}$ . For this choice of damping, the ACF corresponding

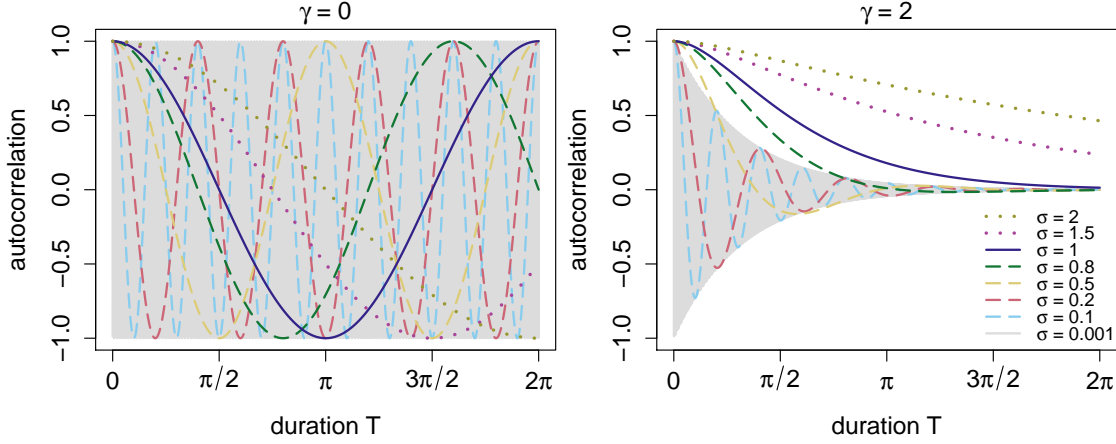


FIG 2. ACFs of Hamiltonian and Langevin dynamics (resp. left and right), for fixed  $\gamma \in \{0, 2\}$  and various component's scales  $\sigma_i > 0$ . The solid blue line corresponds to a reference scale  $\sigma_{\text{ref}} = 1$ . Dashed lines corresponds to smaller scales ( $\sigma_i < 1$ ). Dotted lines corresponds to larger scales ( $\sigma_i > 1$ ). The grey region corresponds to the ACF of a very small scale ( $\sigma_i = 0.001$ ) oscillating with very thin bandwidth.

to the largest scale yields a monotonously vanishing upper bound over all the correlations. This property highlights that the tuning problem of the integration time  $T$  is easier to solve for Langevin dynamics than for Hamiltonian dynamics.

We note that a similar control of the correlations can be obtained with Randomized HMC, for which a uniform bound relates the worst ACF to the largest scale; see [11]. In Section 3, we connect this approach to the Langevin diffusion and compare their exponential mixing rates quantitatively. We also extend their robustness beyond the Gaussian framework by establishing uniform bounds on the correlations for strongly log-concave targets.

### 3. Quantitative exponential mixing rates

To obtain simultaneous control of the ACFs of Hamiltonian dynamics, the main approach suggested in the literature consists on drawing at random the length of each Hamiltonian trajectory. With this approach, ACFs are averaged over multiple trajectories. The smoothing effect induced can enable control of the worst ACF, depending on the distribution chosen; see [11, 38, 57]. In this work we consider exponentially distributed integration times with rate  $\lambda > 0$ . With the term Randomized HMC we will refer to the piecewise deterministic Markov process driven by Hamiltonian dynamics, refreshed with persistence  $\alpha \in [0, 1)$  by independent standard Gaussian momentums  $(\xi_k)_{k \in \mathbb{N}}$ , at random jumping times driven by a homogeneous Poisson process  $(N_t)_{t \geq 0}$  with rate  $\lambda \geq 0$ . Under Assumption 1, Randomized HMC can be defined as the strong solution of the following jump-type SDE.

$$d \begin{bmatrix} \mathbf{X}_t \\ \mathbf{V}_t \end{bmatrix} = \begin{bmatrix} \mathbf{V}_t \\ -\nabla \Phi(\mathbf{X}_t) \end{bmatrix} dt + \begin{bmatrix} \mathbf{0}_d \\ (\alpha \mathbf{V}_{t-} + \sqrt{1 - \alpha^2} \xi_{N_{t-}} - \mathbf{V}_{t-}) dN_t \end{bmatrix}. \quad (5)$$

In the sequel, we connect Randomized HMC to the Langevin diffusion, and compare the two in terms of exponential mixing rates with respect to the 2-Wasserstein distance and the  $\mathbb{L}_2(\Pi_*)$ -norm. These metrics are defined as follows. The 2-Wasserstein distance between any two probability measures  $\nu$  and  $\nu'$  on an Euclidean space is given by

$$W_2(\nu, \nu') \triangleq \inf \{ \mathbb{E}[\|\mathbf{X} - \mathbf{X}'\|^2]^{1/2}, \mathbf{X} \sim \nu, \mathbf{X}' \sim \nu' \}.$$

We note  $\mathbb{L}_2(\Pi_*) \triangleq \{f : \mathbb{R}^{2d} \rightarrow \mathbb{R}, \int f^2 d\Pi_* < \infty\}$  the set of square integrable functions with respect to  $\Pi_*$ . For any such  $f$  and  $g$ , the scalar product and the norm on  $\mathbb{L}_2(\Pi_*)$  are respectively defined by  $\langle f, g \rangle \triangleq \int f g d\Pi_*$  and  $\|f\| \triangleq \langle f, f \rangle^{1/2}$ . We also note  $\mathbb{L}_2^0(\Pi_*) \triangleq \{f \in \mathbb{L}_2(\Pi_*), \int f d\Pi_* = 0\}$  the set of centered functions in  $\mathbb{L}_2(\Pi_*)$ . Some of our results directly relate to the actual target  $\Pi$ , marginal distribution of  $\Pi_*$ . To this end, for any  $\nu$  probability measure on  $\mathbb{R}^{2d}$ , we note  $\nu_{\mathbf{x}}$  its marginal probability measure defined on Borel sets  $A$  of  $\mathbb{R}^d$  by  $\nu_{\mathbf{x}}(A) \triangleq \nu(A \times \mathbb{R}^d)$ . Similarly, we note  $\mathbb{L}_2^0(\Pi) \triangleq \{f \in \mathbb{L}_2^0(\Pi_*), f(\mathbf{x}, \mathbf{v}) = f(\mathbf{x}, \mathbf{0}_d), (\mathbf{x}, \mathbf{v}) \in \mathbb{R}^{2d}\}$  the set of functions in  $\mathbb{L}_2^0(\Pi_*)$  that depend only on the position. We use the notation  $\mathbf{P}^t$  for any Markov kernel characterized by a SDE on  $\mathbb{R}^{2d}$ ; e.g. solution of (2) or (5). Any such kernel can be defined on Borel sets  $A$  of  $\mathbb{R}^{2d}$  by

$$\mathbf{P}^t((\mathbf{x}, \mathbf{v}), A) \triangleq \mathbb{P}((\mathbf{X}_t, \mathbf{V}_t) \in A | (\mathbf{X}_0, \mathbf{V}_0) = (\mathbf{x}, \mathbf{v})), \quad (\mathbf{x}, \mathbf{v}) \in \mathbb{R}^{2d}.$$

Let  $\nu \mathbf{P}^t$  stand for the distribution of  $(\mathbf{X}_t, \mathbf{V}_t)$  starting from  $(\mathbf{X}_0, \mathbf{V}_0) \sim \nu$ . For any  $f \in \mathbb{L}_2(\Pi_*)$  define

$$\mathbf{P}^t f(\mathbf{x}, \mathbf{v}) \triangleq \mathbb{E}[f(\mathbf{X}_t, \mathbf{V}_t) | (\mathbf{X}_0, \mathbf{V}_0) = (\mathbf{x}, \mathbf{v})], \quad (\mathbf{x}, \mathbf{v}) \in \mathbb{R}^{2d}.$$

Main arguments of this section rely on establishing useful relationships between the infinitesimal generators of Randomized HMC and the Langevin diffusion. We note  $C_c^\infty(\mathbb{R}^{2d})$  the set of smooth functions with compact support on  $\mathbb{R}^{2d}$ , and  $\mathcal{L}^H$  the infinitesimal generator of Hamiltonian dynamics (a.k.a Liouville operator). This generator is formally defined on tests functions  $f \in C_c^\infty(\mathbb{R}^{2d})$  such that for any  $(\mathbf{x}, \mathbf{v}) \in \mathbb{R}^{2d}$

$$\mathcal{L}^H f(\mathbf{x}, \mathbf{v}) \triangleq \mathbf{v}^\top \nabla_{\mathbf{x}} f(\mathbf{x}, \mathbf{v}) - \nabla \Phi(\mathbf{x})^\top \nabla_{\mathbf{v}} f(\mathbf{x}, \mathbf{v}).$$

In addition, we introduce the following generators corresponding to two types of momentum refreshments. The generator  $\mathcal{R}_\alpha^{PP}$  refers to discrete refreshments with persistence  $\alpha \in [0, 1]$  with jumps characterized by a standard Poisson Process. The generator  $\mathcal{R}^{BM}$  refers to continuous refreshments induced by a standard Brownian motion. These generators are formally defined for  $\xi \sim \mathcal{N}_d(\mathbf{0}_d, \mathbf{I}_d)$  by

$$\begin{aligned} \mathcal{R}_\alpha^{PP} f(\mathbf{x}, \mathbf{v}) &\triangleq \mathbb{E} \left[ f(\mathbf{x}, \alpha \mathbf{v} + \sqrt{1 - \alpha^2} \xi) \right] - f(\mathbf{x}, \mathbf{v}) \\ \mathcal{R}^{BM} f(\mathbf{x}, \mathbf{v}) &\triangleq -\mathbf{v}^\top \nabla_{\mathbf{v}} f(\mathbf{x}, \mathbf{v}) + \text{tr}(\nabla_{\mathbf{v}}^2 f(\mathbf{x}, \mathbf{v})). \end{aligned}$$

The generator of Randomized HMC with rate  $\lambda \geq 0$  and persistence  $\alpha \in [0, 1]$  is noted  $\mathcal{L}_{\lambda, \alpha}^{RH}$  while the generator of the Langevin diffusion with damping  $\gamma \geq 0$  is noted  $\mathcal{L}_\gamma^{LD}$ . Built upon the two types of refreshment introduced, explicit definitions for these generators are as follows

$$\begin{aligned} \mathcal{L}_{\lambda, \alpha}^{RH} &\triangleq \mathcal{L}^H + \lambda \mathcal{R}_\alpha^{PP} \\ \mathcal{L}_\gamma^{LD} &\triangleq \mathcal{L}^H + \gamma \mathcal{R}^{BM}. \end{aligned}$$

Given that  $\mathcal{L}^H$  is a common element of these two generators, their proximity depends only on the proximity of the two generators of refreshment, and therefore does not rely on any assumption with respect to the potential function. Convergence of the Randomized HMC generator towards the generator of the Langevin diffusion is shown in [Proposition 1](#) for tests functions  $f \in C_c^\infty(\mathbb{R}^{2d})$ . The convergence is established with respect to the supremum norm  $\|f\|_\infty \triangleq \sup |f|$ . A proof of this result is derived in [Appendix A.1](#).

**Proposition 1.** *If  $\lambda = \frac{2\gamma}{1 - \alpha^2}$  then any  $f \in C_c^\infty$  yields  $\|\mathcal{L}_{\lambda, \alpha}^{RH} f - \mathcal{L}_\gamma^{LD} f\|_\infty \rightarrow 0$  as  $\alpha \rightarrow 1$ .*

[Proposition 1](#) describes the Langevin diffusion as a limit of Randomized HMC. Convergence of the generators holds when the persistence  $\alpha \rightarrow 1$  while the refreshment rate  $\lambda = 2\gamma/(1 - \alpha^2) \rightarrow \infty$ . Intuitively, the more partial and frequent the refreshments by a Poisson Process become, the closer they get from continuous refreshments induced by a Brownian motion. Convergence of infinitesimal generators is a powerful tool to establish weak convergence of Markov processes; see [\[34\]](#). Detailed

implications of this result in terms of weak convergence for Randomized HMC are beyond the scope of this work. We now connect and compare the two processes in terms of exponential mixing rates.

Several sufficient conditions to ensure geometric ergodicity of Randomized HMC with respect to the total variation distance have been derived in [11, Theorem 3.9]. These conditions are similar to the ones proposed in [51] to ensure geometric ergodicity of the Langevin diffusion. More precisely, in [11] the authors show that similar Lyapunov functions can be derived for Randomized HMC and for the Langevin diffusion. However, the minorization condition established for Randomized HMC relies on an alternative approach to account for discontinuities of the sample paths. Beyond these qualitative results, we are not aware of any quantitative comparison between the exponential mixing rates of the two processes prior to this work. Yet, quantitative mixing rates have been established for the Langevin diffusion in [24], and for Randomized HMC in [26]. In these works, explicit bounds on the mixing rates are derived with respect to the 2-Wasserstein distance, and extended to the  $\mathbb{L}_2(\Pi_*)$ -norm for Randomized HMC. These rates are established for strongly-log concave targets admitting sufficiently smooth densities with respect to Lebesgue's measure. The class of target distributions considered corresponds to potential functions satisfying [Assumption 2](#).

**Assumption 2.** *The potential  $\Phi \in C^2(\mathbb{R}^d)$ , such that for some constants  $M \geq m > 0$*

$$m\mathbf{I}_d \preceq \nabla^2 \Phi(\mathbf{x}) \preceq M\mathbf{I}_d, \quad \mathbf{x} \in \mathbb{R}^d.$$

Under [Assumption 2](#), exponential mixing rates of the Langevin diffusion with respect to the 2-Wasserstein distance have been established for various damping regimes in [24, Theorem 1]. In particular, by choosing  $\gamma = \sqrt{M+m}$ , an exponential decay of the form  $e^{-rt}$  with rate  $r = m/\sqrt{M+m}$  is obtained. For Randomized HMC, exponential mixing rates for every persistence  $\alpha \in [0, 1)$  have been derived in [26, Theorem 3]. In particular, the following mixing rate and refreshment intensity are suggested:

$$r = \frac{(1+\alpha)m}{2\sqrt{M+m}} - \frac{\alpha m^{3/2}}{4(M+m)}, \quad \lambda = \frac{1}{1-\alpha^2} \left( 2\sqrt{M+m} - \frac{(1-\alpha)m}{\sqrt{M+m}} \right). \quad (6)$$

In the case of full momentum refreshments ( $\alpha = 0$ ), the mixing rate obtained for Randomized HMC boils down to  $r = (m/2)/\sqrt{M+m}$ . We remark that the mixing rate established in [24, Theorem 1] for the Langevin diffusion is faster by a factor two. In addition, the mixing rate of Randomized HMC increases as  $\alpha \rightarrow 1$  while  $\lambda \rightarrow \infty$ . This observation suggests that any discrete refreshment strategy can be improved by choosing more frequent and partial refreshments. In particular, it supports the intuition that continuous refreshments induced by a Brownian motion may enable faster mixing than discrete refreshments induced by a Poisson process. Yet as  $\alpha \rightarrow 1$ , the bound of [26, Theorem 3] does not match the bound of [24, Theorem 1]. More precisely, the mixing rate of Randomized HMC converges to a value strictly lower than  $m/\sqrt{M+m}$ . In [Theorem 1](#), we show that the mixing rate of Randomized HMC can be sharpened for any  $\alpha \in (0, 1)$  without additional assumption. In particular, we establish a bound that matches the mixing rate of the Langevin diffusion as  $\alpha \rightarrow 1$ .

**Theorem 1.** *Suppose that [Assumption 2](#) holds. Let  $\mathbf{P}^t$  be the Markov transition kernel of Randomized HMC, solution of (5), with persistence  $\alpha \in [0, 1)$  and refreshment intensity  $\lambda = \frac{2\sqrt{M+m}}{1-\alpha^2}$ . Then there exist  $C, C' \leq 1.56$  such that for any  $t > 0$*

$$\begin{aligned} W_2((\nu \mathbf{P}^t)_{\mathbf{x}}, \Pi) &\leq C e^{-rt} W_2(\nu_{\mathbf{x}}, \Pi), \quad \nu = \nu_{\mathbf{x}} \otimes \mathcal{N}_d(\mathbf{0}_d, \mathbf{I}_d) \\ \|\mathbf{P}^t f\| &\leq C' e^{-rt} \|f\|, \quad f \in \mathbb{L}_0^2(\Pi) \end{aligned}$$

with an exponential rate of mixing

$$r = \frac{(1+\alpha)m}{2\sqrt{M+m}}.$$

A proof of [Theorem 1](#) is derived in [Appendix A.2](#). The rate of convergence obtained increases as  $\alpha \rightarrow 1$ , while its limit coincides with the rate  $m/\sqrt{M+m}$  established in [24, Theorem 1] for the Langevin diffusion. Compared to (6), the mixing rate is strictly faster for any  $\alpha \in (0, 1)$ , although the two rates get relatively close for large condition number  $M/m \rightarrow \infty$ . Similarly to [24, 26], our analysis is based on a synchronous coupling construction. More precisely, we study the distance between two copies of the process starting from different values, synchronized with the same Poisson process and Gaussian refreshments. This construction is relatively standard, although deriving sharp convergence rates relies on a carefully chosen twist of the metric to optimize the 2-Wasserstein contraction. The main argument in the proof relies on establishing uniform bounds on the coupling generator for which we obtain sufficient and necessary conditions in [Appendix A.3](#); see (20). In particular, the refreshment intensity  $\lambda = 2\sqrt{M+m}/(1-\alpha^2)$  is chosen in order to maximize the exponential rate of convergence under a sharper constraint; see (37). Remarkably, this refreshment intensity coincides with the interpolation curve in [Proposition 1](#) for  $\gamma = \sqrt{M+m}$ . Restricting our attention to the actual target  $\Pi$  rather than  $\Pi_*$  is useful for obtaining small explicit constants  $C, C'$  defined in [Appendix A.2](#); see (23) and (31).

Finally, we establish convergence of the Langevin diffusion with respect to the  $\mathbb{L}_2(\Pi_*)$ -norm in [Proposition 2](#). This result is a consequence of the 2-Wasserstein convergence previously derived in [24, Theorem 1]. This extension is achieved by following similar arguments compared to the ones used for Randomized HMC in [Theorem 1](#). A sketch of proof is presented in [Appendix A.4](#).

**Proposition 2.** *Suppose that [Assumption 2](#) holds. Let  $\mathbf{P}^t$  be the Markov transition kernel of the Langevin diffusion, solution of (2), with friction  $\gamma > \sqrt{M}$ . Then there exist  $C' \leq 1.56$  such that for any  $t > 0$  and any function  $f \in \mathbb{L}_0^2(\Pi)$  that depends only on position*

$$\|\mathbf{P}^t f\| \leq C' e^{-rt} \|f\|,$$

with an exponential rate of mixing

$$r = \frac{m \wedge (\gamma^2 - M)}{\gamma}.$$

The mixing rate in [Proposition 2](#) is a continuous function of  $\gamma^2$  that increases on  $(M, M+m]$  and decreases on  $[M+m, \infty)$ . The optimum is therefore achieved for  $\gamma = \sqrt{M+m}$  and yields  $r = m/\sqrt{M+m}$ . This rate coincides with the limit of the rate obtained in [Theorem 1](#) as  $\alpha \rightarrow 1$ . As illustrated in [Section 2](#), a positive damping can enable uniform control of the ACFs for the Langevin diffusion. Our result extends this property beyond the Gaussian framework; i.e. to any target  $\Pi$  satisfying [Assumption 2](#). Indeed for any  $f : \mathbb{R}^d \rightarrow \mathbb{R}$  such that  $\int f^2 d\Pi \in (0, \infty)$ , the map  $g(\mathbf{x}, \mathbf{v}) \triangleq (f(\mathbf{x}) - \int f d\Pi)/(\int f^2 d\Pi)^{1/2}$  defined for  $(\mathbf{x}, \mathbf{v}) \in \mathbb{R}^{2d}$  is such that  $g \in \mathbb{L}_2^0(\Pi)$  and  $\|g\| = 1$ , therefore [Proposition 2](#) applies:

$$\text{Corr}(f(\mathbf{X}_t), f(\mathbf{X}_0)) = \langle g, \mathbf{P}^t g \rangle \leq \|g\| \|\mathbf{P}^t g\| \leq C' e^{-rt}. \quad (7)$$

Combined together, our results describe the Langevin diffusion as a limit of Randomized HMC achieving the fastest exponential mixing rate, for strongly log-concave targets with smooth enough densities. This observation motivates the construction and study of samplers directly based on the Langevin dynamics rather than the Hamiltonian dynamics.

#### 4. Metropolis Adjusted Langevin Trajectories

In this section, we introduce a Metropolis adjusted sampler built upon a standard time discretization of the Langevin diffusion. We explain its foundations and establish connections with previous approaches aiming for the Langevin diffusion; see [13, 15, 40, 60, 64, 70]. Compared to these approaches, the Metropolis correction is applied to a whole Langevin trajectory of length  $T > 0$ . This

mechanism allows us to get rid of the perturbations induced by momentum flips, by performing full refreshments of the velocity at the start of each trajectory. We describe this sampler as an extension of HMC, for which we advocate the use of a positive friction to enable robust tuning of the integration time  $T > 0$ . We present this extension as an alternative to GHMC, for which the tuning question is arguably more natural and easier to answer.

For any time-step  $h > 0$ , we introduce  $\eta = e^{-\gamma h/2}$ . We also let  $\xi, \xi' \sim \mathcal{N}_d(\mathbf{0}_d, \mathbf{I}_d)$  be independent. Starting from  $(\mathbf{x}_0, \mathbf{v}_0) \in \mathbb{R}^{2d}$ , we consider the following discretization

$$\mathbf{v}'_0 = \eta \mathbf{v}_0 + \sqrt{1 - \eta^2} \xi \quad (\text{O})$$

$$\mathbf{v}_{1/2} = \mathbf{v}'_0 - (h/2) \nabla \Phi(\mathbf{x}_0) \quad (\text{B})$$

$$\mathbf{x}_1 = \mathbf{x}_0 + h \mathbf{v}_{1/2} \quad (\text{A})$$

$$\mathbf{v}'_1 = \mathbf{v}_{1/2} - (h/2) \nabla \Phi(\mathbf{x}_1) \quad (\text{B})$$

$$\mathbf{v}_1 = \eta \mathbf{v}'_1 + \sqrt{1 - \eta^2} \xi' \quad (\text{O})$$

The updates noted by the letters O, B and A correspond to exact solutions of a splitting of (2) into three parts. These are respectively referred in the literature as momentum refreshment, acceleration and free transport parts of the Langevin dynamics; see [44]. The BAB composition boils down to the Störmer-Verlet update introduced in Section 1. Combined with an infinitesimal momentum refreshment as  $h \rightarrow 0$ , the OBABO composition yields a natural time discretization of the Langevin diffusion, built as an extension of the Leapfrog integrator for Hamiltonian dynamics. For this reason, this splitting scheme has received a significant interest; see [13, 15, 56, 64, 70]. Several other splittings of the Langevin diffusion have been proposed and studied; see [1, 69]. This work focuses on the OBABO update in order to preserve several properties of the Störmer-Verlet update, useful for constructing a Metropolis correction. On the principle, our construction could rely on other integrators, as long as these are time-reversible and volume preserving; see [13].

For any  $\gamma > 0$ , the distribution of  $\mathbf{z}_1 = (\mathbf{x}_1, \mathbf{v}_1)$  given  $\mathbf{z}_0 = (\mathbf{x}_0, \mathbf{v}_0)$  admits a positive density  $\mathbf{z}_1 \mapsto q_{h,\gamma}(\mathbf{z}_0, \mathbf{z}_1)$  with respect to Lebesgue's measure on  $\mathbb{R}^{2d}$ . This density is formally defined as the product of the two conditional densities corresponding to the Gaussian distributions of  $\mathbf{x}_1$  given  $(\mathbf{x}_0, \mathbf{v}_0)$  and  $\mathbf{v}_1$  given  $(\mathbf{x}_0, \mathbf{v}_0, \mathbf{x}_1)$ . The case  $\gamma = 0$  boils down to considering the deterministic Störmer-Verlet update. The OBABO update characterizes a Markov kernel defined for any Borel set  $A$  of  $\mathbb{R}^{2d}$  by

$$\mathbf{Q}_{h,\gamma}(\mathbf{z}_0, A) \triangleq \begin{cases} \int_A q_{h,\gamma}(\mathbf{z}_0, \mathbf{z}_1) d\mathbf{z}_1 & \text{if } \gamma > 0 \\ \delta_{\mathbf{z}_0}(A) & \text{if } \gamma = 0. \end{cases}$$

For any distribution  $\nu_0$  on  $\mathbb{R}^{2d}$ , starting from  $\mathbf{z}_0 \sim \nu_0$  we define the numerical Langevin trajectory for  $i \geq 1$  by

$$\mathbf{z}_i \sim \mathbf{Q}_{h,\gamma}(\mathbf{z}_{i-1}, \cdot) \quad (8)$$

We refer to the synchronized processes  $(\mathbf{Z}_t)_{t \geq 0}$  and  $(\mathbf{z}_i)_{i \geq 0}$  for the respective solutions of (2) and (8), starting from  $\mathbf{Z}_0 = \mathbf{z}_0 \sim \nu_0$  with identical momentum refreshments. This synchronization is formally ensured in the OBABO update by considering  $\xi = \xi_{0,h/2}$  and  $\xi' = \xi_{h/2,h}$  such that for  $t > s \geq 0$

$$\xi_{s,t} \triangleq \sqrt{\frac{2\gamma}{1 - e^{-\gamma(t-s)}}} \int_s^t e^{-\gamma(t-u)} d\mathbf{W}_u. \quad (9)$$

In Proposition 3, we show that numerical Langevin trajectories built upon recursive OBABO updates are strongly accurate. Similar results have been proposed and discussed in [9, 13].

**Proposition 3.** *Suppose that Assumption 1 holds. Let  $(\mathbf{Z}_t)_{t \geq 0}$  and  $(\mathbf{z}_i)_{i \geq 0}$  be the respective solutions of (2) and (8), synchronized with respect to (9). For any fixed  $d \geq 1$ ,  $T > 0$  and  $\gamma \geq 0$ , there exists  $C > 0$  such that for any square integrable start  $\mathbf{Z}_0 \sim \nu_0$  on  $\mathbb{R}^{2d}$  and any  $t, h \in (0, T]$*

$$(\mathbb{E}[|\mathbf{Z}_{\lfloor t/h \rfloor h} - \mathbf{z}_{\lfloor t/h \rfloor}|^2])^{1/2} \leq C (1 + \mathbb{E}[|\mathbf{Z}_0|^2])^{1/2} h.$$

**Proposition 3** ensures that, measured by the  $\mathbb{L}_2$ -norm, the numerical error of approximating Langevin trajectories with the OBABO update scales at worst linearly with the time-step  $h > 0$ . Beyond its natural interpretation, this claim is used to establish several results in [Section 5](#). A detailed proof is therefore derived in [Appendix B.1](#).

We introduce a Metropolis correction applied to numerical Langevin trajectories of length  $T > 0$ . This correction involves a local numerical error, defined for  $h > 0$  and  $\mathbf{x}, \mathbf{y} \in \mathbb{R}^d$  by

$$\mathcal{E}_h(\mathbf{x}, \mathbf{y}) \triangleq \Phi(\mathbf{y}) - \Phi(\mathbf{x}) - \frac{1}{2}(\mathbf{y} - \mathbf{x})^\top (\nabla \Phi(\mathbf{y}) + \nabla \Phi(\mathbf{x})) + \frac{h^2}{8} \left( |\nabla \Phi(\mathbf{y})|^2 - |\nabla \Phi(\mathbf{x})|^2 \right). \quad (10)$$

Composed by  $L = \lfloor T/h \rfloor$  steps, a Langevin trajectory  $(\mathbf{x}_0, \mathbf{v}_0), \dots, (\mathbf{x}_L, \mathbf{v}_L) \in \mathbb{R}^{2d}$  is drawn from (8). The trajectory is faced with an accept-reject test to compensate for the total error

$$\Delta(\mathbf{x}_0, \dots, \mathbf{x}_L) \triangleq \sum_{i=1}^L \mathcal{E}_h(\mathbf{x}_{i-1}, \mathbf{x}_i). \quad (11)$$

Applied to the positions in the OBABO discretization, the local error  $\mathcal{E}_h$  boils down to the energy difference induced by the Störmer Verlet update. Indeed the BAB composition yields

$$\mathcal{E}_h(\mathbf{x}_0, \mathbf{x}_1) = \Phi(\mathbf{x}_1) - \Phi(\mathbf{x}_0) + \frac{1}{2}(|\mathbf{v}'_1|^2 - |\mathbf{v}'_0|^2) = -\log \left( \frac{\Pi_*(\mathbf{x}_1, \mathbf{v}'_1)}{\Pi_*(\mathbf{x}_0, \mathbf{v}'_0)} \right). \quad (12)$$

The total error  $\Delta$  corresponds to the sum of energy differences incurred by the Leapfrog integrator (disregarding the partial velocity refreshments). Therefore, it can be interpreted as the error of approximating the Hamiltonian part of Langevin dynamics. Each numerical Langevin trajectory is finally accepted with probability  $1 \wedge \exp\{-\Delta\}$ . The resulting algorithm, named Metropolis Adjusted Langevin Trajectories (MALT), is presented hereafter; see [Algorithm 2](#).

---

**Algorithm 2:** Metropolis Adjusted Langevin Trajectories

---

**Input** : Starting point  $(\mathbf{X}^0, \mathbf{V}^0) \in \mathbb{R}^{2d}$ , number of MCMC samples  $N \geq 1$ , step-size  $h > 0$ , integration time  $T \geq h$ , and friction  $\gamma \geq 0$ .

1 Set  $L \leftarrow \lfloor T/h \rfloor$   
2 **for**  $n \leftarrow 1$  to  $N$  **do**  
3   **draw a full refresh of the momentum**  $\mathbf{V}' \sim \mathcal{N}_d(\mathbf{0}_d, \mathbf{I}_d)$   
4   **set**  $(\mathbf{x}_0, \mathbf{v}_0) \leftarrow (\mathbf{X}^{n-1}, \mathbf{V}')$  and  $\Delta \leftarrow 0$   
5   **for**  $i \leftarrow 1$  to  $L$  **do**  
6     **draw an OBABO update step**  $(\mathbf{x}_i, \mathbf{v}_i) \sim \mathbf{Q}_{h, \gamma}((\mathbf{x}_{i-1}, \mathbf{v}_{i-1}), .)$   
7     **update the energy difference**  $\Delta \leftarrow \Delta + \mathcal{E}_h(\mathbf{x}_{i-1}, \mathbf{x}_i)$   
8   **end**  
9   **set**  $(\mathbf{X}^n, \mathbf{V}^n) \leftarrow (\mathbf{x}_L, \mathbf{v}_L)$   
10   **draw a uniform random variable**  $U$  on  $(0, 1)$   
11   **if**  $U > \exp\{-\Delta\}$  **then**  
12     **reject and flip the momentum**  $(\mathbf{X}^n, \mathbf{V}^n) \leftarrow (\mathbf{X}^{n-1}, -\mathbf{V}')$   
13   **end**  
14 **end**  
15 **return**  $(\mathbf{X}^1, \mathbf{V}^1), \dots, (\mathbf{X}^N, \mathbf{V}^N)$ .

---

Propose a  
Langevin  
trajectory.

From (11) and (12), we see that the total energy error  $\Delta$  in [Algorithm 1](#) and [Algorithm 2](#) coincide when  $\gamma = \alpha = 0$ . In other words, MALT is an extension of HMC to any choice of friction  $\gamma \geq 0$ . In [Proposition 4](#), we show that MALT defines a reversible Markov kernel with respect to  $\Pi$ . We recall that a kernel  $\mathbf{P}$  is reversible with respect to  $\Pi$  if for any Borel sets  $A, B$  of  $\mathbb{R}^d$

$$\int_B \Pi(\mathrm{d}\mathbf{x}) \mathbf{P}(\mathbf{x}, A) = \int_A \Pi(\mathrm{d}\mathbf{x}) \mathbf{P}(\mathbf{x}, B).$$

**Proposition 4.** For any  $\gamma \geq 0$  and  $T \geq h > 0$ , the sequence  $(\mathbf{X}_i)_{i \geq 0}$  in [Algorithm 2](#) defines a Markov chain characterized by a kernel  $\mathbf{P}$  reversible with respect to  $\Pi$ .

A proof is derived in [Appendix B.2](#). The claim is known for HMC; see [3, Remark 13]. For  $\gamma > 0$ , the result follows from remarking that the acceptance ratio  $\exp\{-\Delta\}$  in [Algorithm 2](#) writes as the product of the single step acceptance ratios obtained in [13, Eq 5.13]. Our analysis is more generally built upon a Markov kernel on the space of trajectories  $\mathbf{z}_{0:L} \triangleq (\mathbf{z}_0, \dots, \mathbf{z}_L)$ . In particular, the kernel is shown to be reversible with respect to the extended measure

$$\mu(d\mathbf{z}_{0:L}) \triangleq \Pi_*(d\mathbf{z}_0) \prod_{i=1}^L \mathbf{Q}_{h,\gamma}(\mathbf{z}_{i-1}, d\mathbf{z}_i). \quad (13)$$

We highlight that reversibility is ensured only when full momentum refreshment are performed at the start of each trajectory. In particular, momentum flips are completely erased in [Algorithm 2](#) whereas these are not in [Algorithm 1](#) if  $\alpha > 0$ . The length of the trajectories  $T > 0$  in MALT is an additional degree of freedom compared to one-step Metropolis corrections aiming for the Langevin diffusion; see [13, 15, 40, 60, 64, 70]. We argue that applying a Metropolis correction to whole Langevin trajectories improves flexibility of tuning and enables a neat study of its Markov kernel. In particular, we present MALT as an extension of HMC for which the tuning of  $T > 0$  can be made robust by choosing a positive friction  $\gamma > 0$ . This property is illustrated in [Section 2](#) and [Section 3](#) by deriving uniform bounds on the ACFs of the Langevin diffusion. It is further supported by [Proposition 5](#), in which we show that MALT is ergodic in total variation for any  $T \geq h > 0$  if a positive friction  $\gamma > 0$  is chosen. The total variation between two measures  $\nu, \nu'$  on  $\mathbb{R}^d$  is noted  $\|\nu - \nu'\|_{\text{TV}} \triangleq \sup\{|\nu(A) - \nu'(A)|, A \text{ Borel set of } \mathbb{R}^d\}$ .

**Proposition 5.** Let  $\mathbf{P}$  be the Markov kernel of the chain  $(\mathbf{X}_i)_{i \geq 0}$  in [Algorithm 2](#), and suppose that  $\gamma > 0$ . Then for any  $T \geq h > 0$  and for  $\Pi$ -almost every  $\mathbf{x} \in \mathbb{R}^d$  we have

$$\lim_{n \rightarrow \infty} \|\delta_{\mathbf{x}} \mathbf{P}^n - \Pi\|_{\text{TV}} = 0.$$

A proof is derived in [Appendix B.3](#). For any  $\gamma > 0$ , the measure  $\mu$  defined in (13) admits a positive density with respect to Lebesgue's measure, ensuring  $\Pi$ -irreducibility and aperiodicity of the Markov kernel. Beyond their convergence in total variation, ergodic chains satisfy a strong law of large numbers; see [66, Eq 6]. We argue that a positive friction simplifies considerably the study of MALT's ergodicity. Convergence in total variation has been established for HMC in [31, Theorem 2] under [Assumption 1](#) with Lipschitz constant  $M > 0$ , provided that  $T \geq h > 0$  satisfy

$$\left(1 + hM^{1/2}\omega(hM^{1/2})\right)^{\lfloor T/h \rfloor} < 2, \quad \omega(s) = (1 + s/2 + s^2/4). \quad (14)$$

We highlight that a positive choice of friction in [Algorithm 2](#) avoids this restrictive condition. This fact illustrates further MALT's robustness with respect to tuning. We note that ergodicity has also been established for Randomized HMC in [46], as soon as  $T > 0$  is drawn such that  $\mathbb{P}(\lfloor T/h \rfloor = 1) > 0$ . The study of geometric ergodicity for [Algorithm 2](#) is beyond our scope.

## 5. Optimal scaling

In this section, we consider the problem of tuning the time step  $h > 0$  in MALT for any choice of friction  $\gamma \geq 0$  and integration time  $T > 0$ . Our study connects to several results known as *optimal scaling*; see [68] and [65] for initial results on RWM and MALA and [5] for HMC. One goal of these works is to derive scaling limits of Metropolis adjusted algorithms as the dimension  $d$  goes to infinity. The results obtained rely on assuming that the target distribution has a product

form; i.e. that the components are IID. Although simplistic, this framework allows for a neat study of the accept-reject mechanism for high-dimensional targets. This study provides simple tuning guidelines of the time step to obtain a non trivial acceptance rate. This result is convenient for assessing the number of gradient evaluations to reach a certain integration time, as a scaling of the dimension. We consider here the following assumption:

**Assumption 3.** *The potential satisfies  $\Phi(\mathbf{x}) = \sum_{i=1}^d \phi(\mathbf{x}(i))$  for some  $\phi \in \mathcal{C}^4(\mathbb{R})$ , such that the derivatives  $\phi^{(k)}$  for  $k = 2, 3, 4$  are uniformly bounded and  $\int_{\mathbb{R}} x^8 \exp(-\phi(x)) dx < \infty$ .*

We highlight that the smoothness and integrability conditions above are similar, although slightly weaker than to the ones suggested in [5, Proposition 5.5] for HMC. Under [Assumption 3](#), the asymptotic dynamics of MALT can be described in terms of independent components of the Langevin diffusion defined in (2). Throughout this section, we note  $(X_t, V_t) \in \mathbb{R}^2$  for the solution of a single component of (2) initiated at stationarity:  $(X_0, V_0) \sim e^{-\phi} \otimes \mathcal{N}(0, 1)$ . The  $d$ -dimensional MALT chain will have target potential satisfying [Assumption 3](#) with marginal potential  $\phi$  (independent of the dimension) and increasing dimension  $d$ . The product form of the target together with the proposal density enforces a product structure also on the proposal. Put differently, the (position and velocity) marginals of the MALT trajectory are independent and identically distributed as MALT trajectories of a single particle MALT chain targeting  $e^{-\phi}$ .

We note  $\mu_{\mathbf{x}}(A) \triangleq \mu(\{\mathbf{x}_{0:L} \in A\})$  the marginal measure of  $\mathbf{x}_{0:L} \triangleq (\mathbf{x}_0, \dots, \mathbf{x}_L)$  characterized by (13). For any fixed choice of physical time  $T$  and friction  $\gamma$  we establish asymptotic normality of the total energy difference.

**Theorem 2.** *Suppose that [Assumption 3](#) holds. Choose  $h = \ell d^{-1/4}$  for some constant  $\ell > 0$ . For any  $T > 0$  and  $\gamma \geq 0$ , let  $L = \lfloor T/h \rfloor$  and  $\mathbf{x}_{0:L} \sim \mu_{\mathbf{x}}$ . Then as  $d \rightarrow \infty$*

$$\Delta(\mathbf{x}_{0:L}) \Rightarrow \mathcal{N}\left(\frac{1}{2}\ell^4 \Sigma, \ell^4 \Sigma\right),$$

such that for  $S(x, v) \triangleq \frac{1}{12}v^3\phi'''(x) + \frac{1}{4}v\phi''(x)\phi'(x)$  we have

$$\Sigma = \mathbb{E} \left[ \left( \int_0^T S(X_t, V_t) dt \right)^2 \right].$$

The proof is given in [Appendix C.1](#). To deliver it we had to extend the optimal scaling framework for Metropolis-Hastings methods recently introduced in Section 3 of [74] to also include algorithms based on trajectories, such as HMC and MALT. This is achieved through the study of the asymptotic properties of the *total energy difference*  $\Delta$ , or equivalently the log Metropolis-Hastings rates  $-\Delta$ , as they are called in [74]. Establishing strong accuracy of the trajectories for the function  $S$  is crucial. Our analysis relies on approximating  $S$  by a sum of Lipschitz functions for which strong accuracy follows by [Proposition 3](#). Next, we use [Theorem 2](#) to deliver guidelines for the tuning of MALT chains. We generalise the results discussed in Sections 3 and 4 of [5] so that they also hold for non-negative friction  $\gamma$ . In the special case of  $\gamma = 0$  we recover the results on HMC.

**Proposition 6.** *Under the assumptions of [Theorem 2](#) the following statements hold:*

(i) *The acceptance rate satisfies, with  $\Psi$  denoting the CDF of a standard Gaussian*

$$\mathbb{E} \left[ 1 \wedge e^{-\Delta(\mathbf{x}_{0:L})} \right] \xrightarrow{d \rightarrow \infty} a(\ell) \triangleq 2\Psi\left(-\frac{\ell^2 \sqrt{\Sigma}}{2}\right).$$

(ii) Let  $f: \mathbb{R} \rightarrow \mathbb{R}$  be locally Lipschitz such that  $|f(x) - f(y)| \leq C(|y| + |x|)|x - y|$  for some  $C > 0$ . Note  $\Upsilon_f \triangleq \mathbb{E}[(f(X_T) - f(X_0))^2]$ . Then

$$\mathbb{E}[(f(\mathbf{X}^{n+1}(1)) - f(\mathbf{X}^n(1)))^2] \xrightarrow{d \rightarrow \infty} \Upsilon_f a(\ell).$$

(iii) Set  $X'_T = X_T \mathbf{1}_{[0, a(\ell)]}(U) + X_0 \mathbf{1}_{(a(\ell), 1]}(U)$  for a uniform random variable  $U$ . Then

$$(\mathbf{X}^n(1), \mathbf{X}^{n+1}(1)) \Rightarrow (X_0, X'_T).$$

Point (i) identifies the asymptotic average acceptance rate under the  $h = \ell d^{-1/4}$  scaling. Note that  $h = \ell d^{-1/4}$  is the only decay rate of the time-step that will lead to a non-trivial distributional limit in [Theorem 2](#) and to a non-trivial limiting average acceptance rate. Any other decay rate will lead to a limiting acceptance rate of either zero or one (to see this formally check proof of [proposition 7](#)). This result for general friction  $\gamma$  is exactly the same as for the HMC case  $\gamma = 0$  studied in Section 3.3 of [\[5\]](#). Apart from extending the results from the HMC case to general friction, point (ii) generalises Section 3.4 of [\[5\]](#) where only the mean function is considered. The result describes the asymptotic lag-one autocorrelation of different functions which can be used as heuristic indicators of the performance of the MALT chains. For the mean function, it corresponds to the asymptotic expected squared jump distance, a performance criteria often used for adaptive tuning of MCMC methods (see [\[62\]](#)). Under [Assumption 3](#) we can guarantee this for functions growing as fast as quadratic but with a stronger moment condition we could extend this further for functions that grow even more rapidly.

Point (iii) is again an extension of the results in HMC case, studied in Section 3.5 of [\[5\]](#). It describes the limiting behaviour of each marginal coordinate of MALT chain (with other coordinates integrated out with respect to the stationary measure). If MALT is initiated in stationarity and only a single coordinate is observed, then its behaviour can be described in terms of a Langevin trajectory and an independent coin. Like in the HMC case (and unlike the RWM and MALA cases) it is important to know that the rest of the coordinates are in stationarity, as a single coordinate is not Markovian with respect to its own filtration, not even asymptotically. [\[5, Section 4\]](#) considers two measures of efficiency for HMC, the number of successful transitions per gradient evaluation and the expected squared jump distance per gradient evaluation. Maximising the first one is equivalent to minimising the computational cost of a single accepted transition, while maximising the second will also prioritise schemes which move further.

Number of successful transitions per gradient evaluation is proportional to the acceptance rate and inversely proportional to the number of steps  $L = \lfloor T/h \rfloor$ . For a fixed  $T$  this corresponds to maximizing  $h \mathbb{E}[1 \wedge e^{-\Delta(\mathbf{x}_0: \mathbf{L})}]$ . Similar reasoning holds for other measures of efficiency. We will consider the following measures of efficiency. For  $f$  as in [Proposition 6\(ii\)](#) we define *expected squared  $f$ -distance* per gradient evaluation as

$$\frac{1}{L} \mathbb{E}[(f(\mathbf{X}^{n+1}(1)) - f(\mathbf{X}^n(1)))^2],$$

If we set  $f$  to be linear we recover the expected squared jump distance per gradient evaluation as in [\[5\]](#). This efficiency measure is proportional to the Dirichlet form of MALT evaluated at  $f$  divided by the length of MALT trajectory. For fixed  $T$  and  $\gamma$  the efficiency measures corresponding to different functions  $f$  asymptotically differ from each other only by a factor that is independent of the time-step. Hence, optimising any of them is asymptotically equivalent. We are now in position to show that the step-size decay rate  $d^{-1/4}$  is optimal according to any of these asymptotic measures.

**Proposition 7.** *Let the [Assumption 3](#) be satisfied and let  $f$  be as in [Proposition 6\(ii\)](#). Let  $T, \ell > 0$  and  $\gamma \geq 0$  be constants. Let  $h \rightarrow 0$  be a sequence of time-steps and  $L = \lfloor T/h \rfloor$ . If either  $d^{1/4}h \rightarrow 0$  or  $d^{1/4}h \rightarrow \infty$ , then*

$$d^{1/4} \times \frac{1}{L} \mathbb{E}[(f(\mathbf{X}^{n+1}(1)) - f(\mathbf{X}^n(1)))^2] \xrightarrow{d \rightarrow \infty} 0.$$

If  $d^{1/4}h \rightarrow \ell$  for some  $\ell \in (0, \infty)$ , then for  $\text{eff}(\ell) \triangleq \ell a(\ell)$  we have

$$d^{1/4} \times \frac{1}{L} \mathbb{E} \left[ (f(\mathbf{X}^{n+1}(1)) - f(\mathbf{X}^n(1)))^2 \right] \xrightarrow{d \rightarrow \infty} \Upsilon_f \times \text{eff}(\ell).$$

There exists a unique optimal  $\ell^*$  maximising  $\text{eff}(\ell^*)$ , for which the corresponding optimal acceptance rate equals

$$a(\ell^*) \approx 0.651.$$

This extends the optimal scaling results in Section 4 of [5] to MALT chains. The guidelines for tuning MALT are the same as for HMC:

Scale the step  $h \propto d^{-1/4}$  and tune it to accept 65.1% of proposals.

It is remarkable that the optimal choice of  $\ell$  does not depend on the function  $f$  considered, nor the distribution  $\Pi$ . The same is however, not true for the choices of  $T$  and  $\gamma$ . Using Proposition 7 we can deduce that for an appropriate constant  $C \approx 0.619$  we have  $\text{eff}(\ell^*) = C\Sigma^{-1/4}$ . This implies that the smaller the  $\Sigma$  the larger time-steps optimised sampler takes. However, the constants  $\Upsilon_f$  also depend on  $T$  and  $\gamma$  and as a consequence the choice of  $T$  and  $\gamma$  such that the corresponding  $\ell^*(T, \gamma)$  maximises an efficiency measure depends greatly on the choice of that efficiency measure (in terms of  $f$ ). The findings are not consistent (and are even contradictory) across a simple selection of functions  $f$  even in the case of the standard Gaussian potential.

For a standard Gaussian marginal potential  $\phi(x) = \frac{x^2}{2}$  we have  $\phi'(x) = x$ ,  $\phi''(x) = 1$  and  $\phi''' = 0$ . The identity  $d(X_t^2) = 2X_t dX_t = 2X_t V_t$ , the stationarity of  $(X_t, V_t)$  and Isserlis' theorem imply

$$\begin{aligned} \Sigma_{\gamma, T} &= \frac{1}{16} \mathbb{E} \left[ \left( \int_0^T V_t X_t dt \right)^2 \right] = \frac{1}{64} \mathbb{E} \left[ (X_T^2 - X_0^2)^2 \right] = \frac{1}{32} (\mathbb{E}[X_0^4] - \mathbb{E}[X_0^2 X_T^2]) \\ &= \frac{1}{16} (\mathbb{E}[X_0^2]^2 - \mathbb{E}[X_0 X_T]^2) = \frac{1}{16} (1 - \rho_\gamma^2(T)), \end{aligned}$$

where  $\rho_\gamma(T) = \text{Corr}(X_0, X_T)$  follows formula (4) with  $\sigma_i = 1$ .

The expression of the optimal (rescaled) time-step  $\ell_\gamma^*(T)$  is proportional to  $(1 - \rho_\gamma^2(T))^{-1/4}$ . The map  $T \mapsto \ell_\gamma^*(T)$  fluctuates a lot for small friction especially for high correlated samples: for  $\gamma = 0$  it even diverges for any  $T = k\pi$ ,  $k \in \mathbb{N}$ . At the contrary, the map  $T \mapsto \ell_\gamma^*(T)$  fluctuates less as  $\gamma$  increases, and becomes monotonously decreasing as soon as  $\gamma \geq 2$ . This suggests that the joint tuning of  $\ell$  and  $T$  is more stable when choosing a positive friction.

## 6. Numerical illustrations

In this section, we illustrate how a positive choice of friction in MALT can improve robustness of tuning of the integration time. Integrated Auto-Correlations (IAC) can be quite erratic functions of  $T > 0$  for HMC; see [11]. These can be smoothed when averaged over multiple draws of  $T$  with Randomized HMC. Our study supports the idea that MALT yields an alternative to tackle the lack of robustness of HMC with respect to tuning. We also discuss similarities and discrepancies with the Randomized HMC approach. For HMC, we argue that an optimal integration time  $T > 0$  with respect to the Euclidean square jump distance can yield arbitrary poor mixing for small components. To tackle the problem, we advocate the use of a stronger measure of efficiency: the worst Effective Sample Size (ESS) among the  $d$  components.

Let  $(X_n)_{n \geq 0}$  be a real random sequence such that  $\mathbb{E}[X_n]$  and  $\mathbb{E}[X_n X_{n+k}]$  do not depend on  $n$ . Let  $f$  be a square integrable function. We consider the estimator of  $\mathbb{E}[f(X_0)]$  defined by

$$\hat{f}_N = \frac{1}{N} \sum_{n=1}^N f(X_n).$$

We assume that the following IAC series converges absolutely

$$\text{IAC}_f = 1 + 2 \sum_{n=1}^{\infty} \text{Corr}(f(X_n), f(X_0)).$$

The variance of  $\hat{f}_N$  is equivalent to  $(\text{IAC}_f/N) \times \mathbb{V}(f(X_0))$  as  $N \rightarrow \infty$ . In our framework,  $(X_n)_{n \geq 1}$  are one-dimensional functionals of successive trajectories with integration time  $T > 0$  (or mean integration time  $T$  for RHMC). The unit cost of generating each variable is considered proportional to the number of gradient evaluations, therefore proportional to the integration time. To reduce the variance of  $\hat{f}_N$ , one can either increase  $N$  or increase  $T$  to reduce  $\text{IAC}_f(T)/N$ . Both solutions having linear costs, increasing  $T$  is only profitable if it allows for decreasing  $\text{IAC}_f(T)$  at least linearly. This motivates the optimization of a rescaled ESS per integration time

$$\text{ESS}_f(T) \propto (T \times \text{IAC}_f(T))^{-1}$$

In the sequel, we compare MALT, RHMC and HMC in terms of worst ESS per integration time for various functions. Our investigation is composed by explicit computations and numerical comparisons, first on a Gaussian, second on a unimodal Gaussian mixture, third on a multivariate Student. Heterogeneity of scales is considered in each example.

**Example 1: Gaussian.** Assume that  $\Phi(\mathbf{x}) = \sum_{i=1}^d \mathbf{x}(i)^2 / (2\sigma_i^2)$ , similarly to [Section 2](#). We first study and compare the efficiencies of exact trajectories in MALT, RHMC and HMC, for estimating the mean and variance. The chains built upon these successive trajectories are obtained by letting  $h \rightarrow 0$  in [Algorithm 2](#) for MALT and HMC. For RHMC we consider the sequence of positions evaluated at the jumping times of the continuous time process (5) with full refreshments.

From (3), there exist  $c_{i,\gamma}(T) > 0$  and IID vectors  $(\boldsymbol{\xi}^n)_{n \geq 1} \sim \mathcal{N}_d(\mathbf{0}_d, \mathbf{I}_d)$  such that successive Langevin trajectories are defined as follows, starting from  $\mathbf{X}^0 \sim \Pi$

$$\mathbf{X}^n(i) = \rho_{i,\gamma}(T) \mathbf{X}^{n-1}(i) + c_{i,\gamma}(T) \boldsymbol{\xi}^n(i) \quad (15)$$

The sequence  $(\mathbf{X}^n(i))_{n \geq 0}$  is an autoregressive process with root  $\rho_{i,\gamma}(T)$ . By Isserlis' theorem, any Gaussian vector  $(X_1, X_2) \in \mathbb{R}^2$  is such that  $\text{Corr}(X_1^2, X_2^2) = (\text{Corr}(X_1, X_2))^2$  therefore

$$\begin{aligned} \text{Corr}(\mathbf{X}^n(i), \mathbf{X}^0(i)) &= (\rho_{i,\gamma}(T))^n \\ \text{Corr}((\mathbf{X}^n(i))^2, (\mathbf{X}^0(i))^2) &= (\rho_{i,\gamma}(T))^{2n} \end{aligned} \quad (16)$$

When  $\gamma = 2/\sigma_{\max}$  for MALT, the worst ACFs are achieved for the largest scale  $\sigma_{\max} \triangleq \max_i \sigma_i$ . These ACFs for the mean and variance correspond to  $\rho_{\max}(T)$  and  $\rho_{\max}^2(T)$  where

$$\rho_{\max}(T) \triangleq e^{-T/\sigma_{\max}} (1 + T/\sigma_{\max}).$$

For HMC ( $\gamma = 0$ ), the worst ACFs for the mean and variance are respectively

$$u_{\max}(T) \triangleq \max_{1 \leq i \leq d} \cos(T/\sigma_i), \quad w_{\max}(T) \triangleq \max_{1 \leq i \leq d} \cos^2(T/\sigma_i).$$

The RHMC sequence with full refreshments is defined as follows. Let  $(\tau_n)_{n \geq 1}$  be random integration times, drawn IID from the exponential distribution with rate  $\lambda > 0$ . We note  $T = \mathbb{E}[\tau_1] = \lambda^{-1}$  the average duration of each Hamiltonian trajectory. Starting from  $\mathbf{Y}^0 \sim \Pi$ , the solution writes

$$\mathbf{Y}^n(i) = \cos\left(\frac{\tau_n}{\sigma_i}\right) \mathbf{Y}^{n-1}(i) + \sigma_i \sin\left(\frac{\tau_n}{\sigma_i}\right) \boldsymbol{\xi}^n(i). \quad (17)$$

**Proposition 8.** *The sequence  $(\mathbf{Y}^n(i))_{n \geq 0}$  defined by (17) is not jointly Gaussian. Moreover*

$$\begin{aligned}\text{Corr}(\mathbf{Y}^n(i), \mathbf{Y}^0(i)) &= \mathbb{E}[\cos(\tau_1/\sigma_i)]^n = (r_i(T))^n, & r_i(T) &\triangleq \frac{\sigma_i^2}{\sigma_i^2 + T^2}, \\ \text{Corr}((\mathbf{Y}^n(i))^2, (\mathbf{Y}^0(i))^2) &= \mathbb{E}[\cos^2(\tau_1/\sigma_i)]^n = (s_i(T))^n, & s_i(T) &\triangleq \frac{\sigma_i^2 + 2T^2}{\sigma_i^2 + 4T^2}.\end{aligned}$$

*Proof.* Direct computations are derived for  $\sigma_i = 1$ . Note  $Y_n = \mathbf{Y}^n(i)$  and  $\xi_n = \xi^n(i)$ .

$$\begin{aligned}\text{Corr}(Y_n, Y_0) &= \mathbb{E}[\cos(\tau_1)Y_{n-1}Y_0] = \mathbb{E}[\cos(\tau_1)]\text{Corr}(Y_{n-1}, Y_0) = \mathbb{E}[\cos(\tau_1)]^n \\ a_n &\triangleq \text{Corr}(Y_n^2, Y_0^2) = \text{Corr}((\cos^2(\tau_1)Y_{n-1}^2 + \sin^2(\tau_1)\xi_n^2 + 2\cos(\tau_1)\sin(\tau_1)Y_{n-1}\xi_n), Y_0^2) \\ &= (1/2)(\mathbb{E}[\cos^2(\tau_1)]\mathbb{E}[Y_n^2Y_0^2] + \mathbb{E}[\sin^2(\tau_1)]\mathbb{E}[\xi_n^2Y_0^2] - 1) \\ &= (1/2)(\mathbb{E}[\cos^2(\tau_1)](2a_{n-1} + 1) + \mathbb{E}[\sin^2(\tau_1)] - 1) \\ &= a_{n-1}\mathbb{E}[\cos^2(\tau_1)] = \mathbb{E}[\cos^2(\tau_1)]^n\end{aligned}$$

Computing the moments of the exponential distribution yields  $\mathbb{E}[\cos(\tau_1)] = 1/(1 + \lambda^{-2})$  while

$$\mathbb{E}[\cos^2(\tau_1)] = (1/2)\mathbb{E}[\cos(2\tau_1) + 1] = \frac{1}{2}\left(\frac{1}{1 + 4\lambda^{-2}} + 1\right) = \frac{1 + 2\lambda^{-2}}{1 + 4\lambda^{-2}}$$

In particular  $(r_i(T))^2 \neq s_i(T)$ , therefore  $(\mathbf{Y}^n(i))_{n \geq 0}$  cannot be jointly Gaussian, otherwise Isserlis' theorem would yield a contradiction.  $\square$

**Proposition 8** for RHMC show that the worst ACFs of the mean and variance are respectively

$$r_{\max}(T) \triangleq \frac{1}{1 + (T/\sigma_{\max})^2}, \quad s_{\max}(T) \triangleq \frac{1 + 2(T/\sigma_{\max})^2}{1 + 4(T/\sigma_{\max})^2}.$$

**Proposition 8** also highlights some similarities and discrepancies between RHMC and MALT. In both cases, the worst ACFs are controlled by the largest scale. Yet, we observe that  $r_{\max}$  has a quadratic decay to 0 while  $s_{\max} \rightarrow 1/2$  as  $T \rightarrow \infty$ . This lack of convergence for the square function has been noticed in [38] for uniformly drawn integration times as well. In particular, both  $r_{\max}$  and  $s_{\max}$  decay slower than  $\rho_{\max}$  and  $\rho_{\max}^2$  as  $T \rightarrow \infty$ . This ordering is reversed for small values of  $T$  however. Numerically, we obtain that  $\rho_{\max} < r_{\max}$  for  $T > 5.1$  while  $\rho_{\max}^2 < s_{\max}$  for  $T > 0.8$ . We now consider the problem of optimizing the worst ESS per time over  $d = 50$  components with heterogeneous variances  $\sigma_i^2 = i/d$ . In [Figure 3](#), we compare MALT, RHMC, and HMC for estimating the mean with  $\varrho_f \in \{\rho_{\max}, r_{\max}, u_{\max}\}$ , and the variance with  $\varrho_f \in \{\rho_{\max}^2, s_{\max}, w_{\max}\}$ . We normalize the worst ESS per time as a proportion of the efficiency achieved for an isotropic target with an ideal HMC sampler as  $T = \pi/2$  (independent samples). For  $f(x) = x$  and  $f(x) = x^2$ , [\(16\)](#) and **Proposition 8** show that the  $n^{\text{th}}$  autocorrelations are of the form  $\varrho_f^n$ , the worst ESS writes therefore as

$$\text{ESS}_f(T) = \frac{\pi}{2T} \left( \frac{1 - \varrho_f(T)}{1 + \varrho_f(T)} \right).$$

[Figure 3](#) shows that both MALT and RHMC yield smooth efficiencies with respect to  $T$ . We highlight that none of these efficiencies depend on the number of components whereas the efficiency of HMC becomes more and more erratic as  $d$  increases. This phenomenon is illustrated for  $d = 50$  components, as opposed to the ideal efficiency obtained for an isotropic target (independent of  $d$ ). On  $(\pi/2, 3\pi/2)$ , ideal HMC produces negatively correlated samples yielding super-efficient estimators of the mean, but sub-optimal estimators of the variance. We observe that RHMC achieves a better efficiency than MALT for estimating the mean whereas this ordering is reversed when estimating the variance. **Proposition 8** indicates that the dashed pink lines of RHMC can be interpreted as smoothed versions of the dotted grey lines of ideal HMC, which explains intuitively

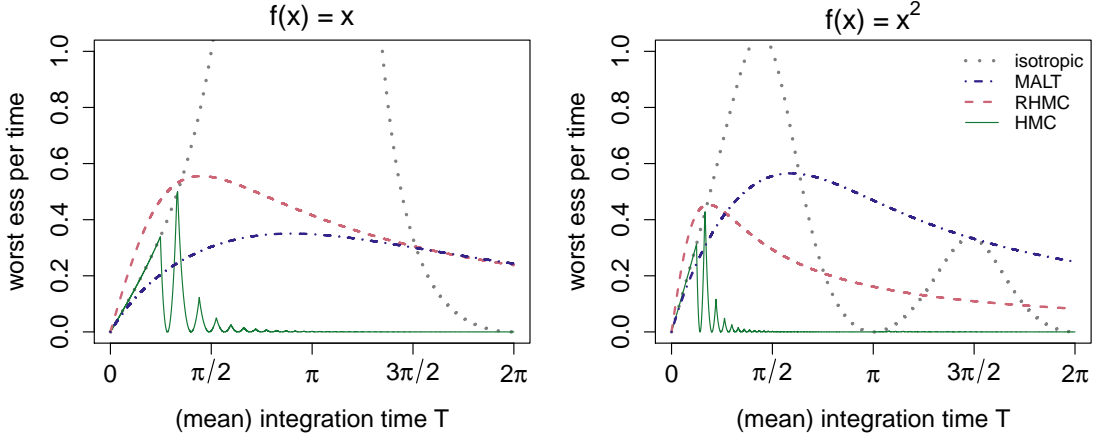


FIG 3. *Gaussian*. Worst ESS per integration time for estimating the mean and variance (resp. left and right). The dotted grey lines correspond to an ideally preconditioned HMC sampler (isotropic target). The dot-dashed blue lines correspond to MALT for  $\gamma = 2/\sigma_{\max}$ . The dashed pink lines correspond to Randomized HMC with full refreshments. The solid green lines correspond to HMC.

the differences observed between  $f(x) = x$  and  $f(x) = x^2$ . This discrepancy is illustrated more generally between odd and even functions in the sequel.

The sensitivity of MALT to the choice of friction is investigated numerically. We observe that any  $\gamma \in [1/\sigma_{\max}, 2/\sigma_{\max}]$  achieves a similar efficiency, roughly optimized for  $\gamma \approx 1.5/\sigma_{\max}$ . Intuitively the worst ESS per time is optimized in a slightly underdamped regime to adapt to the finite length of the trajectories. We focus on the discrete approximation and consider the problem of choosing a (mean) number of steps  $L$  to ensure a relatively good efficiency for every function. The time step  $h = 0.20$  is chosen to obtain acceptance rates slightly above 65% for MALT for a friction  $\gamma = 1.5/\sigma_{\max}$ . The same measure of efficiency is interpreted as ESS per gradient evaluation by setting  $T = Lh$ . In the sequel,  $L$  is chosen to optimize the worst efficiency between  $f(x) = x$  and  $f(x) = x^2$ . Figure 3 indicates that the efficiency of HMC is quite sensitive to small variations of  $T$  whereas these have little impact on the efficiency of MALT and RHMC. This problem is emphasized by the time discretization: in our example, the worst ESS for  $f(x) = x^2$  is negligible for every value of  $L > 1$  with HMC.

In Table 1, worst ESS per gradient evaluation are compared numerically between MALT, RHMC, and HMC for various choices of functions. The choice  $L = 1$  is optimal for HMC, which boils down to MALA. We also illustrate the efficiency of HMC for  $L = 3$ . Monte Carlo estimates are computed on a sample of size  $N = 10^6$ .

TABLE 1  
*Gaussian*. Worst ESS per gradient evaluation for various odd/even functions.

$f(x)$	odd				even			
	$x$	$x^3$	$\text{sgn}(x)$	$\sin(x)$	$x^2$	$x^4$	$e^{- x }$	$\cos(x)$
MALT: $L = 8$	0.25	0.31	0.31	0.27	<b>0.40</b>	<b>0.42</b>	<b>0.43</b>	<b>0.40</b>
RHMC: $L = 5$	<b>0.40</b>	<b>0.43</b>	<b>0.45</b>	<b>0.41</b>	0.29	0.31	0.31	0.29
HMC: $L = 3$	0.19	0.25	0.26	0.21	0.00	0.00	0.00	0.00
MALA ( $L = 1$ )	0.06	0.08	0.09	0.07	0.12	0.12	0.16	0.13

Table 1 highlights that MALT and RHMC are more robust than HMC or MALA in terms of worst ESS. Neither MALT nor RHMC dominates the other for every function, yet MALT achieves slightly higher ESS for even functions while the ordering is reversed for odd functions.

**Example 2: Gaussian mixture.** For  $\mathbf{a} \in \mathbb{R}^d$  and a positive definite matrix  $\Sigma \in \mathbb{R}^{d \times d}$ , we consider the mixture of  $\mathcal{N}_d(\mathbf{a}, \Sigma)$  and  $\mathcal{N}_d(-\mathbf{a}, \Sigma)$  with equal weights. Noting  $\mathbf{b} = \Sigma^{-1}\mathbf{a}$ , we define the potential and its derivatives for  $\mathbf{x} \in \mathbb{R}^d$

$$\begin{aligned}\Phi(\mathbf{x}) &= \frac{1}{2}|\mathbf{x} - \mathbf{a}|_{\Sigma^{-1}}^2 - \log(1 + \exp(-2\mathbf{x}^\top \mathbf{b})) \\ \nabla\Phi(\mathbf{x}) &= \Sigma^{-1}\mathbf{x} - \mathbf{b} + 2\mathbf{b}(1 + \exp(-2\mathbf{x}^\top \mathbf{b}))^{-1} \\ \nabla^2\Phi(\mathbf{x}) &= \Sigma^{-1} - 4\mathbf{b}\mathbf{b}^\top \exp(-2\mathbf{x}^\top \mathbf{b})(1 + \exp(-2\mathbf{x}^\top \mathbf{b}))^{-2}\end{aligned}$$

The target is strongly log-concave if  $|\mathbf{a}|_{\Sigma^{-1}} < 1$ . In that case, the bound  $0 \leq e^u/(1 + e^u)^2 \leq 1/4$  shows that [Assumption 2](#) holds with constants  $m = (1 - |\mathbf{a}|_{\Sigma^{-1}}^2)/\sigma_{\max}(\Sigma)$  and  $M = 1/\sigma_{\min}(\Sigma)$ , where  $\sigma_{\min}(\Sigma)$  and  $\sigma_{\max}(\Sigma)$  denote the smallest and largest eigen values of  $\Sigma$ . Heterogeneity of scales is introduced among  $d = 50$  components such that  $\Sigma = \text{diag}_{1 \leq i \leq d}(\sigma_i^2)$  where  $\sigma_i^2 = i/d$ . The distance between the centers of the mixture is set by  $\mathbf{a}(i) = \sqrt{i}/(2d)$  to obtain  $|\mathbf{a}|_{\Sigma^{-1}} = 1/2$ . In [Figure 4](#) and [Table 2](#), we compare numerically the worst ESS per gradient evaluation for MALT, RHMC and HMC for a time step  $h = 0.20$  on samples of size  $N = 10^6$ . The friction in MALT is chosen empirically as  $\gamma = 1/\sigma_{\max}$ , while the number of steps in [Table 2](#) is chosen in order to optimize the worst efficiency between  $f(x) = x$  and  $f(x) = x^2$ . Similarly to the Gaussian example, the optimal number of steps for HMC is  $L = 1$  (i.e. MALA). We compute the efficiency of HMC for  $L = 3$  as well.

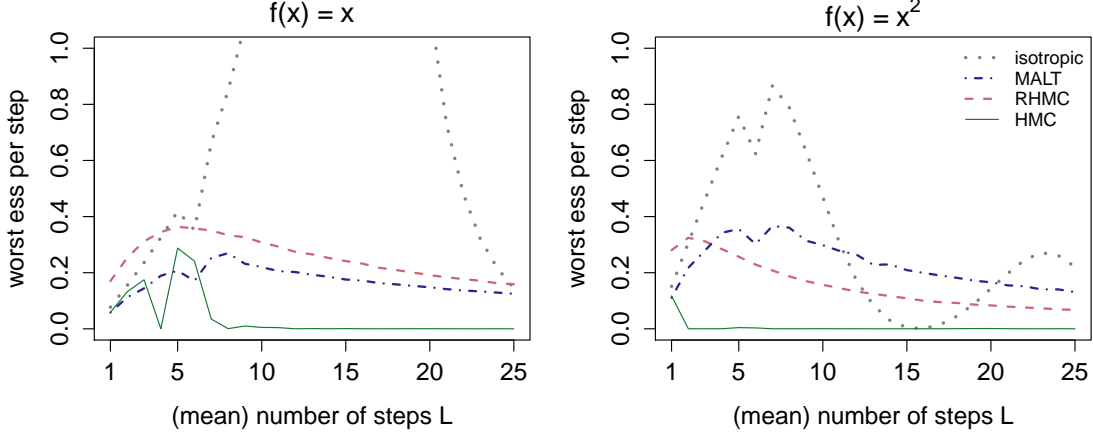


FIG 4. Gaussian mixture. Worst ESS per gradient evaluation for estimating the mean and variance (resp. left and right). The dotted grey lines correspond to an ideally preconditioned HMC sampler (isotropic:  $\Sigma = \mathbf{I}_d$ ). The dot-dashed blue lines correspond to MALT for  $\gamma = 1/\sigma_{\max}$ . The dashed pink lines correspond to Randomized HMC with full refreshments. The solid green lines correspond to HMC.

TABLE 2  
Gaussian mixture. Worst ESS per gradient evaluation for various odd/even functions.

$f(x)$	odd				even			
	$x$	$x^3$	$\text{sgn}(x)$	$\sin(x)$	$x^2$	$x^4$	$e^{- x }$	$\cos(x)$
MALT: $L = 8$	0.27	0.32	0.31	0.27	<b>0.36</b>	<b>0.37</b>	<b>0.38</b>	<b>0.36</b>
RHMC: $L = 4$	<b>0.35</b>	<b>0.38</b>	<b>0.41</b>	<b>0.36</b>	0.29	0.29	0.33	0.29
HMC: $L = 3$	0.17	0.23	0.24	0.19	0.00	0.00	0.00	0.00
MALA ( $L = 1$ )	0.06	0.08	0.09	0.07	0.11	0.13	0.16	0.12

[Figure 4](#) and [Table 2](#) show that MALT and RHMC both achieve higher efficiency than HMC and MALA, on a unimodal Gaussian mixture. Supported by [Section 3](#), this observation confirms that MALT and RHMC have robustness properties on strongly log-concave targets as well. A similar discrepancy between odd and even functions is observed when comparing MALT and RHMC.

**Example 3: Student.** For a positive definite matrix  $\Sigma \in \mathbb{R}^{d \times d}$ , we consider the multivariate Student with  $k \geq 1$  degrees of freedom. The potential and its gradient are defined for  $\mathbf{x} \in \mathbb{R}^d$  by

$$\Phi(\mathbf{x}) = \frac{(k+d)}{2} \log(k + |\mathbf{x}|_{\Sigma^{-1}}^2)$$

$$\nabla \Phi(\mathbf{x}) = \Sigma^{-1} \mathbf{x} (k+d) (k + |\mathbf{x}|_{\Sigma^{-1}}^2)^{-1}$$

The target has  $k-1$  moments. In particular, [Assumption 2](#) does not hold while [Assumption 1](#) does. For any  $k > 2$ , the covariance matrix is proportional to  $\Sigma$ . Heterogeneity of scales is introduced among  $d = 50$  components by setting  $\Sigma = \text{diag}_{1 \leq i \leq d}(\sigma_i^2)$  where  $\sigma_i^2 = i/d$ . In [Figure 5](#) and [Table 3](#), we compare numerically the worst ESS per gradient evaluation for MALT, RHMC and HMC on a Student with  $k = 20$  degrees of freedom for a time step  $h = 0.20$ . The friction in MALT is chosen empirically as  $\gamma = 1/\sigma_{\max}$ , while the number of steps in [Table 3](#) is chosen in order to optimize the worst efficiency between  $f(x) = x$  and  $f(x) = x^2$ . Here the optimal number of steps for HMC is  $L = 3$ . We also compute the efficiency of MALA.

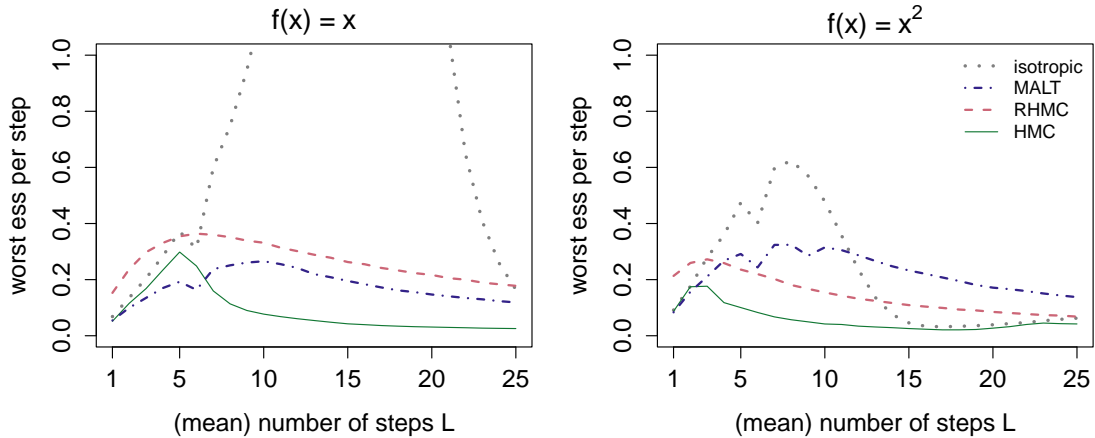


FIG 5. *Student.* Worst ESS per gradient evaluation for estimating the mean and variance (resp. left and right). The dotted grey lines correspond to an ideally preconditioned HMC sampler (isotropic:  $\Sigma = \mathbf{I}_d$ ). The dot-dashed blue lines correspond to MALT for  $\gamma = 1/\sigma_{\max}$ . The dashed pink lines correspond to Randomized HMC with full refreshments. The solid green lines correspond to HMC.

TABLE 3  
*Student.* Worst ESS per gradient evaluation for various odd/even functions.

$f(x)$	odd				even			
	$x$	$x^3$	$\text{sgn}(x)$	$\sin(x)$	$x^2$	$x^4$	$e^{- x }$	$\cos(x)$
MALT: $L = 8$	0.25	0.30	0.29	0.28	<b>0.33</b>	<b>0.37</b>	0.26	<b>0.33</b>
RHMC: $L = 5$	<b>0.35</b>	<b>0.37</b>	<b>0.40</b>	<b>0.37</b>	0.24	0.26	<b>0.28</b>	0.25
HMC: $L = 3$	0.17	0.19	0.24	0.20	0.18	0.19	0.17	0.18
MALA ( $L = 1$ )	0.05	0.07	0.08	0.07	0.09	0.08	0.14	0.11

[Figure 5](#) and [Table 3](#) give an illustration of the robustness of MALT and RHMC on a distribution with polynomial tails. We observe that heterogeneity of scales in the covariance matrix have slightly less impact on the worst ESS of HMC, although its performance still breaks down in higher dimension. When comparing MALT and RHMC: apart from one example, a similar discrepancy between odd and even functions is observed.

## 7. Conclusion

In this work we have investigated several tuning problems for HMC, known to be quite sensitive to the choice of integration time. In particular, we have highlighted that Hamiltonian trajectories of fixed length fail to control the worst ACF under heterogeneity of scales. One main solution suggested in the literature consists on randomizing the length of Hamiltonian trajectories. The Langevin diffusion is presented as an alternative to introduce randomness in Hamiltonian trajectories, through a continuous momentum refreshment of the velocities. Our analysis shows that a positive damping enables control of the worst ACF, ensuring robustness of tuning. We present the Langevin diffusion as a limit of Randomized HMC achieving the fastest mixing rate for strongly log-concave distributions. Our results motivate the construction of a sampler built upon this diffusion, named Metropolis Adjusted Langevin Trajectories (MALT).

We present MALT as a robust extension to HMC for which the tuning question is arguably easier to answer than for GHMC. The efficiency of MALT relies on the choice of three parameters: the integration time  $T > 0$ , the time-step  $h > 0$ , and the damping parameter  $\gamma \geq 0$ . The tuning of these parameters appears to be easier than answering **Q1** in [Section 1](#) for GHMC for several reasons. As highlighted in [Section 2](#), a positive damping enables control of the worst ACF simplifying the choice of integration time  $T$ . Contrary to a positive persistence  $\alpha \in (0, 1)$  in GHMC, momentum flips are erased by full refreshments for any damping in MALT. Finally, an optimal scaling guideline for tuning the time-step is provided for any choice of friction. In particular, our study shows that the  $d^{1/4}$  scaling of [\[5\]](#) is recovered without additional assumption. Tuning the parameters of MALT can be guided by simple rules. Just as for HMC, the time-step may be tuned to achieve approximately a 65% acceptance rate. The choice of the damping parameter can be guided by quantitative mixing rates for the Langevin diffusion. An accurate tuning can rely on a graphical control of the worst ACF. We advocate the use of the worst ESS per gradient evaluation as a measure of efficiency. The choice of integration time for a positive damping appears to be much easier than for HMC since the autocorrelations vanish with  $T \rightarrow \infty$ .

Our contributions motivate the study of adaptive tuning solutions for MALT, together with further comparisons with HMC and its variations, both from a theoretical and numerical viewpoint. These questions will be investigated in future works.

## 8. Acknowledgements

LRD was supported by the EPSRC grant EP/R034710/1. JV was supported by the EPSRC grants EP/R022100/1 and EP/T004134/1. We wish to thank the following people for helpful discussions at various stages of the project: Nicolas Chopin, George Deligiannidis, Samuel Livingstone, Jesús María Sanz-Serna and Giorgos Vasdekis.

## Appendix A: Proofs of the quantitative mixing rates

### A.1. Proof of [Proposition 1](#)

Let  $f \in C_c^\infty$ . By assumption there is a constant  $B > 0$  such that:  $f$  and its derivatives are zero on the complement of the compact set  $S(B) \triangleq \{(\mathbf{x}, \mathbf{v}) \in \mathbb{R}^{2d} : |\mathbf{x}| \vee |\mathbf{v}| \leq B\}$ , and for any  $(\mathbf{x}, \mathbf{v}) \in S(B)$  we have  $|\nabla_{\mathbf{v}} f(\mathbf{x}, \mathbf{v})| \leq B$  and  $\nabla_{\mathbf{v}}^2 f(\mathbf{x}, \mathbf{v}) \preceq B\mathbf{I}_d$ . We note  $\beta = \sqrt{1 - \alpha^2}$  and assume that  $\beta \in (0, 1/2]$ . Let  $\xi \sim \mathcal{N}_d(\mathbf{0}_d, \mathbf{I}_d)$ , and define

$$g_\xi(\beta) \triangleq f\left(\mathbf{x}, \sqrt{1 - \beta^2}\mathbf{v} + \beta\xi\right) - f(\mathbf{x}, \mathbf{v}).$$

We remark that for any  $(\mathbf{x}, \mathbf{v}) \notin S(2B + |\boldsymbol{\xi}|)$  we have  $g_{\boldsymbol{\xi}}(\beta) = 0$  for any  $\beta \in (0, 1/2]$ . Taylor's theorem ensures that there is a function  $\beta \mapsto R_{\boldsymbol{\xi}}(\beta)$  such that

$$g_{\boldsymbol{\xi}}(\beta) = g_{\boldsymbol{\xi}}(0) + \beta g'_{\boldsymbol{\xi}}(0) + (\beta^2/2)g''_{\boldsymbol{\xi}}(0) + (\beta^2/2)R_{\boldsymbol{\xi}}(\beta).$$

We have  $R_{\boldsymbol{\xi}}(\beta) \rightarrow 0$  almost surely as  $\beta \rightarrow 0$  and for any  $\beta \in (0, 1/2]$  there exists a random variable  $\delta_{\boldsymbol{\xi}} \in (0, \beta]$  such that  $R_{\boldsymbol{\xi}}(\beta) = g''_{\boldsymbol{\xi}}(\delta_{\boldsymbol{\xi}}) - g''_{\boldsymbol{\xi}}(0)$ . Direct computations yields

$$\begin{aligned} g'_{\boldsymbol{\xi}}(\beta) &= \left( -\frac{\beta}{(1-\beta^2)^{1/2}} \mathbf{v} + \boldsymbol{\xi} \right)^\top \nabla_{\mathbf{v}} f(\mathbf{x}, \sqrt{1-\beta^2} \mathbf{v} + \beta \boldsymbol{\xi}) \\ g''_{\boldsymbol{\xi}}(\beta) &= -\frac{1}{(1-\beta^2)^{3/2}} \mathbf{v}^\top \nabla_{\mathbf{v}} f(\mathbf{x}, \sqrt{1-\beta^2} \mathbf{v} + \beta \boldsymbol{\xi}) \\ &\quad + \left( -\frac{\beta}{(1-\beta^2)^{1/2}} \mathbf{v} + \boldsymbol{\xi} \right)^\top \nabla_{\mathbf{v}}^2 f(\mathbf{x}, \sqrt{1-\beta^2} \mathbf{v} + \beta \boldsymbol{\xi}) \left( -\frac{\beta}{(1-\beta^2)^{1/2}} \mathbf{v} + \boldsymbol{\xi} \right). \end{aligned}$$

Furthermore for  $\lambda = \frac{2\gamma}{1-\alpha^2}$ , we have

$$\|\mathcal{L}_{\lambda, \alpha}^{\text{RH}} f - \mathcal{L}_{\gamma}^{\text{LD}} f\|_{\infty} = \gamma \|(2/(1-\alpha^2))\mathcal{R}_{\alpha}^{\text{PP}} f - \mathcal{R}^{\text{BM}} f\|_{\infty}.$$

For any deterministic square matrix  $\mathbf{A}$  we have  $\mathbb{E}[\boldsymbol{\xi}^\top \mathbf{A} \boldsymbol{\xi}] = \text{tr}(\mathbf{A})$ . This yields

$$\begin{aligned} (2/(1-\alpha^2))\mathcal{R}_{\alpha}^{\text{PP}} f(\mathbf{x}, \mathbf{v}) &= (2/\beta)\mathbb{E}[g'_{\boldsymbol{\xi}}(0)] + \mathbb{E}[g''_{\boldsymbol{\xi}}(0)] + \mathbb{E}[R_{\boldsymbol{\xi}}(\beta)] \\ &= -\mathbf{v}^\top \nabla_{\mathbf{v}} f(\mathbf{x}, \mathbf{v}) + \mathbb{E}[\boldsymbol{\xi}^\top \nabla_{\mathbf{v}}^2 f(\mathbf{x}, \mathbf{v}) \boldsymbol{\xi}] + \mathbb{E}[R_{\boldsymbol{\xi}}(\beta)] \\ &= \mathcal{R}^{\text{BM}} f(\mathbf{x}, \mathbf{v}) + \mathbb{E}[R_{\boldsymbol{\xi}}(\beta)]. \end{aligned}$$

We see that  $\|\mathcal{L}_{\lambda, \alpha}^{\text{RH}} f - \mathcal{L}_{\gamma}^{\text{LD}} f\|_{\infty} \rightarrow 0$  as soon as  $\mathbb{E}[R_{\boldsymbol{\xi}}(\beta)]$  converges to zero uniformly over  $(\mathbf{x}, \mathbf{v}) \in \mathbb{R}^{2d}$ . This condition is satisfied because  $R_{\boldsymbol{\xi}}(\beta)$  can be uniformly dominated by an integrable random variable, i.e.

$$\begin{aligned} |R_{\boldsymbol{\xi}}(\beta)| &\leq |g''_{\boldsymbol{\xi}}(\delta_{\boldsymbol{\xi}})| + |g''_{\boldsymbol{\xi}}(0)| \\ &\leq 2(8|\mathbf{v}|B + (|\mathbf{v}| + |\boldsymbol{\xi}|)^2 B) \mathbf{1}_{(\mathbf{x}, \mathbf{v}) \in S(2B + |\boldsymbol{\xi}|)} \\ &\leq 2(16B^2 + 8B|\boldsymbol{\xi}| + (2B + 2|\boldsymbol{\xi}|)^2 B). \end{aligned}$$

By Taylor's theorem  $R_{\boldsymbol{\xi}}(\beta) \rightarrow 0$  almost surely as  $\beta \rightarrow 0$ . The claim of the Proposition follows from applying the dominated convergence theorem.

## A.2. Proof of Theorem 1

The proof relies on establishing a contraction rate for a twisted Wasserstein distance between two copies of Randomized HMC. The coupling is synchronized with the same homogeneous Poisson process  $(\mathbf{N}_t)_{t \geq 0}$  with rate  $\lambda$ , and the same independent standard Gaussian refreshments  $(\boldsymbol{\xi}_k)_{k \in \mathbb{N}}$ . Let us denote for any  $t \geq 0$  the two processes  $\mathbf{Z}_t \triangleq (\mathbf{X}_t, \mathbf{V}_t)$  and  $\mathbf{Z}'_t \triangleq (\mathbf{X}'_t, \mathbf{V}'_t)$ , defined through the following system of SDEs:

$$\begin{aligned} d\mathbf{V}_t &= -\nabla \Phi(\mathbf{X}_t) dt + \left( \sqrt{1-\alpha^2} \boldsymbol{\xi}_{\mathbf{N}_t} - (1-\alpha) \mathbf{V}_t \right) d\mathbf{N}_t, & d\mathbf{X}_t &= \mathbf{V}_t dt, \\ d\mathbf{V}'_t &= -\nabla \Phi(\mathbf{X}'_t) dt + \left( \sqrt{1-\alpha^2} \boldsymbol{\xi}_{\mathbf{N}_t} - (1-\alpha) \mathbf{V}'_t \right) d\mathbf{N}_t, & d\mathbf{X}'_t &= \mathbf{V}'_t dt. \end{aligned} \tag{18}$$

Let  $\nu$  and  $\nu'$  be any two probability measures on  $\mathbb{R}^{2d}$ . We initialize the two processes from an arbitrary coupling  $(\mathbf{Z}_0, \mathbf{Z}'_0) \sim \zeta$  such that  $\mathbf{Z}_0 \sim \nu$ ,  $\mathbf{Z}'_0 \sim \nu'$ . Both copies are Randomized HMC

processes, yet we remark that the joint process  $(\mathbf{Z}_t, \mathbf{Z}'_t)$  is also a Markov process. We note  $\mathcal{L}_{\lambda, \alpha}^{\text{Couple}}$  its joint infinitesimal generator, characterized by the system of SDEs (18) for  $j \in \{1, 2\}$ .

The main arguments of this proof rely on a uniform bound on the generator  $\mathcal{L}_{\lambda, \alpha}^{\text{Couple}}$  applied to a twisted distance between the coupled processes, established in [Lemma 1](#). This bound is proven in [Appendix A.3](#). The twist of the metric is determined by three real numbers  $a, b, c$  such that

$$\mathbf{A} \triangleq \begin{pmatrix} a\mathbf{I}_d & b\mathbf{I}_d \\ b\mathbf{I}_d & c\mathbf{I}_d \end{pmatrix} \succ \mathbf{0}_{d \times d}. \quad (19)$$

For any such positive definite matrix  $\mathbf{A}$  and any vector  $\mathbf{z} \in \mathbb{R}^{2d}$ , we note  $|\mathbf{z}|_{\mathbf{A}} \triangleq (\mathbf{z}^\top \mathbf{A} \mathbf{z})^{1/2}$  its  $\mathbf{A}$ -norm. For any  $q \geq 1$ , we define the  $(q, \mathbf{A})$ -Wasserstein metric between any two probability measures  $\nu$  and  $\nu'$  on  $\mathbb{R}^{2d}$  by

$$W_{q, \mathbf{A}}(\nu, \nu') \triangleq \inf\{\mathbb{E}[|\mathbf{X} - \mathbf{X}'|_{\mathbf{A}}^q]^{1/q}, \mathbf{X} \sim \nu, \mathbf{X}' \sim \nu'\}.$$

**Lemma 1.** *The values  $a = 2(M + m)/(1 + \alpha)$ ,  $b = \sqrt{M + m}$  and  $c = 2$  are such that the matrix  $\mathbf{A}$  defined in (19) is positive definite. Moreover almost surely for  $t \geq 0$ , we have*

$$\mathcal{L}_{\lambda, \alpha}^{\text{Couple}} |\mathbf{Z}_t - \mathbf{Z}'_t|_{\mathbf{A}}^2 \leq -2r |\mathbf{Z}_t - \mathbf{Z}'_t|_{\mathbf{A}}^2, \quad r = \frac{(1 + \alpha)m}{2\sqrt{M + m}}. \quad (20)$$

An application of Grönwall's inequality to [Lemma 1](#) yields contraction for the twisted  $\mathbb{L}_2$ -norm. We obtain for any  $t \geq 0$

$$\mathbb{E}[|\mathbf{Z}_t - \mathbf{Z}'_t|_{\mathbf{A}}^2] \leq e^{-2rt} \mathbb{E}[|\mathbf{Z}_0 - \mathbf{Z}'_0|_{\mathbf{A}}^2]. \quad (21)$$

Taking square roots and considering the infimum over the couplings  $(\mathbf{Z}_0, \mathbf{Z}'_0) \sim \zeta$  such that  $\mathbf{Z}_0 \sim \nu$ ,  $\mathbf{Z}'_0 \sim \nu'$  yields

$$W_{2, \mathbf{A}}(\nu \mathbf{P}^t, \nu' \mathbf{P}^t) \leq e^{-rt} W_{2, \mathbf{A}}(\nu, \nu') \quad (22)$$

Establishing the 2-Wasserstein convergence for the Euclidean distance follows from unfolding the twist of the metric. We consider the inequality (21) for a particular coupling  $(\mathbf{Z}_0, \mathbf{Z}'_0) \sim \zeta$  with marginals  $\nu = \nu_{\mathbf{x}} \otimes \mathcal{N}_d(\mathbf{0}_d, \mathbf{I}_d)$  and  $\nu' = \Pi_* = \Pi \otimes \mathcal{N}_d(\mathbf{0}_d, \mathbf{I}_d)$  defined as follows. We start from  $\mathbf{V}_0 = \mathbf{V}'_0 \sim \mathcal{N}_d(\mathbf{0}_d, \mathbf{I}_d)$ , independently drawn from an arbitrary coupling of the positions  $(\mathbf{X}_0, \mathbf{X}'_0) \sim \zeta_{\mathbf{x}}$  such that  $\mathbf{X}_0 \sim \nu_{\mathbf{x}}$  and  $\mathbf{X}'_0 \sim \Pi$ . We remark that for any  $\mathbf{x}, \mathbf{v} \in \mathbb{R}^d$  we have

$$c(a|\mathbf{x}|^2 + 2b\mathbf{x}^\top \mathbf{v} + c|\mathbf{v}|^2) = (ac - b^2)|\mathbf{x}|^2 + |b\mathbf{x} + c\mathbf{v}|^2 \geq (ac - b^2)|\mathbf{x}|^2.$$

Combining this inequality with (21) yields

$$\mathbb{E} \left[ |\mathbf{X}_t - \mathbf{X}'_t|^2 \right] \leq \frac{c}{ac - b^2} \mathbb{E} \left[ |\mathbf{Z}_t - \mathbf{Z}'_t|_{\mathbf{A}}^2 \right] \leq \frac{ce^{-2rt}}{ac - b^2} \mathbb{E} \left[ |\mathbf{Z}_0 - \mathbf{Z}'_0|_{\mathbf{A}}^2 \right].$$

Using that  $\mathbf{V}_0 - \mathbf{V}'_0 = 0$  the last term can be substituted by

$$\mathbb{E} \left[ |\mathbf{Z}_0 - \mathbf{Z}'_0|_{\mathbf{A}}^2 \right] = a \mathbb{E} \left[ |\mathbf{X}_0 - \mathbf{X}'_0|^2 \right].$$

Taking square roots and considering the infimum over the couplings  $(\mathbf{X}_0, \mathbf{X}'_0) \sim \zeta_{\mathbf{x}}$  such that  $\mathbf{X}_0 \sim \nu_{\mathbf{x}}$  and  $\mathbf{X}'_0 \sim \Pi$  yields

$$W_2((\nu \mathbf{P}^t)_{\mathbf{x}}, \Pi) \leq C e^{-rt} W_2(\nu_{\mathbf{x}}, \Pi), \quad C \triangleq \sqrt{\frac{ac}{ac - b^2}}.$$

In particular,  $(\Pi_* \mathbf{P}^t)_{\mathbf{x}} = \Pi$  for any  $t > 0$  because  $\Pi_*$  is invariant. A direct computation of the constant  $C$  yields

$$C = \sqrt{4/(3 - \alpha)} \leq \sqrt{2}. \quad (23)$$

We now extend the convergence to the  $\mathbb{L}_2(\Pi_*)$ -norm using a similar sketch of proof as for [26, Theorem 3]. We introduce  $(\mathbf{P}^t)^*$  and  $(\mathcal{L}_{\lambda,\alpha}^{\text{Couple}})^*$  the respective adjoints of  $\mathbf{P}^t$  and  $\mathcal{L}_{\lambda,\alpha}^{\text{Couple}}$ . These adjoints are characterized by the distribution of Randomized HMC ran backwards in time. In a weak sense, the backward dynamics are similar to the forward dynamics up to a flip of the drift term. In [Lemma 2](#) we present a uniform bound on the adjoint generator, similar to the one obtained in [Lemma 1](#) for the forward process. The twist of the metric differs to take into account the change of sign in the velocities. It is determined by

$$\mathbf{A}' \triangleq \begin{pmatrix} a\mathbf{I}_d & -b\mathbf{I}_d \\ -b\mathbf{I}_d & c\mathbf{I}_d \end{pmatrix} \succ \mathbf{0}_{d \times d}. \quad (24)$$

**Lemma 2.** *The values  $a = 2(M+m)/(1+\alpha)$ ,  $b = \sqrt{M+m}$  and  $c = 2$  are such that the matrix  $\mathbf{A}'$  defined in (24) is positive definite. Moreover almost surely for  $t \geq 0$ , we have*

$$(\mathcal{L}_{\lambda,\alpha}^{\text{Couple}})^* |\mathbf{Z}_t - \mathbf{Z}'_t|^2_{\mathbf{A}'} \leq -2r |\mathbf{Z}_t - \mathbf{Z}'_t|^2_{\mathbf{A}'}, \quad r = \frac{(1+\alpha)m}{2\sqrt{M+m}}. \quad (25)$$

The result of [Lemma 2](#) can be derived following the same arguments used for [26, Theorem 3], its proof is therefore omitted. Similarly to (21) and (22), this result yields a  $(2, \mathbf{A}')$ -Wasserstein contraction for the adjoint  $(\mathbf{P}^t)^*$ . For any  $\nu, \nu'$  two probability measures of  $\mathbb{R}^{2d}$

$$W_{2,\mathbf{A}'}(\nu(\mathbf{P}^t)^*, \nu'(\mathbf{P}^t)^*) \leq e^{-rt} W_{2,\mathbf{A}'}(\nu, \nu'). \quad (26)$$

For  $f : \mathbb{R}^{2d} \rightarrow \mathbb{R}$  we introduce the Lipschitz norm with respect to  $\mathbf{A}$  as

$$\|f\|_{\text{Lip},\mathbf{A}} \triangleq \sup_{\mathbf{z}_1 \neq \mathbf{z}_2} \frac{|f(\mathbf{z}_1) - f(\mathbf{z}_2)|}{|\mathbf{z}_1 - \mathbf{z}_2|_{\mathbf{A}}}.$$

Using the dual formulation of the  $(1, \mathbf{A})$ -Wasserstein distance, for any measures  $\nu, \nu'$  on  $\mathbb{R}^{2d}$

$$W_{2,\mathbf{A}}(\nu, \nu') \geq W_{1,\mathbf{A}}(\nu, \nu') = \sup_{\|f\|_{\text{Lip},\mathbf{A}} \leq 1} \int f d(\nu - \nu').$$

Let  $\mathbf{z}_1, \mathbf{z}_2 \in \mathbb{R}^{2d}$ . We combine this dual formulation with (22) and (26) for  $\nu = \delta_{\mathbf{z}_1}$  and  $\nu' = \delta_{\mathbf{z}_2}$ . In particular for any  $f, g$  such that  $\|f\|_{\text{Lip},\mathbf{A}} \leq 1$  and  $\|g\|_{\text{Lip},\mathbf{A}'} \leq 1$  we obtain

$$\begin{aligned} |\mathbf{P}^t f(\mathbf{z}_1) - \mathbf{P}^t f(\mathbf{z}_2)| &\leq e^{-rt} |\mathbf{z}_1 - \mathbf{z}_2|_{\mathbf{A}} \\ |(\mathbf{P}^t)^* g(\mathbf{z}_1) - (\mathbf{P}^t)^* g(\mathbf{z}_2)| &\leq e^{-rt} |\mathbf{z}_1 - \mathbf{z}_2|_{\mathbf{A}'} \end{aligned} \quad (27)$$

We also note that [26, Equation (4.12)] yields

$$|\mathbf{z}_1 - \mathbf{z}_2|_{\mathbf{A}'} \leq (C')^2 |\mathbf{z}_1 - \mathbf{z}_2|_{\mathbf{A}}, \quad C' \triangleq \left( \frac{ac + b^2 + 2\sqrt{acb^2}}{ac - b^2} \right)^{1/4}. \quad (28)$$

Let  $f \in \mathbb{L}_2^0(\Pi)$ . By definition,  $f$  depends only on the position therefore  $\|f\|_{\text{Lip},\mathbf{A}} = \|f\|_{\text{Lip},\mathbf{A}'}$ . Applying successively (27) with  $g = \mathbf{P}^t f$  and (28) yields

$$\begin{aligned} \|(\mathbf{P}^t)^* \mathbf{P}^t f\|_{\text{Lip},\mathbf{A}'} &\leq e^{-rt} \|\mathbf{P}^t f\|_{\text{Lip},\mathbf{A}'} \leq (C')^2 e^{-rt} \|\mathbf{P}^t f\|_{\text{Lip},\mathbf{A}} \\ &\leq (C')^2 e^{-2rt} \|f\|_{\text{Lip},\mathbf{A}} = (C')^2 e^{-2rt} \|f\|_{\text{Lip},\mathbf{A}'}. \end{aligned} \quad (29)$$

We refer to the proof of [59, Proposition 30] with  $\kappa = 1 - (C')^2 e^{-2rt}$  for any  $t > \log(C')/r$ . We argue that  $(\mathbf{P}^t)^* \mathbf{P}^t$  is a reversible kernel with spectral radius at most  $(C')^2 e^{-2rt}$  on the Lipschitz functions of  $\mathbb{L}_2^0(\Pi)$ . This subset being dense, the spectral radius extends to every function of  $\mathbb{L}_2^0(\Pi)$ . Noting  $\langle \cdot, \cdot \rangle$  for the scalar product in  $\mathbb{L}_2^0(\Pi_*)$ , we obtain that for any  $f \in \mathbb{L}_2^0(\Pi)$

$$\|\mathbf{P}^t f\|^2 = \langle f, (\mathbf{P}^t)^* \mathbf{P}^t f \rangle \leq \|f\| \|(\mathbf{P}^t)^* \mathbf{P}^t f\| \leq (C')^2 e^{-2rt} \|f\|^2. \quad (30)$$

The second claim of the Theorem follows from taking square roots. A direct computation of  $C'$  yields

$$C' = \left( \frac{5 + \alpha + 4\sqrt{1 + \alpha}}{3 - \alpha} \right)^{1/4} \leq (3 + 2\sqrt{2})^{1/4} \leq 1.56. \quad (31)$$

### A.3. Proof of Lemma 1

In the sequel, we note  $\mathbf{H}_t$  the  $d \times d$  matrix defined by

$$\mathbf{H}_t \triangleq \int_0^1 \nabla^2 \Phi(s\mathbf{X}_t + (1-s)\mathbf{X}'_t) ds.$$

Taylor's theorem yields  $\nabla \Phi(\mathbf{X}_t) - \nabla \Phi(\mathbf{X}'_t) = \mathbf{H}_t \tilde{\mathbf{X}}_t$ , and  $m\mathbf{I}_d \preceq \mathbf{H}_t \preceq M\mathbf{I}_d$  by [Assumption 2](#). For the purpose of computations, we make repeated use of the shorthand notations  $\tilde{\mathbf{X}}_t \triangleq \mathbf{X}_t - \mathbf{X}'_t$ , and  $\tilde{\mathbf{V}}_t \triangleq \mathbf{V}_t - \mathbf{V}'_t$  in the following. From [\(18\)](#) we rewrite  $(\tilde{\mathbf{X}}_t, \tilde{\mathbf{V}}_t)_{t \geq 0}$  as a stochastic jump process driven by the following SDE

$$\begin{aligned} d\tilde{\mathbf{V}}_t &= -\mathbf{H}_t \tilde{\mathbf{X}}_t dt - (1-\alpha)\tilde{\mathbf{V}}_t d\mathbf{N}_t \\ d\tilde{\mathbf{X}}_t &= \tilde{\mathbf{V}}_t dt \end{aligned}$$

Applying the product rule to this SDE yields

$$\begin{aligned} d|\tilde{\mathbf{X}}_t|^2 &= 2\tilde{\mathbf{X}}_t^\top \tilde{\mathbf{V}}_t dt \\ d\tilde{\mathbf{X}}_t^\top \tilde{\mathbf{V}}_t &= (-\tilde{\mathbf{X}}_t^\top \mathbf{H}_t \tilde{\mathbf{X}}_t + |\tilde{\mathbf{V}}_t|^2)dt - (1-\alpha)\tilde{\mathbf{X}}_t^\top \tilde{\mathbf{V}}_t d\mathbf{N}_t \\ d|\tilde{\mathbf{V}}_t|^2 &= -2\tilde{\mathbf{X}}_t^\top \mathbf{H}_t \tilde{\mathbf{V}}_t dt - (1-\alpha^2)|\tilde{\mathbf{V}}_t|^2 d\mathbf{N}_t \end{aligned}$$

Applying the generator  $\mathcal{L}_{\lambda, \alpha}^{\text{Couple}}$  on  $|\mathbf{Z}_t - \mathbf{Z}'_t|_{\mathbf{A}}^2 = a|\tilde{\mathbf{X}}_t|^2 + 2b\tilde{\mathbf{X}}_t^\top \tilde{\mathbf{V}}_t + c|\tilde{\mathbf{V}}_t|^2$  yields

$$\begin{aligned} \mathcal{L}_{\lambda, \alpha}^{\text{Couple}} |\mathbf{Z}_t - \mathbf{Z}'_t|_{\mathbf{A}}^2 &= 2a\tilde{\mathbf{X}}_t^\top \tilde{\mathbf{V}}_t - 2b\tilde{\mathbf{X}}_t^\top \mathbf{H}_t \tilde{\mathbf{X}}_t - 2b(1-\alpha)\lambda\tilde{\mathbf{X}}_t^\top \tilde{\mathbf{V}}_t + 2b|\tilde{\mathbf{V}}_t|^2 - 2c\tilde{\mathbf{X}}_t^\top \mathbf{H}_t \tilde{\mathbf{V}}_t \\ &\quad - c(1-\alpha^2)\lambda|\tilde{\mathbf{V}}_t|^2 \\ &= -(\tilde{\mathbf{X}}_t^\top, \tilde{\mathbf{V}}_t^\top) \underbrace{\begin{pmatrix} 2b\mathbf{H}_t & (b(1-\alpha)\lambda - a)\mathbf{I}_d + c\mathbf{H}_t \\ (b(1-\alpha)\lambda - a)\mathbf{I}_d + c\mathbf{H}_t & (c(1-\alpha^2)\lambda - 2b)\mathbf{I}_d \end{pmatrix}}_{\triangleq \mathbf{S}_t} \begin{pmatrix} \tilde{\mathbf{X}}_t \\ \tilde{\mathbf{V}}_t \end{pmatrix}. \end{aligned}$$

We define

$$\mathbf{A} \triangleq \begin{pmatrix} a\mathbf{I}_d & b\mathbf{I}_d \\ b\mathbf{I}_d & c\mathbf{I}_d \end{pmatrix}.$$

The inequality  $\mathcal{L}_{\lambda, \alpha}^{\text{Couple}} |\mathbf{Z}_t - \mathbf{Z}'_t|_{\mathbf{A}}^2 \leq -2r|\mathbf{Z}_t - \mathbf{Z}'_t|_{\mathbf{A}}^2$  is therefore satisfied whenever  $\mathbf{S}_t - 2r\mathbf{A}$  is a positive semi-definite matrix. By diagonalizing each block of this last matrix in the same basis, we obtain necessary and sufficient conditions for ensuring that its  $2d$  eigen values are simultaneously non-negative:  $\mathbf{S}_t - 2r\mathbf{A} \succeq 0$  iff for each eigen value  $\sigma$  of  $\mathbf{H}_t$ , we have

$$-2ra + 2b\sigma \geq 0 \tag{32}$$

$$-2rc + c(1-\alpha^2)\lambda - 2b \geq 0 \tag{33}$$

$$[-2rb + b(1-\alpha)\lambda - a + ch]^2 \leq [-2ra + 2b\sigma][-2rc + c(1-\alpha^2)\lambda - 2b] \tag{34}$$

The inequalities [\(32\)](#), [\(33\)](#) and [\(34\)](#) ensure that the two diagonal elements and the determinant of the  $2 \times 2$  submatrix corresponding to a given eigen value  $\sigma$  (composed by the corresponding diagonal elements of each block), are non-negative. To solve these inequalities, we first choose  $a, b, c$  such that the constraints [\(32\)](#) and [\(34\)](#) are saturated for the less favorable choice of eigen value  $\sigma$ , then we check that [\(33\)](#) holds for the resulting values of  $a, b, c$ .

Without loss of generality we fix  $c = 2$ , and then choose  $a$  such that [\(32\)](#) is an equality when  $\sigma = m$ . Consequently,  $b$  is also fixed since both sides of [\(34\)](#) must be zero when  $\sigma = m$ , we get

$$\begin{cases} 2ra = 2bm \\ 2rb = b(1-\alpha)\lambda - a + 2m \end{cases} \Leftrightarrow \begin{cases} a = 2m/s \\ b = 2r/s \end{cases}, \quad s \triangleq 1 - \frac{r}{m}((1-\alpha)\lambda - 2r). \tag{35}$$

For any real numbers  $x, y, z, w$  such that  $xz > 0$  and  $w/z = y/x = m$  the map  $\sigma \mapsto (x\sigma - y)^2/(z\sigma - w)$  is increasing when  $\sigma > m$ . As a consequence, (34) holds for any  $\sigma \in [m, M]$  iff it holds for  $\sigma = M$ . This condition is satisfied whenever

$$\begin{aligned} [2(M - m)]^2 &\leq [2b(M - m)][2((1 - \alpha^2)\lambda - 2r) - 2b] \\ \Leftrightarrow M - m &\leq b((1 - \alpha^2)\lambda - 2r - b) \\ \Leftrightarrow M + m &\leq a + \alpha(1 - \alpha)\lambda b - b^2 \end{aligned}$$

where the last equivalence follows from substituting  $b((1 - \alpha)\lambda - 2r)$  by  $a - 2m$ , in line with (35). By multiplying both sides by  $s^2$ , we conclude that (34) holds for any  $h \in [m, M]$  iff

$$(M + m)s^2 - (2m + 2\alpha(1 - \alpha)\lambda r)s + 4r^2 \leq 0. \quad (36)$$

Moreover, the set of solutions  $s \in \mathbb{R}$  to (36) is non empty only when

$$16r^2(M + m) - (2m + 2\alpha(1 - \alpha)\lambda r)^2 \leq 0. \quad (37)$$

For the purpose of computations, we parametrize the refreshment angle, intensity, and the exponential convergence rate with respect to  $x, y \geq 0$  such that

$$\alpha(1 - \alpha)\lambda = x\sqrt{M + m}, \quad r = y\left(\frac{m}{\sqrt{M + m}}\right).$$

Plugging this parametrization into (37) simplifies to

$$\begin{aligned} 16y^2m^2 - (2m + 2yxm)^2 &\leq 0 \quad \Leftrightarrow \quad 16y^2 - (2 + 2yx)^2 \leq 0 \\ &\Leftrightarrow (4y - 2 - 2yx)(2x + 2 + 2yx) \leq 0 \\ &\Leftrightarrow y(2 - x) \leq 1. \end{aligned}$$

We remark that the largest exponential convergence rate is obtained by choosing  $y = 1/(2 - x)$  for  $0 \leq x < 2$ . This choice saturates (37), therefore (36) now has a unique positive solution that fixes the choice of  $\delta$ , indeed

$$\begin{aligned} s = \frac{m + \alpha(1 - \alpha)\lambda r}{M + m} &\Leftrightarrow 1 - \frac{r}{m}((1 - \alpha)\lambda - 2r) = 1 - \frac{(M - \alpha(1 - \alpha)\lambda r)}{(M + m)} \\ &\Leftrightarrow yx(M + m) - 2\alpha ym = \alpha M - \alpha yxm \\ &\Leftrightarrow x(M + m) - (2 - x)\alpha M + x\alpha m = 2\alpha m \\ &\Leftrightarrow x(M + m + \alpha M + \alpha m) = 2\alpha m + 2\alpha M \\ &\Leftrightarrow x = 2\alpha/(1 + \alpha). \end{aligned}$$

We remark therefore that  $x \in [0, 1)$  because  $\alpha \in [0, 1)$ . Since the constraint (36) is also saturated, we know (33) holds for any  $x \in [0, 1)$  because  $(1 - \alpha^2)\lambda - 2r - b = (M - m)/b$  is non-negative. Moreover, direct computations of  $s$  and  $r$  in (35) yields explicit values for  $a, b, c$  as follows:

$$a = 2(M + m)/(1 + \alpha), \quad b = \sqrt{M + m}, \quad c = 2. \quad (38)$$

Both  $a$  and  $c$  are positive, therefore  $A$  is positive definite for any  $\alpha \in [0, 1)$  since

$$ac - b^2 = (M + m)(3 - \alpha)/(1 + \alpha) > 0.$$

#### A.4. Proof of Proposition 2

For  $a = \gamma^2$ ,  $b = \gamma$  and  $c = 2$ , consider the matrices

$$\mathbf{A} \triangleq \begin{pmatrix} a\mathbf{I}_d & b\mathbf{I}_d \\ b\mathbf{I}_d & c\mathbf{I}_d \end{pmatrix}, \quad \mathbf{A}' \triangleq \begin{pmatrix} a\mathbf{I}_d & -b\mathbf{I}_d \\ -b\mathbf{I}_d & c\mathbf{I}_d \end{pmatrix}.$$

Note the forward Langevin processes  $(\mathbf{Z}_t)_{t \geq 0}$  and  $(\mathbf{Z}'_t)_{t \geq 0}$ , solutions of (2) coupled with the same Brownian motion. We refer to the proof of [24, Proposition 1] (for  $v = 0$ ), which obtains

$$\frac{d}{dt} |\mathbf{Z}_t - \mathbf{Z}'_t|_{\mathbf{A}}^2 \leq -2r |\mathbf{Z}_t - \mathbf{Z}'_t|_{\mathbf{A}}^2.$$

We remark that a similar inequality can be proven for the backward processes, with respect to the  $\mathbf{A}'$ -norm. Applying Gronwall's inequality then yields both

$$\begin{aligned} W_{2,\mathbf{A}}(\nu \mathbf{P}^t, \nu' \mathbf{P}^t) &\leq e^{-rt} W_{2,\mathbf{A}}(\nu, \nu') \\ W_{2,\mathbf{A}'}(\nu(\mathbf{P}^t)^*, \nu'(\mathbf{P}^t)^*) &\leq e^{-rt} W_{2,\mathbf{A}'}(\nu, \nu') \end{aligned}$$

The claim of the proposition follows from using the exact same arguments as in the proof of Theorem 1 starting from (26); see Appendix A.2. The same constant  $C' = (3 + 2\sqrt{2})^{1/4} \leq 1.56$  is obtained for any choice of friction.

## Appendix B: Proofs of the properties of MALT

### B.1. Proof of Proposition 3

We refer to a generic theorem established in [54, Theorem 1.1]. The claim of the proposition follows from checking that sufficient conditions to invoke this theorem are satisfied. This task boils down to establishing local accuracy for the numerical Langevin trajectories. We introduce a few notations before stating these conditions, established in Lemma 3.

For any  $t \geq 0$ ,  $i \geq 0$  and any function  $f$  such that  $f(\mathbf{Z}_t, \mathbf{z}_i)$  is integrable, we note the conditional expectation starting from  $\mathbf{z}_0$  by  $\mathbb{E}^{\mathbf{z}_0}[f(\mathbf{Z}_t, \mathbf{z}_i)] \triangleq \mathbb{E}[f(\mathbf{Z}_t, \mathbf{z}_i) | \mathbf{Z}_0 = \mathbf{z}_0]$ . Whenever  $f(\mathbf{Z}_t, \mathbf{z}_i)$  is square integrable, we note the  $\mathbb{L}_2$ -norm from  $\mathbf{z}_0$  by  $\|f(\mathbf{Z}_t, \mathbf{z}_i)\|_{\mathbb{L}_2}^{\mathbf{z}_0} \triangleq \mathbb{E}^{\mathbf{z}_0}[f(\mathbf{Z}_t, \mathbf{z}_i)^2]^{1/2}$ .

**Lemma 3.** (Local accuracy) Suppose that Assumption 1 holds. For any fixed  $d \geq 1$ ,  $T > 0$  and  $\gamma \geq 0$ , there exists  $C > 0$  such that for any  $h \in (0, T]$  and  $\mathbf{z}_0 = (\mathbf{x}_0, \mathbf{v}_0) \in \mathbb{R}^{2d}$

$$\begin{aligned} |\mathbb{E}^{\mathbf{z}_0}[\mathbf{Z}_h - \mathbf{z}_1]| &\leq C(1 + |\mathbf{z}_0|^2)^{1/2} h^2 \\ (\mathbb{E}^{\mathbf{z}_0}[|\mathbf{Z}_h - \mathbf{z}_1|^2])^{1/2} &\leq C(1 + |\mathbf{z}_0|^2)^{1/2} h^{3/2} \end{aligned}$$

Combined with [54, Theorem 1.1], this result yields the claim of the proposition. The proof of Lemma 3 is derived hereafter. The density  $\Pi \propto e^{-\Phi}$  is integrable, therefore the potential  $\Phi \in C^1(\mathbb{R}^d)$  has a minimum, which is also a zero of  $\nabla \Phi$ . In other words there exists  $\mathbf{x}^* \in \arg \min \Phi$  such that  $\nabla \Phi(\mathbf{x}^*) = \mathbf{0}_d$ , and we note  $\mathcal{D} \triangleq |\mathbf{x}^*|$ . Assumption 1 ensures that for any  $\mathbf{x} \in \mathbb{R}^d$ , we have  $|\nabla \Phi(\mathbf{x})| \leq M(|\mathbf{x}| + \mathcal{D})$ . We make repeated use of this bound in the sequel.

We set  $d \geq 1$ ,  $T > 0$  and  $\gamma \geq 0$  to be fixed for the rest of the proof. We first show that the constant  $A \triangleq (1 + 2T(d\gamma + M^2\mathcal{D}^2))e^{(2M^2+2)T}$  is such that for any  $\mathbf{z}_0 = (\mathbf{x}_0, \mathbf{v}_0) \in \mathbb{R}^{2d}$  and  $t \in (0, T]$

$$\mathbb{E}^{\mathbf{z}_0}[|\mathbf{Z}_t|^2] \leq A(1 + |\mathbf{z}_0|^2). \quad (39)$$

For  $f(\mathbf{x}, \mathbf{v}) = |\mathbf{x}|^2 + |\mathbf{v}|^2$ , Young's inequality applied to the generator  $\mathcal{L}$  yields

$$\begin{aligned} \mathcal{L}f(\mathbf{x}, \mathbf{v}) &= -2\langle \gamma \mathbf{v} + \nabla \Phi(\mathbf{x}), \mathbf{v} \rangle + 2\langle \mathbf{v}, \mathbf{x} \rangle + 2d\gamma \\ &\leq -2\gamma |\mathbf{v}|^2 + (|\nabla \Phi(\mathbf{x})|^2 + |\mathbf{v}|^2) + (|\mathbf{x}|^2 + |\mathbf{v}|^2) + 2d\gamma \\ &\leq (2M^2 + 2)f(\mathbf{x}, \mathbf{v}) + 2(d\gamma + M^2\mathcal{D}^2) \end{aligned}$$

Dynkin's formula applies to the norm-like function  $f$ ; see [53, Theorem 1.1] for a justification. For  $a = 2M^2 + 2$  and  $b = 2(d\gamma + M^2\mathcal{D}^2)$  this bound yields

$$\mathbb{E}^{\mathbf{z}_0}[f(\mathbf{Z}_t)] = f(\mathbf{z}_0) + \int_0^t \mathbb{E}^{\mathbf{z}_0}[\mathcal{L}f(\mathbf{Z}_s)]ds \leq (bt + f(\mathbf{z}_0)) + a \int_0^t \mathbb{E}^{\mathbf{z}_0}[f(\mathbf{Z}_s)]ds.$$

Grönwall's inequality in its integral form yields  $\mathbb{E}^{\mathbf{z}_0}[f(\mathbf{Z}_t)] \leq (bt + f(\mathbf{z}_0))e^{at}$ , and (39) follows for  $A = (1 + bT)e^{aT}$ .

We apply the inequality (39) in the sequel to bound the local errors between  $\mathbf{Z}_h$  and  $\mathbf{z}_1$ . To this end, we write down their respective explicit solutions. Integrating the Langevin SDE defined in (2) yields the following solution; see [9, Lemma 7.1, eqs 43, 44].

$$\begin{aligned} \mathbf{V}_h &= e^{-\gamma h} \mathbf{v}_0 - h \nabla \Phi(\mathbf{x}_0) - \int_0^h (h-s) \nabla^2 \Phi(\mathbf{X}_s) \mathbf{V}_s ds + \int_0^h (1 - e^{-\gamma(h-s)}) \nabla \Phi(\mathbf{X}_s) ds + \mathbf{G}_h \\ \mathbf{X}_h &= \mathbf{x}_0 + h \mathbf{v}_0 - \int_0^h (h-s) [\nabla \Phi(\mathbf{X}_s) + \gamma \mathbf{V}_s] ds + \sqrt{2\gamma} \int_0^h (h-s) d\mathbf{W}_s \end{aligned}$$

where

$$\mathbf{G}_h \triangleq \sqrt{2\gamma} \int_0^h e^{-\gamma(h-s)} d\mathbf{W}_s.$$

Define  $\boldsymbol{\xi} = \boldsymbol{\xi}_{0,h/2}$  and  $\boldsymbol{\xi}' = \boldsymbol{\xi}_{h/2,h}$  with respect to (9). The OBABO update unfolds as

$$\begin{aligned} \mathbf{v}_1 &= \eta \left( \eta \mathbf{v}_0 + \sqrt{1-\eta^2} \boldsymbol{\xi} - h \nabla \Phi(\mathbf{x}_0) - (h/2)(\nabla \Phi(\mathbf{x}_1) - \nabla \Phi(\mathbf{x}_0)) \right) + \sqrt{1-\eta^2} \boldsymbol{\xi}' \\ \mathbf{x}_1 &= \mathbf{x}_0 + h(\eta \mathbf{v}_0 + \sqrt{1-\eta^2} \boldsymbol{\xi}) - (h^2/2) \nabla \Phi(\mathbf{x}_0) \end{aligned} \quad (40)$$

From (9) we obtain that  $\mathbf{G}_h = \sqrt{1-\eta^2}(\eta \boldsymbol{\xi} + \boldsymbol{\xi}')$ . As a result, the difference between the Langevin solution and the OBABO update yields

$$\begin{aligned} \mathbf{V}_h - \mathbf{v}_1 &= -h(1-\eta) \nabla \Phi(\mathbf{x}_0) + (h/2)(\nabla \Phi(\mathbf{x}_1) - \nabla \Phi(\mathbf{x}_0)) - \int_0^h (h-s) \nabla^2 \Phi(\mathbf{X}_s) \mathbf{V}_s ds \\ &\quad + \int_0^h (1 - e^{-\gamma(h-s)}) \nabla \Phi(\mathbf{X}_s) ds \\ \mathbf{X}_h - \mathbf{x}_1 &= h(1-\eta) \mathbf{v}_0 + \int_0^h (h-s) [\nabla \Phi(\mathbf{x}_0) - \nabla \Phi(\mathbf{X}_s) - \gamma \mathbf{V}_s] ds + \mathbf{G}'_h \end{aligned}$$

where

$$\mathbf{G}'_h \triangleq \sqrt{2\gamma} \int_0^h (h-s) d\mathbf{W}_s - h \sqrt{1-\eta^2} \boldsymbol{\xi}.$$

Young's inequality yields

$$\mathbb{E}[|\mathbf{G}'_h|^2] \leq 2d(2\gamma h^3/3 + \gamma h^3) \leq 4d\gamma h^3.$$

The vector  $\mathbf{G}'_h$  is centered. Applying Jensen's and Young's inequalities yields the decompositions

$$|\mathbb{E}^{\mathbf{z}_0}[\mathbf{Z}_h - \mathbf{z}_1]| \leq \|\mathbf{V}_h - \mathbf{v}_1\|_{\mathbb{L}_2}^{\mathbf{z}_0} + \|\mathbf{X}_h - \mathbf{x}_1 - \mathbf{G}'_h\|_{\mathbb{L}_2}^{\mathbf{z}_0} \quad (41)$$

$$(\mathbb{E}^{\mathbf{z}_0}[|\mathbf{Z}_h - \mathbf{z}_1|^2])^{1/2} \leq \sqrt{2} \left( \|\mathbf{V}_h - \mathbf{v}_1\|_{\mathbb{L}_2}^{\mathbf{z}_0} + \|\mathbf{X}_h - \mathbf{x}_1 - \mathbf{G}'_h\|_{\mathbb{L}_2}^{\mathbf{z}_0} + h^{3/2} \sqrt{4d\gamma} \right) \quad (42)$$

The claim of Lemma 3 follows from bounding the two norms on the right hand sides. For any

$s \in (0, h]$ , we have  $\|\mathbf{Z}_s\|_{\mathbb{L}_2}^{\mathbf{z}_0} \leq \sqrt{A}(1 + |\mathbf{z}_0|^2)^{1/2}$  by (39). Minkowski's inequality yields

$$\begin{aligned} \|\mathbf{V}_h - \mathbf{v}_1\|_{\mathbb{L}_2}^{\mathbf{z}_0} &\leq (\gamma h^2 M/2)(|\mathbf{x}_0| + \mathcal{D}) + (h^2 M/2)(|\mathbf{v}_0| + \|\boldsymbol{\xi}\|_{\mathbb{L}_2} + (h/2)(|\mathbf{x}_0| + \mathcal{D})) \\ &\quad + \int_0^h (h-s)M\|\mathbf{V}_s\|_{\mathbb{L}_2}^{\mathbf{z}_0} ds + \gamma \int_0^h (h-s)M(\|\mathbf{X}_s\|_{\mathbb{L}_2}^{\mathbf{z}_0} + \mathcal{D}) ds \\ &\leq (h^2 M/2) \left[ \left( (\gamma + \sqrt{T}/2)(|\mathbf{x}_0| + \mathcal{D}) + |\mathbf{v}_0| + \sqrt{d} \right) + (1 + \gamma) \sup_{0 \leq s \leq h} \|\mathbf{Z}_s\|_{\mathbb{L}_2}^{\mathbf{z}_0} \right] \\ &\leq (M/2) \left[ 2(\gamma + \sqrt{T}/2)(1 + \mathcal{D}) + 2(1 + \sqrt{d}) + (1 + \gamma)A^{1/2} \right] (1 + |\mathbf{z}_0|^2)^{1/2} h^2 \\ \|\mathbf{X}_h - \mathbf{x}_1 - \mathbf{G}'_h\|_{\mathbb{L}_2}^{\mathbf{z}_0} &\leq (\gamma h^2/2)|\mathbf{v}_0| + \int_0^h (h-s) \left( M|\mathbf{x}_0| + M\|\mathbf{X}_s\|_{\mathbb{L}_2}^{\mathbf{z}_0} + \gamma\|\mathbf{V}_s\|_{\mathbb{L}_2}^{\mathbf{z}_0} \right) ds \\ &\leq (h^2/2) \left[ \gamma|\mathbf{v}_0| + M|\mathbf{x}_0| + (M + \gamma) \sup_{0 \leq s \leq h} \|\mathbf{Z}_s\|_{\mathbb{L}_2}^{\mathbf{z}_0} \right] \\ &\leq (1/2) \left[ (\gamma + M)(1 + A^{1/2}) \right] (1 + |\mathbf{z}_0|^2)^{1/2} h^2 \end{aligned}$$

As a result, for  $B \triangleq 2M(\gamma + \sqrt{T}/2)(1 + \mathcal{D}) + 2M(1 + \sqrt{d}) + (\gamma + \gamma M + M)A^{1/2}$  we obtain

$$\|\mathbf{V}_h - \mathbf{v}_1\|_{\mathbb{L}_2}^{\mathbf{z}_0} + \|\mathbf{X}_h - \mathbf{x}_1 - \mathbf{G}'_h\|_{\mathbb{L}_2}^{\mathbf{z}_0} \leq B(1 + |\mathbf{z}_0|^2)^{1/2} h^2.$$

Plugging this bound into the decompositions (41) and (42), we get for any  $h \in (0, T]$

$$\begin{aligned} |\mathbb{E}^{\mathbf{z}_0}[\mathbf{Z}_h - \mathbf{z}_1]| &\leq B(1 + |\mathbf{z}_0|^2)^{1/2} h^2 \\ (\mathbb{E}^{\mathbf{z}_0}[|\mathbf{Z}_h - \mathbf{z}_1|^2])^{1/2} &\leq (\sqrt{2T}B + \sqrt{8d\gamma})(1 + |\mathbf{z}_0|^2)^{1/2} h^{3/2} \end{aligned}$$

This yields the claim of Lemma 3 for  $C = B \vee (\sqrt{2T}B + \sqrt{8d\gamma})$ .

## B.2. Proof of Proposition 4

We introduce  $\Gamma(B) \triangleq \mathbb{P}(\boldsymbol{\xi} \in B)$ , where  $\boldsymbol{\xi} \sim \mathcal{N}_d(\mathbf{0}_d, \mathbf{I}_d)$ , defined for any Borel set  $B$  of  $\mathbb{R}^d$ . We also define the Gibbs update, corresponding to the conditional distribution of  $\mu$  given  $\mathbf{x}_0$ .

$$\mathbf{G}(\mathbf{z}_{0:L}, d\mathbf{z}'_{0:L}) \triangleq \delta_{\mathbf{x}_0}(d\mathbf{x}'_0) \Gamma(d\mathbf{v}'_0) \prod_{i=1}^L \mathbf{Q}_{h,\gamma}(\mathbf{z}_{i-1}, d\mathbf{z}_i) \quad (43)$$

The Gibbs kernel  $\mathbf{G}$  is reversible with respect to  $\mu$  by construction. Built upon a deterministic proposal of the backward trajectory  $\beta(\mathbf{z}_{0:L}) \triangleq (\varphi(\mathbf{z}_L), \varphi(\mathbf{z}_{L-1}), \dots, \varphi(\mathbf{z}_0))$ , we introduce a Metropolis update defined for any Borel set  $A$  of  $\mathbb{R}^{2d(L+1)}$

$$\mathbf{M}(\mathbf{z}_{0:L}, A) \triangleq (1 \wedge e^{-\Delta(\mathbf{z}_{0:L})}) \delta_{\beta(\mathbf{z}_{0:L})}(A) + (1 - 1 \wedge e^{-\Delta(\mathbf{z}_{0:L})}) \delta_{\mathbf{z}_{0:L}}(A).$$

The Metropolis kernel  $\mathbf{M}$  is also reversible with respect to  $\mu$ . For  $\gamma = 0$ , this follows from (11), (12) and [3, Theorem 3]. For  $\gamma > 0$  the distribution  $\mu$  admits a density with respect to Lebesgue's measure. From (11) and [13, Eq 5.13] we obtain that the corresponding density  $\mu$  is such that

$$-\Delta(\mathbf{z}_{0:L}) = \sum_{i=1}^L \log \left( \frac{\Pi_*(\mathbf{z}_i) q_{h,\gamma}(\varphi(\mathbf{z}_i), \varphi(\mathbf{z}_{i-1}))}{\Pi_*(\mathbf{z}_{i-1}) q_{h,\gamma}(\mathbf{z}_{i-1}, \mathbf{z}_i)} \right) = \log \left( \frac{\mu(\beta(\mathbf{z}_{0:L}))}{\mu(\mathbf{z}_{0:L})} \right). \quad (44)$$

Finally, we consider the cycle  $\mathbf{K} = \mathbf{G}\mathbf{M}\mathbf{G}$  defined on Borel sets  $A$  of  $\mathbb{R}^{2d(L+1)}$

$$\mathbf{K}(\mathbf{z}_{0:L}, A) \triangleq \int \mathbf{G}(\mathbf{z}_{0:L}, d\mathbf{z}'_{0:L}) \mathbf{M}(\mathbf{z}'_{0:L}, d\mathbf{z}''_{0:L}) \mathbf{G}(\mathbf{z}''_{0:L}, A).$$

The palindromic structure of  $\mathbf{K} = \mathbf{GMG}$  ensures reversibility with respect to  $\mu$ . Since the transition  $\mathbf{G}(\mathbf{z}_{0:L}, \cdot)$  only depends on the starting position  $\mathbf{x}_0 \in \mathbb{R}^d$  and  $\Pi$  is the marginal of  $\mu$ , we obtain that  $\mathbf{P}(\mathbf{x}_0, A) \triangleq \mathbf{K}(\mathbf{z}_{0:L}, A \times \mathbb{R}^{d(2L+1)})$  defines marginally a Markov kernel on  $\mathbb{R}^d$ , reversible with respect to  $\Pi$ . In particular, the distribution of  $(\mathbf{X}_n)_{n \geq 0}$  in [Algorithm 2](#) coincides with the distribution of a Markov chain generated by  $\mathbf{P}$ .

### B.3. Proof of [Proposition 5](#)

The claim of the proposition follows from establishing that  $\mathbf{P}$  is both  $\Pi$ -irreducible and aperiodic; see [\[66, Theorem 4\]](#). We prove these two results here. For any  $\gamma > 0$  and any position  $\mathbf{x}_0 \in \mathbb{R}^d$ , the kernel  $\mathbf{G}$  in [\(43\)](#) defines a density with respect to Lebesgue's measure on  $\mathbb{R}^{d(2L+1)}$

$$g(\mathbf{x}_0, (\mathbf{v}_0, \mathbf{z}_{1:L})) \triangleq \psi(\mathbf{v}_0) \prod_{i=1}^L q_{h,\gamma}(\mathbf{z}_{i-1}, \mathbf{z}_i).$$

By definition, this conditional density is positive everywhere, and  $\Delta(\mathbf{x}_{0:L}) < \infty$  for any  $\mathbf{x}_{0:L} \in \mathbb{R}^{d(L+1)}$ . Subsequently, for any Borel set  $A$  of  $\mathbb{R}^d$  such that  $\Pi(A) > 0$ , we have

$$\mathbf{P}(\mathbf{x}_0, A) \geq \int g(\mathbf{x}_0, (\mathbf{v}_0, \mathbf{z}_{1:L}))(1 \wedge e^{-\Delta(\mathbf{x}_{0:L})}) d(\mathbf{v}_0, \mathbf{z}_{1:L}) > 0 \quad (45)$$

Since  $\mathbf{P}(\mathbf{x}_0, A) > 0$  for any  $\mathbf{x}_0 \in \mathbb{R}^d$  and any  $A$  such that  $\Pi(A) > 0$ , we conclude that  $\mathbf{P}$  is  $\Pi$ -irreducible. Suppose now that  $\mathbf{P}$  is periodic. Then there exist two disjoint sets  $A_1, A_2$  with  $\Pi(A_1) > 0$  and  $\Pi(A_2) > 0$  such that  $\mathbf{P}(\mathbf{x}_0, A_2) = 1$  for any  $\mathbf{x}_0 \in A_1$ . However [\(45\)](#) implies that  $\mathbf{P}(\mathbf{x}_0, A_1) > 0$  for any such  $\mathbf{x}_0 \in A_1$ , yielding a contradiction. We conclude that  $\mathbf{P}$  is aperiodic.

## Appendix C: Proofs of optimal scaling

### C.1. Proof of [Theorem 2](#)

Analogously to [\(10\)](#) and [\(11\)](#) denote for  $x, y \in \mathbb{R}$

$$\varepsilon_h(x, y) = \phi(y) - \phi(x) - \frac{y-x}{2} (\phi'(y) + \phi'(x)) - \frac{h^2}{8} (\phi'(y)^2 - \phi'(x)^2) \quad (46)$$

and for  $x_{0:L} \in \mathbb{R}^{L+1}$

$$\Delta_h(x_{0:L}) = \sum_{i=1}^L \varepsilon_h(x_{i-1}, x_i). \quad (47)$$

The product structure of the potentials imposed by [Assumption 3](#) enforces a product structure also on the associated total energy differences in the following sense

$$\Delta(\mathbf{x}_{0:L}) = \sum_{j=1}^d \Delta_{h,j}(\mathbf{x}_{0:L}(j)), \quad (48)$$

where  $\Delta_{h,j}(\mathbf{x}_{0:L}(j))$  are IID copies of a random variable  $\Delta_h(\mathbf{x}_{0:L})$  given by a single particle MALT trajectory  $x_{0:L}$  of the same length and time-step, but one-dimensional potential  $\phi$  (initiated in stationarity).

To prove that total energy difference random variables  $\Delta(\mathbf{x}_{0:L})$  satisfy a form of CLT, we use an extension of the framework introduced in [\[74, Section 3\]](#). More precisely, [Theorem 2](#) is as a

direct application of [74, Theorem 8]. To invoke it, we need to understand asymptotic behaviour of single particle MALT trajectories as the dimension increases. Specifically, we need to verify the following two conditions:

**Proposition 9.** *Let  $T > 0$ ,  $\gamma \geq 0$  and  $\ell > 0$  and take a sequence of time-steps  $h \rightarrow 0$  and  $L = \lfloor T/h \rfloor$ . Assume one-dimesional potential  $\phi$  satisfies [Assumption 3](#) and let  $x_0 \sim \Pi$ . Then*

(i)

$$\frac{1}{h^4} \mathbb{E} [\Delta_h^2(x_{0:L})] \xrightarrow{h \rightarrow 0} \Sigma = \mathbb{E} \left[ \left( \int_0^T S(X_t, V_t) dt \right)^2 \right]$$

(ii)

$$\frac{1}{h^4} \mathbb{E} [\Delta_h^2(x_{0:L}) \mathbb{1}_{\Delta_h > h}] \xrightarrow{h \rightarrow 0} 0.$$

Proof is given in [Appendix C.2](#).

Some care is required to argue that the results of [74, Section 3] do actually carry over from the classical Metropolis-Hastings setting to the MALT trajectory setting considered here. The results of [74, Section 3] concern objects called *log Metropolis-Hastings random variables* that are related to the Kullback-Leibler divergence between the forward  $\Pi(dx)q(x, dy)$  and reverse  $\Pi(dy)q(y, dx)$  transition kernels. The total energy difference random variables defined here are a generalisation, they can also be related to the Kullback-Leibler divergence between the forward distribution  $\mu(z_{0:L})$  and the skew-backward distribution  $\mu(\beta(z_{0:L}))$ .

The proofs of [74, Section 3] depend entirely on the symmetry property of log-MH random variables featured in the following proposition. They do not rely on the exact definition of log-MH random variables, only on their symmetric property. Therefore, the only thing we need to do in order to extend the results to the trajectory setting is to verify this symmetry is still satisfied, the proofs from that point on remain literally the same.

**Proposition 10.** *Let  $\Delta(\mathbf{x}_{0:L})$  be a total energy difference function of MALT and abbreviate  $\mathbf{x}_{L:0} = (\mathbf{x}_L, \dots, \mathbf{x}_0)$ . Then*

(i)  $\Delta(\mathbf{x}_{0:L}) = -\Delta(\mathbf{x}_{L:0})$ .

(ii) *Let  $f : \mathbb{R} \rightarrow \mathbb{R}$  be a measurable functions such that  $f \circ \Delta$  is integrable with respect to  $\mu$ . Then  $\mathbb{E}_\mu[f(-\Delta)e^{-\Delta}] = \mathbb{E}_\mu[f(\Delta)]$ .*

*Proof.* Part (i) of the proposition is immediate from (10) and (11). To establish Part (ii) we split the cases  $\gamma > 0$  and  $\gamma = 0$ . In the positive friction case, by (44) the measure  $\mu$  has a positive density with respect to Lebesgue measure on  $\mathbb{R}^{2d(L+1)}$  such that

$$\mu(\mathbf{z}_{0:L})e^{-\Delta(\mathbf{x}_{0:L})} = \mu(\beta(\mathbf{z}_{0:L})).$$

Combining this equality to the change of variable  $\mathbf{z}'_{0:L} = \beta(\mathbf{z}_{0:L})$  with unit Jacobian, we obtain

$$\begin{aligned} \mathbb{E}_\mu[f(-\Delta(\mathbf{x}_{0:L}))|e^{-\Delta(\mathbf{x}_{0:L})}] &= \int_{\mathbb{R}^{2d(L+1)}} |f(-\Delta(\mathbf{x}_{0:L}))|e^{-\Delta(\mathbf{x}_{0:L})} \mu(\mathbf{z}_{0:L}) d\mathbf{z}_{0:L} \\ &= \int_{\mathbb{R}^{2d(L+1)}} |f(\Delta(\mathbf{x}_{L:0}))| \mu(\beta(\mathbf{z}_{0:L})) d\mathbf{z}_{0:L} \\ &= \int_{\mathbb{R}^{2d(L+1)}} |f(\Delta(\mathbf{x}'_{0:L}))| \mu(\mathbf{z}'_{0:L}) d\mathbf{z}'_{0:L} = \mathbb{E}_\mu[|f(\Delta(\mathbf{x}_{0:L}))|] < \infty. \end{aligned}$$

This ensures that the quantity  $\mathbb{E}[f(-\Delta(\mathbf{x}_{0:L}))e^{-\Delta(\mathbf{x}_{0:L})}]$  is well defined. Repeating the calculation without the absolute values yields the desired identity. Now, when  $\gamma = 0$  the measure  $\mu$  is characterized by the density  $\Pi_*$  on  $\mathbb{R}^{2d}$ . Each trajectory is a deterministic function of its starting point  $\mathbf{z}_{0:L} = (\mathbf{z}_0, \dots, \theta_h^L(\mathbf{z}_0))$ . We apply the change of variable  $\mathbf{z}'_0 = \varphi \circ \theta_h^L(\mathbf{z}_0)$  with unit Jacobian. Note  $\mathbf{z}'_{0:L} = (\mathbf{z}'_0, \dots, \theta_h^L(\mathbf{z}'_0))$  and remark that time-reversibility of the Leapfrog update yields  $\mathbf{z}'_{0:L} = (\varphi \circ \theta_h^L(\mathbf{z}_0), \dots, \varphi(\mathbf{z}_0))$ . Since  $\varphi$  leaves  $\Pi_*$  invariant, we obtain

$$\begin{aligned}\mathbb{E}_\mu[|f(-\Delta(\mathbf{x}_{0:L}))|e^{-\Delta(\mathbf{x}_{0:L})}] &= \int_{\mathbb{R}^{2d}} |f(-\Delta(\mathbf{x}_{0:L}))| e^{-\Delta(\mathbf{x}_{0:L})} \Pi_*(\mathbf{z}_0) d\mathbf{z}_0 \\ &= \int_{\mathbb{R}^{2d}} |f(\Delta(\mathbf{x}_{L:0}))| \Pi_*(\theta_h^L(\mathbf{z}_0)) d\mathbf{z}_0 \\ &= \int_{\mathbb{R}^{2d}} |f(\Delta(\mathbf{x}'_{0:L}))| \Pi_*(\mathbf{z}'_0) d\mathbf{z}'_0 = \mathbb{E}_\mu[|f(\Delta(\mathbf{x}_{0:L}))|] < \infty.\end{aligned}$$

Again, the same calculation without absolute values establishes the desired identity.  $\square$

### C.2. Proof of [Proposition 9](#)

The center of the proof for both (i) and (ii) is showing that

$$\frac{1}{h^2} \Delta_h(x_{0:L}) = \int_0^T S(X_t, V_t) dt + R_h, \quad (49)$$

where the reminder  $R_h$  satisfies  $\mathbb{E}[R_h^2] \rightarrow 0$  as  $h \rightarrow \infty$ . This is done by approximating the leading terms of a Taylor's expansion of  $\Delta_h(x_{0:L})$  with Langevin dynamics over the entire MALT trajectory and controlling the square expectations of the error terms. For this task we need to extend strong accuracy results (see [Proposition 3](#)) beyond Lipschitz functions. This is enabled by the following lemma proven in [Appendix C.3](#).

**Lemma 4.** *Let  $T > 0$ ,  $\gamma \geq 0$  and  $h \in (0, 1]$  and take  $L$  so that  $hL \leq T$ . Assume one-dimesional potential  $\phi$  satisfies [Assumption 3](#) and let  $x_0 \sim \Pi$ . There exists constants  $A_1, A_2, A_3, A_4 > 0$  independent of the choices of  $h$  and  $L$  such that following statements hold:*

(i)

$$\max_{0 \leq i \leq L} \max(\mathbb{E}[x_i^8], \mathbb{E}[v_i^8]) \leq A_1,$$

(ii)

$$\mathbb{E} \left[ (\phi'(x_L)^2 - \phi'(X_{hL})^2)^2 \right] \leq A_2 h,$$

(iii)

$$\sup_{1 \leq i \leq L} \mathbb{E} \left[ \left( \left( \frac{x_i - x_{i-1}}{h} \right)^3 - \hat{V}_{i-1}^3 \right)^2 \right] \leq A_3 h,$$

(iv)

$$\sup_{1 \leq i \leq L} \mathbb{E} \left[ \left( V_{(i-1)h}^3 - v_{i-1}^3 \right)^2 \right] \leq A_4 h^{2/3}.$$

To show (49) we transform the expression in (47) into the desired form. The sum of third terms of (46) terms appearing in (47) can be dealt with using Ito's lemma

$$\int_0^T V_t \phi''(X_t) \phi'(X_t) dt = \int_0^T \frac{\partial}{\partial x} \left( \frac{1}{2} \phi'(X_t)^2 \right) dX_t = \frac{1}{2} (\phi'(X_T)^2 - \phi'(X_0)^2).$$

Since  $x_0 = X_0$ , this implies

$$\begin{aligned} \mathbb{E} & \left[ \left( \sum_{i=1}^L (\phi'(x_i)^2 - \phi'(x_{i-1})^2) - 2 \int_0^T V_t \phi''(X_t) \phi'(X_t) dt \right)^2 \right] \\ &= \mathbb{E} \left[ (\phi'(x_L)^2 - \phi'(x_0)^2 - \phi'(X_T)^2 + \phi'(X_0)^2)^2 \right] \\ &\leq 2\mathbb{E} \left[ (\phi'(x_L)^2 - \phi'(X_{hL})^2)^2 \right] + 2\mathbb{E} \left[ (\phi'(X_T)^2 - \phi'(X_{hL})^2)^2 \right] \xrightarrow{h \rightarrow 0} 0. \end{aligned} \quad (50)$$

The first term vanishes by [Lemma 4](#) (ii). The second vanishes because  $hL \rightarrow T$ , the function  $\phi'$  is  $M$ -Lipschitz (grows at most linearly) and  $X_t$  is a stationary process with continuous paths and finite fourth moments.

To control the rest of (47) we take advantage of [74, Lemma A.2.] and the fundamental theorem of calculus. For each  $1 \leq i \leq L$  we rewrite using  $\int_0^1 (1-2u)du = 0$

$$\begin{aligned} \phi(x_i) - \phi(x_{i-1}) - \frac{1}{2}(x_i - x_{i-1})(\phi'(x_i) + \phi'(x_{i-1})) \\ &= \frac{1}{2}(x_i - x_{i-1})^2 \int_0^1 (1-2u)\phi''(x_{i-1} + u(x_i - x_{i-1}))du \\ &= \frac{1}{2}(x_i - x_{i-1})^3 \int_0^1 (1-2u)u \int_0^1 \phi'''(x_{i-1} + su(x_i - x_{i-1}))dsdu. \end{aligned}$$

Noting that  $\int_0^1 (1-2u)udu = -\frac{1}{6}$ , we can relate this to a term expressed with Langevin dynamics:

$$\begin{aligned} \phi(x_i) - \phi(x_{i-1}) - \frac{1}{2}(x_i - x_{i-1})(\phi'(x_i) + \phi'(x_{i-1})) + \frac{1}{12}h^3 V_{(i-1)h}^3 \phi'''(X_{(i-1)h}) \\ = R_{i,1} + R_{i,2} + R_{i,3}, \end{aligned} \quad (51)$$

where

$$\begin{aligned} R_{i,1} &= \frac{1}{2} ((x_i - x_{i-1})^3 - h^3 v_{i-1}^3) \int_0^1 (1-2u)u \int_0^1 \phi'''(x_{i-1} + su(x_i - x_{i-1}))dsdu \\ R_{i,2} &= \frac{1}{2} h^3 (v_{i-1}^3 - V_{(i-1)h}^3) \int_0^1 (1-2u)u \int_0^1 \phi'''(x_{i-1} + su(x_i - x_{i-1}))dsdu \\ R_{i,3} &= \frac{1}{2} h^3 V_{(i-1)h}^3 \int_0^1 (1-2u)u \int_0^1 (\phi'''(x_{i-1} + su(x_i - x_{i-1})) - \phi'''(X_{(i-1)h})) dsdu. \end{aligned}$$

We will show that of the  $k = 1, 2, 3$  we have

$$\frac{1}{h^6} \sup_{1 \leq i \leq L} \mathbb{E}[R_{i,k}^2] \xrightarrow{h \rightarrow 0} 0. \quad (52)$$

For the first two term  $R_{i,1}$  and  $R_{i,2}$  we use boundedness of  $\phi'''$  together with respectively points (iii) and (iv) of [Lemma 4](#). For the last term  $R_{i,3}$  we first use Cauchy's inequality (recall  $\mathbb{E}[V_{(i-1)h}^{12}]$  is finite since  $V_t$  is a stationary standard Gaussian process) together with Jensen's inequality, Fubini's theorem and the fact that both  $\phi'''$  and  $\phi^{(4)}$  are bounded.

$$\begin{aligned} \mathbb{E} \left[ (\phi'''(x_{i-1} + su(x_i - x_{i-1})) - \phi'''(X_{(i-1)h}))^4 \right] \\ \leq 8\|\phi^{(4)}\|_\infty \|\phi'''\|_\infty^3 (\mathbb{E} [|x_{i-1} - X_{(i-1)h}|] + \mathbb{E} [|x_i - x_{i-1}|]). \end{aligned}$$

Then use [Proposition 3](#) and [Lemma 4](#) (iii) and (iv) to control this bound as follows:

$$\begin{aligned}\mathbb{E}[|x_i - x_{i-1}|] &\leq \mathbb{E}\left[(x_i - x_{i-1})^6\right]^{1/6} \\ &= E\left[\left((x_i - x_{i-1})^3 - h^3 v_{i-1}^3 + h^3 (v_{i-1}^3 - V_{(i-1)h}^3) + h^3 V_{(i-1)h}^3\right)^2\right]^{1/6} \\ &\leq h \left(3\mathbb{E}\left[\left(\left(\frac{x_i - x_{i-1}}{h}\right)^3 - v_{i-1}^3\right)^2\right] + 3\mathbb{E}\left[(v_{i-1}^3 - V_{i-1}^3)^2\right] + 3\mathbb{E}[V_{i-1}^6]\right)^{1/6}.\end{aligned}$$

Finally, paths of  $(X_t, V_t)$  are almost surely continuous and therefore Riemann integrable. Hence almost surely

$$h \sum_{i=1}^L V_{(i-1)h}^3 \phi'''(X_{(i-1)h}) \xrightarrow{h \rightarrow 0} \int_0^T V_t^3 \phi'''(X_t) dt.$$

Since  $hL \rightarrow T$ ,  $\phi'''$  is bounded and  $V_t$  is standard Gaussian for all  $t$ , the convergence also holds in  $L^2$ -sense

$$\mathbb{E}\left[\left(h \sum_{i=1}^L V_{(i-1)h}^3 \phi'''(X_{(i-1)h}) - \int_0^T V_t^3 \phi'''(X_t) dt\right)^2\right] \xrightarrow{h \rightarrow 0} 0.$$

This, together with [\(51\)](#) and [\(52\)](#) implies as  $h \rightarrow 0$

$$\frac{1}{h^4} \mathbb{E}\left[\left(\sum_{i=1}^L \left(\phi(x_i) - \phi(x_{i-1}) - \frac{1}{2}(x_i - x_{i-1})(\phi'(x_i) + \phi'(x_{i-1}))\right) - \int_0^T V_t^3 \phi'''(X_t) dt\right)^2\right] \rightarrow 0,$$

which in turn, together with [\(50\)](#), shows [\(49\)](#).

Having established [\(49\)](#) point (i) follows by integration

$$\frac{1}{h^4} \mathbb{E}[\Delta_h^2(x_{0:L})] = \mathbb{E}\left[\left(\int_0^T S(X_t, V_t) dt\right)^2\right] - 2\mathbb{E}\left[R_h \int_0^T S(X_t, V_t) dt\right] + \mathbb{E}[R_h^2]$$

and the last two terms vanish as  $h \rightarrow 0$  (use Cauchy's inequality for the middle term).

Proof of point [Proposition 9\(ii\)](#) uses similar arguments. Recall that  $v_t$  is a stationary Gaussian and that by [Assumption 3](#) there exists constants  $M, D$  such that  $\|\phi''\|_\infty \leq M$  and  $|\phi'(x)| \leq M(|x| + D)$ . Note that by [Assumption 3](#), Jensen's inequality and Fubini's theorem

$$\begin{aligned}\mathbb{E}\left[\left(\int_0^T S(X_t, V_t) dt\right)^4\right] &\leq \int_0^T \mathbb{E}[S(X_t, V_t)^4] dt \\ &= 4 \int_0^T \mathbb{E}\left[\frac{1}{12^4} V_t^{12} \phi'''(X_t)^4 + \frac{1}{4^4} V_t^4 \phi''(X_t)^4 \phi'(X_t)^4\right] dt \\ &\leq \frac{T}{3^4 4^3} \|\phi'''\|_\infty^4 \mathbb{E}[V_t^{12}] + \frac{T}{4^3} M^4 \mathbb{E}[V_t^8]^{1/2} \mathbb{E}[(M(|X_t| + D))^8]^{1/2} < \infty.\end{aligned}$$

This and [\(49\)](#) show

$$\begin{aligned}\frac{1}{h^4} \mathbb{E}[\Delta_h^2(x_{0:L}) \mathbb{1}_{\Delta_h(x_{0:L}) > h}] &= \mathbb{E}\left[\left(\int_0^T S(X_t, V_t) dt\right)^2 \mathbb{1}_{\Delta_h(x_{0:L}) > h}\right] \\ &+ 2\mathbb{E}\left[R_h \left(\int_0^T S(X_t, V_t) dt\right) \mathbb{1}_{\Delta_h(x_{0:L}) > h}\right] + \mathbb{E}[R_h^2 \mathbb{1}_{\Delta_h(x_{0:L}) > h}].\end{aligned}$$

The last two terms vanish since  $\mathbb{E}[R_h^2] \rightarrow 0$ . The first term vanishes by a combination of Cauchy and Markov inequalities together with part (i)

$$\begin{aligned} \mathbb{E} \left[ \left( \int_0^T S(X_t, V_t) dt \right)^2 \mathbb{1}_{\Delta_h(x_{0:L}) > h} \right] &\leq \mathbb{E} \left[ \left( \int_0^T S(X_t, V_t) dt \right)^4 \right]^{1/2} \mathbb{P} [\Delta_h^2(x_{0:L}) > h^2]^{1/2} \\ &\leq h \mathbb{E} \left[ \left( \int_0^T S(X_t, V_t) dt \right)^4 \right]^{1/2} \left( \frac{1}{h^4} \mathbb{E} [\Delta_h^2(x_{0:L})] \right)^{1/2} \xrightarrow{h \rightarrow 0} 0. \end{aligned}$$

### C.3. Proof of Lemma 4

[Proposition 3](#) gives us uniform control of deviations between trajectories of MALT and Langevin diffusion, which extends trivially to uniform control of deviations between functional values along the trajectories for all Lipschitz functions. Point (i) is the key result that allows us to extend these findings for functions that are not globally Lipschitz but do not grow to rapidly. This is then done for specific functions required for the analysis of MALT in points (ii), (iii) and (iv).

The proof of (i) we use a "discrete Grönwall's inequality". We will show that for  $0 \leq i \leq L-1$  and some constants  $A, B > 0$

$$\max(\mathbb{E}[x_{i+1}^8], \mathbb{E}[v_{i+1}^8], B) \leq (1 + Ah) \times \max(\mathbb{E}[x_i^8], \mathbb{E}[v_i^8], B). \quad (53)$$

Iterating this inequality and using  $h \leq T/L$  and the elementary inequality  $(1+t) \leq e^t$  gives us the following uniform bound, valid for all  $0 \leq i \leq L$ :

$$\begin{aligned} \max(\mathbb{E}[x_i^8], \mathbb{E}[v_i^8], B) &\leq (1 + Ah)^i \times \max(\mathbb{E}[x_0^8], \mathbb{E}[v_0^8], B) \\ &\leq (1 + AT/L)^L \times \max(\mathbb{E}[x_0^8], \mathbb{E}[v_0^8], B) \\ &\leq e^{AT} \times \max(\mathbb{E}[x_0^8], \mathbb{E}[v_0^8], B). \end{aligned}$$

This establishes (i) with  $A_1 = e^{AT} \max(\mathbb{E}[x_0^8], \mathbb{E}[v_0^8], B)$ , which is finite by [Assumption 3](#), as the MALT trajectory is initiated in stationarity.

[Assumption 3](#) implies  $\phi'$  is  $M$ -Lipschitz and grows at most linearly:  $|\phi'(x)| \leq M(|x| + D)$  for appropriate constants  $M, D$ , so that  $(\phi'(x))^8 \leq 8M^8(|x|^8 + D^8)$ .

First, we deal with the bound on the eight moment of the position. We use Multinomial theorem to expand the exact expression of  $x_{i+1}$  in the OBABO update (40). We then separate the zero-order term with respect to  $h$  from the rest and use the Hölder's inequality to bound them. Note that the number of terms is fixed and finite and recall that we are assuming  $h < 1$ . Using at most linear growth of  $\phi'$  we get for appropriate constants  $A', B' > 0$

$$\begin{aligned} \mathbb{E}[x_{i+1}^8] &= \mathbb{E} \left[ \left( x_i + h e^{-\gamma h/2} v_i + h \sqrt{1 - e^{-\gamma h}} \xi_i - \frac{h^2}{2} \phi'(x_i) \right)^8 \right] \\ &\leq \mathbb{E}[x_i^8] + \sum_{\substack{j_1+j_2+j_3+j_4=8 \\ j_1 < 8}} h^{j_2+j_3+2j_4} \binom{8}{j_1, j_2, j_3, j_4} \mathbb{E}[|x_i|^{j_1} |v_i|^{j_2} |\xi_i|^{j_3} |\phi'(x_i)|^{j_4}] \\ &\leq \mathbb{E}[x_i^8] + h \sum_{\substack{j_1+j_2+j_3+j_4=8 \\ j_1 < 8}} \binom{8}{j_1, j_2, j_3, j_4} \mathbb{E}[x_i^8]^{j_1/8} \mathbb{E}[v_i^8]^{j_2/8} \mathbb{E}[\xi_i^8]^{j_3/8} \mathbb{E}[\phi'(x_i)]^{j_4/8} \\ &\leq \mathbb{E}[x_i^8] + A' h \max(\mathbb{E}[x_i^8], \mathbb{E}[v_i^8], B'). \end{aligned} \quad (54)$$

We derive a similar identity for the evolution of the velocities where we use Multinomial theorem to expand the exact expression of  $v_{i+1}$  in the OBABO update (40). Note that since  $\xi_i, \xi_{i+1}$  are standard Gaussian and independent of each other and of  $v_i$ , there exists a standard Gaussian  $\xi'_i$  that is independent of  $v_i$  and satisfies  $e^{-\gamma h/2}\sqrt{1-e^{-\gamma h}}\xi_i + \sqrt{1-e^{-\gamma h}}\xi_{i+1} = \sqrt{1-e^{-2\gamma h}}\xi'_i$ . Also note that the elementary inequality  $1 - e^{-t} \leq t$  implies  $\sqrt{1-e^{-2\gamma h}} < \sqrt{2\gamma h}$ . This time separate the zero-order and half-order terms with respect to  $h$  and bound the rest using Lipschitz properties of  $\phi'$  and (54). The half-order term vanishes since  $\mathbb{E}[\xi'_i] = 0$ . For appropriate constants  $A, B$  we get

$$\begin{aligned}
\mathbb{E}[v_{i+1}^8] &= \mathbb{E}\left[\left(e^{-\gamma h}v_i - h\phi'(x_i) - \frac{h}{2}(\phi'(x_{i+1}) - \phi'(x_i)) + \sqrt{1-e^{-2\gamma h}}\xi'_i\right)^8\right] \\
&\leq \mathbb{E}[v_i^8] + 8e^{-7\gamma h}\sqrt{1-e^{-2\gamma h}}\mathbb{E}[v_i^7]\mathbb{E}[\xi'_i] \\
&+ \sum_{\substack{j_1+j_2+j_3+j_4=8 \\ j_2+j_3+\frac{1}{2}j_4 \geq 1}} h^{j_2+j_3+\frac{1}{2}j_4} \binom{8}{j_1, j_2, j_3, j_4} \mathbb{E}\left[|v_i|^{j_1}|\phi'(x_i)|^{j_2}|\phi'(x_{i+1}) - \phi'(x_i)|^{j_3}|\xi'_i|^{j_4}\right] \\
&\leq \mathbb{E}[v_i^8] + A'h \max(\mathbb{E}[v_i^8], \mathbb{E}[v_i^8], C^8\mathbb{E}[(x_{i+1} - x_i)^8], B') \\
&\leq \mathbb{E}[v_i^8] + Ah \max(\mathbb{E}[v_i^8], \mathbb{E}[v_i^8], B).
\end{aligned} \tag{55}$$

Together, (54) and (55) imply (53) and establish (i).

To see (ii) use (i), Lipschitz properties of  $\phi'$  and Cauchy's inequality to argue

$$\begin{aligned}
\mathbb{E}\left[(\phi'(x_L)^2 - \phi'(X_{hL})^2)^2\right] &= \mathbb{E}\left[(\phi'(x_L) - \phi'(X_{hL}))^2(\phi'(x_L) + \phi'(X_{hL}))^2\right] \\
&\leq \mathbb{E}\left[|\phi'(x_L) - \phi'(X_{hL})|(|\phi'(x_L)| + |\phi'(X_{hL})|)^3\right] \\
&\leq M^4 \times \mathbb{E}\left[|x_L - X_{hL}|(|x_L| + |X_{hL}| + 2D)^3\right] \\
&\leq M^4 \times \mathbb{E}\left[|x_L - X_{hL}|^2\right]^{\frac{1}{2}} \times \mathbb{E}\left[(|x_L| + |X_{hL}| + 2D)^6\right]^{\frac{1}{2}} \leq A_2 h.
\end{aligned}$$

The final bound follows for an appropriate constant by [Proposition 3](#) and (i).

To show (iii) consider the elementary bound for  $a, b \in \mathbb{R}$

$$\begin{aligned}
(a^3 - b^3)^2 &= (a - b)^2(a^2 + ab + b^2)^2 \\
&= (a - b)^2((a - b)^2 + 3(a - b)b + 3b^2)^2 \\
&\leq 3(a - b)^6 + 27(a - b)^4b^2 + 27(a - b)^2b^4.
\end{aligned}$$

Fix  $1 \leq i \leq L$ . Insert  $a = h^{-1}(x_i - x_{i-1})$  and  $b = v_{i-1}$  in the above bound together with Hölder's inequality gives us

$$\begin{aligned}
\mathbb{E}\left[\left(\left(\frac{x_i - x_{i-1}}{h}\right)^3 - v_{i-1}^3\right)^2\right] &\leq 3\mathbb{E}\left[\left(\frac{x_i - x_{i-1}}{h} - v_{i-1}\right)^6\right] \\
&+ 27\mathbb{E}\left[\left(\frac{x_i - x_{i-1}}{h} - v_{i-1}\right)^6\right]^{2/3} \mathbb{E}[v_{i-1}^6]^{1/3} + 27\mathbb{E}\left[\left(\frac{x_i - x_{i-1}}{h} - v_{i-1}\right)^6\right]^{1/3} \mathbb{E}[v_{i-1}^6]^{2/3}.
\end{aligned}$$

Hence, it is sufficient to show that for an appropriate constant  $A'_3 > 0$

$$\mathbb{E}\left[\left(\frac{x_i - x_{i-1}}{h} - v_{i-1}\right)^6\right] \leq A'_3 h^3.$$

Using the linear growth of  $\phi'$  and the inequality  $1 - e^{-t} \leq t$

$$\begin{aligned}\mathbb{E} \left[ \left( \frac{x_i - x_{i-1}}{h} - v_{i-1} \right)^6 \right] &= \mathbb{E} \left[ \left( (e^{-\gamma h/2} - 1)v_{i-1} + \sqrt{1 - e^{-\gamma h}}\xi_0 - \frac{h}{2}\phi'(x_{i-1}) \right)^6 \right] \\ &\leq 6(1 - e^{-\gamma h/2})^6 \mathbb{E} [v_{i-1}^6] + 6(1 - e^{-\gamma h})^3 \mathbb{E} [\xi_0^6] + \frac{3h^6}{32} [\phi'(x_{i-1})^6] \\ &\leq A'_3 h^3.\end{aligned}$$

To prove (iv) consider the following bound for  $a, b \in \mathbb{R}$

$$\begin{aligned}(a^3 - b^3)^2 &= (a - b)^2(a^2 + ab + b^2)^2 \\ &\leq (a - b)^2(|a| + |b|)^4 \leq (a - b)^{2/3}(|a| + |b|)^{16/3}.\end{aligned}$$

Fix  $1 \leq i \leq L$ . Inserting  $a = V_{(i-1)h}$  and  $b = v_{i-1}$  in the above bound together with Hölder's inequality gives us

$$\mathbb{E} \left[ (V_{(i-1)h}^3 - v_{i-1}^3)^2 \right] \leq \mathbb{E} \left[ (V_{(i-1)h} - v_{i-1})^2 \right]^{1/3} \mathbb{E} \left[ (|V_{(i-1)h}| + |v_{i-1}|)^8 \right]^{2/3}.$$

[Proposition 3](#) implies  $\mathbb{E} \left[ (V_{(i-1)h} - v_{i-1})^2 \right] \leq A'_4 h^2$  for an appropriate constant. Point (i) together with the stationarity of process  $V_t$  ensure the right factor is bounded.

#### C.4. Proofs of miscellaneous results

*Proof of Proposition 6.* (i) This is a direct consequence of weak convergence in [Theorem 2](#) applied to the Lipschitz function  $t \rightarrow 1 \wedge e^t$ . We use Proposition 2.4 in [68] to evaluate  $\mathbb{E}[1 \wedge e^Y]$  for a normal random variable  $Y$  on  $\mathbb{R}$ .

(ii) First note that because of the independence of coordinates and the product structure (48)

$$\begin{aligned}\mathbb{E} \left[ (f(\mathbf{X}^{n+1}(1)) - f(\mathbf{X}^n(1)))^2 \right] &= \mathbb{E} \left[ (f(\mathbf{x}_L(1)) - f(\mathbf{x}_0(1)))^2 1 \wedge e^{-\sum_{j=1}^d \Delta_{h,j}} \right] \\ &= \mathbb{E} \left[ (f(\mathbf{x}_L(1)) - f(\mathbf{x}_0(1)))^2 \right] \mathbb{E} \left[ 1 \wedge e^{-\sum_{j=1}^d \Delta_{h,j}} \right] \\ &\quad + \mathbb{E} \left[ (f(\mathbf{x}_L(1)) - f(\mathbf{x}_0(1)))^2 \left( 1 \wedge e^{-\sum_{j=1}^d \Delta_{h,j}} - 1 \wedge e^{-\sum_{j=1}^d \Delta_{h,j}} \right) \right]\end{aligned}$$

We first show that the second term vanishes with increasing  $d$ . Using Cauchy's inequality and the fact that  $t \mapsto 1 \wedge e^t$  is 1-Lipschitz we argue

$$\begin{aligned}\mathbb{E} \left[ (f(\mathbf{x}_L(1)) - f(\mathbf{x}_0(1)))^2 \left( 1 \wedge e^{-\sum_{j=1}^d \Delta_{h,j}} - 1 \wedge e^{-\sum_{j=1}^d \Delta_{h,j}} \right) \right] &\leq \mathbb{E} \left[ (f(\mathbf{x}_L(1)) - f(\mathbf{x}_0(1)))^4 \right]^{1/2} \mathbb{E} [\Delta_{h,j}^2]^{1/2} \\ &\leq C^2 \mathbb{E} \left[ (\mathbf{x}_L(1) - \mathbf{x}_0(1))^8 \right]^{1/4} \mathbb{E} \left[ (|\mathbf{x}_L(1)| + |\mathbf{x}_0(1)|)^8 \right]^{1/4} \mathbb{E} [\Delta_{h,j}^2]^{1/2}.\end{aligned}$$

The first two factors are finite by [Lemma 4](#)(i) and the third converges to zero by [Proposition 9](#).

Hence, as  $\mathbb{E} \left[ 1 \wedge e^{-\sum_{j=1}^d \Delta_{h,j}} \right] \rightarrow a(\ell)$  by (i), we only need to show

$$\mathbb{E} \left[ (f(\mathbf{x}_L(1)) - f(\mathbf{x}_0(1)))^2 \right] \xrightarrow{d \rightarrow \infty} \mathbb{E} \left[ (f(X_T) - f(X_0))^2 \right].$$

Note that for every dimension  $d$  there exists a Langevin diffusion  $\mathbf{Z}_t$  linked to the MALT trajectory  $\mathbf{z}_{0:L}$  via (9). This ensures  $\mathbf{x}_0 = \mathbf{X}_0$  and implies

$$\begin{aligned}\mathbb{E} \left[ (f(\mathbf{x}_L(1)) - f(\mathbf{x}_0(1)))^2 \right] &= \mathbb{E} \left[ (f(\mathbf{x}_L(1)) - f(\mathbf{X}_T(1)) + f(\mathbf{X}_T(1)) - f(\mathbf{X}_0(1)))^2 \right] \\ &= 2 \mathbb{E} [(f(X_T) - f(X_0))(f(\mathbf{x}_L(1)) - f(\mathbf{X}_T(1)))] \\ &\quad + \mathbb{E} \left[ (f(X_T) - f(X_0))^2 \right] + \mathbb{E} \left[ (f(\mathbf{x}_L(1)) - f(\mathbf{X}_T(1)))^2 \right].\end{aligned}$$

We will show that the last term vanishes. By Cauchy's inequality that means, that the mixed term vanishes as well. By another Cauchy inequality and the elementary bound  $|A - B| \leq |A| + |B|$

$$\begin{aligned}\mathbb{E} \left[ (f(\mathbf{x}_L(1)) - f(\mathbf{X}_T(1)))^2 \right] &\leq C^2 \mathbb{E} \left[ (\mathbf{x}_L(1) - \mathbf{X}_T(1))^2 (|\mathbf{x}_L(1)| + |\mathbf{X}_T(1)|)^2 \right] \\ &\leq C^2 \mathbb{E} \left[ |\mathbf{x}_L(1) - \mathbf{X}_T(1)| (|\mathbf{x}_L(1)| + |\mathbf{X}_T(1)|)^3 \right] \\ &\leq C^2 \mathbb{E} \left[ (\mathbf{x}_L(1) - \mathbf{X}_T(1))^2 \right]^{1/2} \mathbb{E} \left[ (|\mathbf{x}_L(1)| + |\mathbf{X}_T(1)|)^6 \right]^{1/2}.\end{aligned}$$

The first factor vanishes by [Proposition 3](#) and the second is bounded by [Lemma 4](#).

(iii) Again we synchronise the Langevin diffusion with the MALT trajectory via (9), hence  $\mathbf{X}^n(1) = \mathbf{x}_0(1) = X_0$ . We will prove that

$$\mathbb{E} [f(\mathbf{X}^{n+1}(1))] \xrightarrow{d \rightarrow \infty} \mathbb{E} [f(X'_T)]$$

for an arbitrary bounded Lipschitz function  $f$ . By Portmanteau theorem this implies the result.

Note that since the function  $t \mapsto 1 \wedge e^t$  is 1-Lipschitz, [Proposition 9](#) guarantees

$$\begin{aligned}\mathbb{P} \left[ U \text{ is between } 1 \wedge e^{-\sum_{j=1}^d \Delta_{h,j}} \text{ and } 1 \wedge e^{-\sum_{j=2}^d \Delta_{h,j}} \right] \\ \leq \mathbb{E} \left[ \left| 1 \wedge e^{-\sum_{j=1}^d \Delta_{h,j}} - 1 \wedge e^{-\sum_{j=2}^d \Delta_{h,j}} \right| \right] \leq \mathbb{E} [|\Delta_h|] \xrightarrow{d \rightarrow \infty} 0,\end{aligned}$$

Since  $f$  is bounded this implies

$$\left| \mathbb{E} \left[ f(\mathbf{x}_L(1)) \mathbb{1}_{U \leq 1 \wedge e^{-\sum_{j=1}^d \Delta_{h,j}}} \right] - \mathbb{E} \left[ f(\mathbf{x}_L(1)) \mathbb{1}_{U \leq 1 \wedge e^{-\sum_{j=2}^d \Delta_{h,j}}} \right] \right| \xrightarrow{d \rightarrow \infty} 0$$

and

$$\left| \mathbb{E} \left[ f(\mathbf{x}_0(1)) \mathbb{1}_{U > 1 \wedge e^{-\sum_{j=1}^d \Delta_{h,j}}} \right] - \mathbb{E} \left[ f(\mathbf{x}_0(1)) \mathbb{1}_{U > 1 \wedge e^{-\sum_{j=2}^d \Delta_{h,j}}} \right] \right| \xrightarrow{d \rightarrow \infty} 0.$$

Finally, this gives us

$$\begin{aligned}\lim_{d \rightarrow \infty} \mathbb{E} [f(\mathbf{X}^{n+1}(1))] \\ &= \lim_{d \rightarrow \infty} \mathbb{E} \left[ f(\mathbf{x}_L(1)) \mathbb{1}_{U \leq 1 \wedge e^{-\sum_{j=1}^d \Delta_{h,j}}} \right] + \lim_{d \rightarrow \infty} \mathbb{E} \left[ f(\mathbf{x}_0(1)) \mathbb{1}_{U > 1 \wedge e^{-\sum_{j=1}^d \Delta_{h,j}}} \right] \\ &= \lim_{d \rightarrow \infty} \mathbb{E} \left[ f(\mathbf{x}_L(1)) \mathbb{1}_{U \leq 1 \wedge e^{-\sum_{j=2}^d \Delta_{h,j}}} \right] + \lim_{d \rightarrow \infty} \mathbb{E} \left[ f(\mathbf{x}_0(1)) \mathbb{1}_{U > 1 \wedge e^{-\sum_{j=2}^d \Delta_{h,j}}} \right] \\ &= \lim_{d \rightarrow \infty} \mathbb{E} [f(\mathbf{x}_L(1))] \mathbb{P} \left[ U \leq 1 \wedge e^{-\sum_{j=2}^d \Delta_{h,j}} \right] + \lim_{d \rightarrow \infty} \mathbb{E} [f(\mathbf{x}_0(1))] \mathbb{P} \left[ U > 1 \wedge e^{-\sum_{j=2}^d \Delta_{h,j}} \right] \\ &= \mathbb{E} [f(X_T)] a(\ell) + \mathbb{E} [f(X_0)] (1 - a(\ell)) = \mathbb{E} [f(X'_T)].\end{aligned}$$

The first equality holds by design of MALT accept-reject mechanism, the third by independence of the coordinates of MALT trajectory and the fourth by [Proposition 3](#) and point (i).  $\square$

*Proof of Proposition 7.* Mimicking the argument of [75, Theorem 3] we will first establish that

$$\begin{aligned}\mathbb{E} \left[ (f(\mathbf{X}^{n+1}(1)) - f(\mathbf{X}^n(1)))^2 \right] &= \mathbb{E} \left[ (f(\mathbf{x}_L(1)) - f(\mathbf{x}_0(1)))^2 1 \wedge e^{-\sum_{j=1}^d \Delta_{h,j}} \right] \\ &\leq 2\mathbb{E} \left[ (f(\mathbf{x}_L(1)) - f(\mathbf{x}_0(1)))^2 \right] \mathbb{E} \left[ 1 \wedge e^{-\sum_{j=2}^d \Delta_{h,j}} \right].\end{aligned}\quad (56)$$

The statement without the factor of two is apparent if  $\Delta_{h,1}$  is positive. If it is negative we use [Proposition 10](#) and it is crucial that the expression  $(f(\mathbf{x}_L(1)) - f(\mathbf{x}_0(1))^2$  is symmetric with respect to the start  $\mathbf{x}_0(1)$  and end  $\mathbf{x}_L(1)$  point of the trajectory:

$$\begin{aligned}\mathbb{E} \left[ (f(\mathbf{x}_L(1)) - f(\mathbf{x}_0(1)))^2 1 \wedge e^{-\sum_{j=1}^d \Delta_{h,j}} \mathbb{1}_{(-\infty,0]}(\Delta_{h,1}) \right] \\ &\leq \mathbb{E} \left[ (f(\mathbf{x}_L(1)) - f(\mathbf{x}_0(1)))^2 1 \wedge e^{-\sum_{j=2}^d \Delta_{h,j}} e^{-\Delta_{h,1}} \mathbb{1}_{[0,\infty)}(-\Delta_{h,1}) \right] \\ &= \mathbb{E} \left[ (f(\mathbf{x}_0(1)) - f(\mathbf{x}_L(1)))^2 1 \wedge e^{-\sum_{j=2}^d \Delta_{h,j}} \mathbb{1}_{[0,\infty)}(\Delta_{h,1}) \right] \\ &\leq \mathbb{E} \left[ (f(\mathbf{x}_L(1)) - f(\mathbf{x}_0(1)))^2 1 \wedge e^{-\sum_{j=2}^d \Delta_{h,j}} \right].\end{aligned}$$

As  $h \rightarrow 0$  we also have  $\mathbb{E} \left[ (f(\mathbf{x}_L(1)) - f(\mathbf{x}_0(1)))^2 \right] \rightarrow \Upsilon_f$  like in the proof of [Proposition 6\(ii\)](#). Everything therefore hinges on understanding the asymptotics of  $\mathbb{E} \left[ 1 \wedge e^{-\sum_{j=2}^d \Delta_{h,j}} \right]$  as  $h \rightarrow \infty$ .

Clearly, if  $d^{1/4}h \rightarrow 0$ , then  $d^{1/4}h\mathbb{E} \left[ 1 \wedge e^{-\sum_{j=2}^d \Delta_{h,j}} \right] \rightarrow 0$  as  $d$  increases, since the acceptance rate is bounded by one.

Assume now  $d^{1/4}h \rightarrow \infty$ . Note that [Proposition 9](#) implies (see [74, Theorem 7])

$$\frac{\mathbb{E}[\Delta_h]}{\mathbb{E}[\Delta_h^2]} \xrightarrow{h \rightarrow 0} \frac{1}{2}.$$

We split the probability space with respect to the event  $\mathcal{A}_d = \left\{ \sum_{j=2}^d \Delta_{h,j} \geq \frac{d-1}{2} \mathbb{E}[\Delta_h] \right\}$ . Using the above and [Proposition 9](#) with  $dh^4 \rightarrow \infty$  we argue:

$$\begin{aligned}\limsup_{d \rightarrow \infty} d^{1/4}h\mathbb{E} \left[ 1 \wedge e^{-\sum_{j=2}^d \Delta_{h,j}} \mathbb{1}_{\mathcal{A}_d} \right] &\leq \limsup_{d \rightarrow \infty} d^{1/4}h e^{-\frac{d-1}{2}\mathbb{E}[\Delta_h]} \leq \limsup_{d \rightarrow \infty} d^{1/4}h e^{-\frac{d}{5}\mathbb{E}[\Delta_h^2]} \\ &= \limsup_{d \rightarrow \infty} d^{1/4}h e^{-\frac{dh^4}{5}h^{-4}\mathbb{E}[\Delta_h^2]} \leq \limsup_{d \rightarrow \infty} d^{1/4}h e^{-dh^4\frac{\Sigma}{6}} = 0.\end{aligned}$$

On the complement  $\mathcal{A}_d^c$  we use Chebyshev's inequality in addition

$$\begin{aligned}\limsup_{d \rightarrow \infty} d^{1/4}h\mathbb{E} \left[ 1 \wedge e^{-\sum_{j=2}^d \Delta_{h,j}} \mathbb{1}_{\mathcal{A}_d^c} \right] &\leq \limsup_{d \rightarrow \infty} d^{1/4}h\mathbb{P}[\mathcal{A}_d^c] \\ &= \limsup_{d \rightarrow \infty} d^{1/4}h \mathbb{P} \left[ \sum_{j=1}^d (\mathbb{E}[\Delta_{h,j}] - \Delta_{h,j}) \geq \frac{d-1}{2} \mathbb{E}[\Delta_h] \right] \leq \limsup_{d \rightarrow \infty} d^{1/4}h \frac{4d\text{Var}[\Delta_h]}{d^2\mathbb{E}[\Delta_h]^2} \\ &\leq \limsup_{d \rightarrow \infty} d^{1/4}h \frac{17}{d\mathbb{E}[\Delta_h^2]} \leq \limsup_{d \rightarrow \infty} \frac{18}{\Sigma} \frac{1}{d^{3/4}h^3} = 0.\end{aligned}$$

The last two conclusions together with (56) show the sub-optimality of scaling of time-step  $h$  different to  $d^{-1/4}$ . We conclude that  $d^{-1/4}$  scaling is optimal by noting that the claimed non-zero limit is achieved in the case when  $d^{1/4}h \rightarrow \ell$  by [Proposition 6\(ii\)](#).

Finally, to optimise over the choice of  $\ell$  note that the function  $\ell \mapsto 2\ell\Psi\left(-\frac{1}{2}\ell^2\sqrt{\Sigma}\right)$  is smooth and converges to zero both as  $\ell \rightarrow 0$  and  $\ell \rightarrow \infty$ . Since it is positive, its maximum must be

attained at a stationary point. Substituting  $s = \ell^2 \sqrt{\Sigma}/2$  we can find stationary points of  $s \mapsto 2^{3/2} \Sigma^{-1/4} \sqrt{s} \Psi(-s)$  which is equivalent to finding solutions of  $\frac{1}{2} = s \frac{\psi(-s)}{\Psi(-s)}$ , where  $\psi$  is the density of the standard Gaussian. There exists a unique solution  $s^*$  since the function  $s \mapsto s \frac{\psi(-s)}{\Psi(-s)}$  is strictly increasing. Hence,  $\text{eff}(\ell)$  attains its greatest value at a specific value  $\ell^* = \sqrt{2s^* \Sigma^{-1/4}}$  that corresponds to an average acceptance rate  $2\Psi(-s^*)$ , which turns out to numerically equal 0.651 to three decimal places. It also implies

$$\text{eff}(\ell^*) = 2^{3/2} \sqrt{s^*} \Psi(-s^*) \times \Sigma^{-1/4} \approx 0.619219 \times \Sigma^{-1/4}.$$

□

## References

- [1] A. Alamo and J. M. Sanz-Serna. A technique for studying strong and weak local errors of splitting stochastic integrators. *SIAM Journal on Numerical Analysis*, 54(6):3239–3257, 2016.
- [2] C. Andrieu and S. Livingstone. Peskun–tierney ordering for markovian monte carlo: Beyond the reversible scenario. *The Annals of Statistics*, 49(4):1958–1981, 2021.
- [3] C. Andrieu, A. Lee, and S. Livingstone. A general perspective on the metropolis-hastings kernel. *arXiv preprint arXiv:2012.14881*, 2020.
- [4] J. Besag. Comments on “representations of knowledge in complex systems” by u. grenander and mi miller. *J. Roy. Statist. Soc. Ser. B*, 56(591–592):4, 1994.
- [5] A. Beskos, N. Pillai, G. Roberts, J.-M. Sanz-Serna, and A. Stuart. Optimal tuning of the hybrid-monte carlo algorithm. *Bernoulli*, 19(5A):1501–1534, 2013.
- [6] M. Betancourt. Identifying the optimal integration time in hamiltonian monte carlo. *arXiv preprint arXiv:1601.00225*, 2016.
- [7] M. Betancourt, S. Byrne, S. Livingstone, and M. Girolami. The geometric foundations of hamiltonian monte carlo. *Bernoulli*, 23(4A):2257–2298, 2017.
- [8] N. Bou-Rabee and A. Eberle. Mixing time guarantees for unadjusted hamiltonian monte carlo. *arXiv preprint arXiv:2105.00887*, 2021.
- [9] N. Bou-Rabee and H. Owhadi. Long-run accuracy of variational integrators in the stochastic context. *SIAM Journal on Numerical Analysis*, 48(1):278–297, 2010.
- [10] N. Bou-Rabee and J. M. Sanz-Serna. Randomized hamiltonian monte carlo. *The Annals of Applied Probability*, 27(4):2159–2194, 2017.
- [11] N. Bou-Rabee and J. M. Sanz-Serna. Randomized hamiltonian monte carlo. *The Annals of Applied Probability*, 27(4):2159–2194, 2017.
- [12] N. Bou-Rabee and K. Schuh. Convergence of unadjusted hamiltonian monte carlo for mean-field models. *arXiv preprint arXiv:2009.08735*, 2020.
- [13] N. Bou-Rabee and E. Vanden-Eijnden. Pathwise accuracy and ergodicity of metropolized integrators for sdes. *Communications on Pure and Applied Mathematics: A Journal Issued by the Courant Institute of Mathematical Sciences*, 63(5):655–696, 2010.
- [14] N. Bou-Rabee, A. Eberle, and R. Zimmer. Coupling and convergence for hamiltonian monte carlo. *The Annals of Applied Probability*, 30(3):1209–1250, 2020.
- [15] G. Bussi and M. Parrinello. Accurate sampling using langevin dynamics. *Physical Review E*, 75(5):056707, 2007.
- [16] C. M. Campos and J. M. Sanz-Serna. Extra chance generalized hybrid monte carlo. *Journal of Computational Physics*, 281:365–374, 2015.
- [17] B. Carpenter, A. Gelman, M. D. Hoffman, D. Lee, B. Goodrich, M. Betancourt, M. Brubaker, J. Guo, P. Li, and A. Riddell. Stan: A probabilistic programming language. *Journal of statistical software*, 76(1):1–32, 2017.
- [18] Y. Chen, R. Dwivedi, M. J. Wainwright, and B. Yu. Fast mixing of metropolized hamiltonian monte carlo: Benefits of multi-step gradients. *J. Mach. Learn. Res.*, 21:92–1, 2020.
- [19] Z. Chen and S. S. Vempala. Optimal convergence rate of hamiltonian monte carlo for strongly logconcave distributions. *arXiv preprint arXiv:1905.02313*, 2019.

- [20] X. Cheng, N. S. Chatterji, P. L. Bartlett, and M. I. Jordan. Underdamped langevin mcmc: A non-asymptotic analysis. In *Conference on Learning Theory*, pages 300–323. PMLR, 2018.
- [21] S. Chewi, C. Lu, K. Ahn, X. Cheng, T. Le Gouic, and P. Rigollet. Optimal dimension dependence of the metropolis-adjusted langevin algorithm. In *Conference on Learning Theory*, pages 1260–1300. PMLR, 2021.
- [22] A. S. Dalalyan. Theoretical guarantees for approximate sampling from smooth and log-concave densities. *Journal of the Royal Statistical Society: Series B (Statistical Methodology)*, 79(3):651–676, 2017.
- [23] A. S. Dalalyan and A. Karagulyan. User-friendly guarantees for the langevin monte carlo with inaccurate gradient. *Stochastic Processes and their Applications*, 129(12):5278–5311, 2019.
- [24] A. S. Dalalyan and L. Riou-Durand. On sampling from a log-concave density using kinetic langevin diffusions. *Bernoulli*, 26(3):1956–1988, 2020.
- [25] A. S. Dalalyan, A. Karagulyan, and L. Riou-Durand. Bounding the error of discretized langevin algorithms for non-strongly log-concave targets. *arXiv preprint arXiv:1906.08530*, 2019.
- [26] G. Deligiannidis, D. Paulin, A. Bouchard-Côté, and A. Doucet. Randomized hamiltonian monte carlo as scaling limit of the bouncy particle sampler and dimension-free convergence rates. *The Annals of Applied Probability*, 31(6):2612–2662, 2021.
- [27] S. Duane, A. D. Kennedy, B. J. Pendleton, and R. Duncan. Hybrid monte carlo. *Physics letters B*, 195:216–222, 1987.
- [28] A. Durmus and E. Moulines. Nonasymptotic convergence analysis for the unadjusted langevin algorithm. *Annals of Applied Probability*, 27(3):1551–1587, 2017.
- [29] A. Durmus and E. Moulines. High-dimensional bayesian inference via the unadjusted langevin algorithm. *Bernoulli*, 25(4A):2854–2882, 2019.
- [30] A. Durmus, S. Majewski, and B. Miasojedow. Analysis of langevin monte carlo via convex optimization. *The Journal of Machine Learning Research*, 20(1):2666–2711, 2019.
- [31] A. Durmus, É. Moulines, and E. Saksman. Irreducibility and geometric ergodicity of hamiltonian monte carlo. *The Annals of Statistics*, 48(6):3545–3564, 2020.
- [32] R. Dwivedi, Y. Chen, M. J. Wainwright, and B. Yu. Log-concave sampling: Metropolis–hastings algorithms are fast! In *Conference on learning theory*, pages 793–797. PMLR, 2018.
- [33] A. Eberle, A. Guillin, and R. Zimmer. Couplings and quantitative contraction rates for langevin dynamics. *Annals of Probability*, 47(4):1982–2010, 2019.
- [34] S. N. Ethier and T. G. Kurtz. *Markov processes: characterization and convergence*, volume 282. John Wiley & Sons, 2009.
- [35] C. W. Gardiner. *Handbook of stochastic methods*, volume 3. Springer Berlin, 1985.
- [36] P. J. Green and A. Mira. Delayed rejection in reversible jump metropolis–hastings. *Biometrika*, 88(4):1035–1053, 2001.
- [37] W. K. Hastings. Monte carlo sampling methods using markov chains and their applications. *Biometrika*, 57:97–109, 1970.
- [38] M. Hoffman, A. Radul, and P. Sountsov. An adaptive-mcmc scheme for setting trajectory lengths in hamiltonian monte carlo. In *International Conference on Artificial Intelligence and Statistics*, pages 3907–3915. PMLR, 2021.
- [39] M. D. Hoffman and A. Gelman. The no-u-turn sampler: adaptively setting path lengths in hamiltonian monte carlo. *Journal of Machine Learning Research*, 15(1):1593–1623, 2014.
- [40] A. M. Horowitz. A generalized guided monte carlo algorithm. *Physics Letters B*, 268(2):247–252, 1991.
- [41] A. Karagulyan and A. Dalalyan. Penalized langevin dynamics with vanishing penalty for smooth and log-concave targets. *Advances in Neural Information Processing Systems*, 33:17594–17604, 2020.
- [42] A. Kennedy and B. Pendleton. Cost of the generalised hybrid monte carlo algorithm for free field theory. *Nuclear Physics B*, 607(3):456–510, 2001.
- [43] Y. T. Lee, R. Shen, and K. Tian. Logsmooth gradient concentration and tighter runtimes for metropolized hamiltonian monte carlo. In *Conference on Learning Theory*, pages 2565–2597. PMLR, 2020.

- [44] B. Leimkuhler and C. Matthews. Rational construction of stochastic numerical methods for molecular sampling. *Applied Mathematics Research eXpress*, 2013(1):34–56, 2013.
- [45] S. Livingstone and G. Zanella. The barker proposal: combining robustness and efficiency in gradient-based mcmc. *arXiv preprint arXiv:1908.11812*, 2019.
- [46] S. Livingstone, M. Betancourt, S. Byrne, and M. Girolami. On the geometric ergodicity of hamiltonian monte carlo. *Bernoulli*, 25(4A):3109–3138, 2019.
- [47] Y.-A. Ma, N. S. Chatterji, X. Cheng, N. Flammarion, P. L. Bartlett, and M. I. Jordan. Is there an analog of nesterov acceleration for gradient-based mcmc? *Bernoulli*, 27(3):1942–1992, 2021.
- [48] O. Mangoubi and A. Smith. Mixing of hamiltonian monte carlo on strongly log-concave distributions 2: Numerical integrators. In *The 22nd international conference on artificial intelligence and statistics*, pages 586–595. PMLR, 2019.
- [49] O. Mangoubi and A. Smith. Mixing of hamiltonian monte carlo on strongly log-concave distributions: Continuous dynamics. *The Annals of Applied Probability*, 31(5):2019–2045, 2021.
- [50] O. Mangoubi and N. K. Vishnoi. Dimensionally tight bounds for second-order hamiltonian monte carlo. *arXiv preprint arXiv:1802.08898*, 2018.
- [51] J. C. Mattingly, A. M. Stuart, and D. J. Higham. Ergodicity for sdes and approximations: locally lipschitz vector fields and degenerate noise. *Stochastic processes and their applications*, 101(2):185–232, 2002.
- [52] N. Metropolis, A. W. Rosenbluth, M. N. Rosenbluth, A. H. Teller, and E. Teller. Equation of state calculations by fast computing machines. *The journal of chemical physics*, 21(6):1087–1092, 1953.
- [53] S. P. Meyn and R. L. Tweedie. Stability of markovian processes iii: Foster–lyapunov criteria for continuous-time processes. *Advances in Applied Probability*, 25(3):518–548, 1993. .
- [54] G. N. Milstein and M. V. Tretyakov. *Stochastic numerics for mathematical physics*. Springer Science & Business Media, 2013.
- [55] A. Mira et al. On metropolis-hastings algorithms with delayed rejection. *Metron*, 59(3-4):231–241, 2001.
- [56] P. Monmarché. High-dimensional mcmc with a standard splitting scheme for the under-damped langevin. *arXiv preprint arXiv:2007.05455*, 2020.
- [57] R. M. Neal. Mcmc using hamiltonian dynamics. *Handbook of markov chain monte carlo*, 2 (11):2, 2011.
- [58] E. Nelson. *Dynamical Theories of Brownian Motion*, volume 3. Princeton University Press, 1967.
- [59] Y. Ollivier. Ricci curvature of markov chains on metric spaces. *Journal of Functional Analysis*, 256(3):810–864, 2009.
- [60] M. Ottobre, N. S. Pillai, F. J. Pinski, and A. M. Stuart. A function space hmc algorithm with second order langevin diffusion limit. *Bernoulli*, 22(1):60–106, 2016.
- [61] J. Park and Y. Atchadé. Markov chain monte carlo algorithms with sequential proposals. *Statistics and Computing*, 30(5):1325–1345, 2020.
- [62] C. Pasarica and A. Gelman. Adaptively scaling the metropolis algorithm using expected squared jumped distance. *Statistica Sinica*, pages 343–364, 2010.
- [63] N. S. Pillai, A. M. Stuart, and A. H. Thiéry. Optimal scaling and diffusion limits for the langevin algorithm in high dimensions. *The Annals of Applied Probability*, 22(6):2320–2356, 2012.
- [64] A. Ricci and G. Ciccotti. Algorithms for brownian dynamics. *Molecular Physics*, 101(12):1927–1931, 2003.
- [65] G. O. Roberts and J. S. Rosenthal. Optimal scaling of discrete approximations to langevin diffusions. *Journal of the Royal Statistical Society: Series B (Statistical Methodology)*, 60(1):255–268, 1998.
- [66] G. O. Roberts and J. S. Rosenthal. General state space markov chains and mcmc algorithms. *Probability surveys*, 1:20–71, 2004.
- [67] G. O. Roberts and R. L. Tweedie. Exponential convergence of langevin distributions and

their discrete approximations. *Bernoulli*, 2(4):341–363, 1996.

- [68] G. O. Roberts, A. Gelman, and W. R. Gilks. Weak convergence and optimal scaling of random walk metropolis algorithms. *The annals of applied probability*, 7(1):110–120, 1997.
- [69] J. M. Sanz-Serna and K. C. Zygalakis. Wasserstein distance estimates for the distributions of numerical approximations to ergodic stochastic differential equations. *arXiv preprint arXiv:2104.12384*, 2021.
- [70] A. Scemama, T. Lelièvre, G. Stoltz, E. Cancès, and M. Caffarel. An efficient sampling algorithm for variational monte carlo. *The Journal of chemical physics*, 125(11):114105, 2006.
- [71] C. Sherlock, S. Urbas, and M. Ludkin. Apogee to apogee path sampler. *arXiv preprint arXiv:2112.08187*, 2021.
- [72] J. Sohl-Dickstein, M. Mudigonda, and M. DeWeese. Hamiltonian monte carlo without detailed balance. In *International Conference on Machine Learning*, pages 719–726. PMLR, 2014.
- [73] L. Tierney and A. Mira. Some adaptive monte carlo methods for bayesian inference. *Statistics in medicine*, 18(17-18):2507–2515, 1999.
- [74] J. Vogrinc and W. S. Kendall. Counterexamples for optimal scaling of metropolis–hastings chains with rough target densities. *The Annals of Applied Probability*, 31(2):972–1019, 2021.
- [75] J. Vogrinc, S. Livingstone, and G. Zanella. Optimal design of the barker proposal and other locally-balanced metropolis-hastings algorithms. *arXiv preprint arXiv:2201.01123*, 2022.
- [76] J. A. Wagoner and V. S. Pande. Reducing the effect of metropolization on mixing times in molecular dynamics simulations. *The Journal of chemical physics*, 137(21):214105, 2012.
- [77] Z. Wang, S. Mohamed, and N. Freitas. Adaptive hamiltonian and riemann manifold monte carlo. In *International conference on machine learning*, pages 1462–1470. PMLR, 2013.